AN INVESTIGATION INTO G PROTEIN MODULATION OF HIGH VOLTAGE ACTIVATED CALCIUM CURRENTS IN ACUTELY REPLATED CULTURED SENSORY NEURONES OF THE RAT

BY

ANATOLE SEBASTIAN MENON-JOHANSSON

A THESIS FOR THE DEGREE OF DOCTOR OF PHILOSOPHY IN PHARMACOLOGY AT THE UNIVERSITY OF LONDON.

ACADEMIC DEPARTMENT OF PHARMACOLOGY
ROYAL FREE HOSPITAL SCHOOL OF MEDICINE
LONDON.

DECEMBER 1992

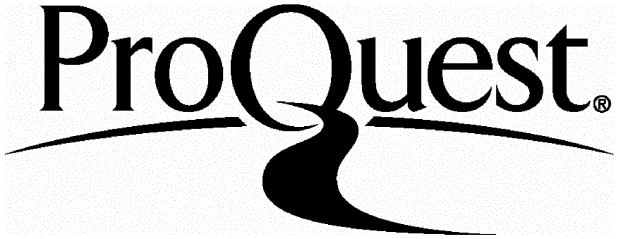

ABSTRACT

Cultured rat dorsal root ganglion (DRG) neurones are a model of their presynaptic terminals in vivo. Acutely replating DRGs before use provides an axotomised cell body ideal for space clamp in electrophysiological recordings. In addition macromolecules can be introduced through transient pores created by the replating procedure.

High voltage activated (HVA) calcium channel currents (I_{Ba}) were recorded in the whole cell configuration of the patch clamp technique. The HVA I_{Ba} in acutely replated DRGs were irreversibly inhibited 57% by ω-CTx-GVIA (1μM). The selective $GABA_B$ agonist, (-)-baclofen (50μM), inhibited the HVA I_{Ba} by 30%. Prior application of ω-CTx-GVIA completely blocked baclofen inhibition of the HVA I_{Ba}. The modulation of the HVA I_{Ba} by baclofen is reduced by pre-incubation with pertussis toxin (PTX). This indicates that a GTP binding (G) protein is involved. PTX ADP-ribosylates the G proteins, $G\alpha_i$ and $G\alpha_o$. To investigate which G protein subtype was involved, cells were replated in the presence of anti-Gα antisera raised against the C-terminal decapeptide of the Gα subunits, $G\alpha_i$ (SG1) and $G\alpha_o$ (OC1/2) at dilutions of 1:100-1:25. Only replating DRGs in the presence of OC1/2 reduced baclofen inhibition of the HVA I_{Ba}. DRGs replated in the presence of the $G\alpha_o$ decapeptide (80μg/ml), also significantly reduced baclofen inhibition of I_{Ba}. Pre-incubation of OC2 with the $G\alpha_o$ decapeptide for one hour at 37°C reversed the effect of both treatments alone.

Using anti-Gα antisera and confocal laser microscopy, Gα localisation was investigated. Using OC1/2 (1:2000), immunoreactivity was observed at the plasma membrane, neurites, attachment plaques, perinuclear region and at points of cell-cell contact. This was blocked by pre-incubation with the $G\alpha_o$ decapeptide (1μg/ml) for one hour at 37°C. Immunoreactivity with SG1 (1:2000-1:500) was also observed in the plasma membrane, cytoplasmic and perinuclear regions. To conclude, $GABA_B$ inhibition of ω-CTx-GVIA sensitive calcium channels in acutely replated DRGs is via $G\alpha_o$.

ACKNOWLEDGEMENTS

Firstly, I would like to thank Professor Annette C Dolphin for her clarity and direction over the last three years.

Secondly, I would like to thank Dr.G.Milligan, University of Glasgow for the anti-G protein antisera.

Thirdly, I would like to thank Mrs P.A.Hems and Professor C.A.Pasternak for awarding me the Hems Memorial Fund in July 1990 to attend the conference "Calcium entry and action at the presynaptic terminal" in Baltimore.

I would also like to thank Dr. Hugh Pearson and Mr. Chris Thrasivoulou for their assistance in the technical aspects of my thesis.

I would also like to acknowledge the Medical Research Council for their financial support.

This thesis is dedicated to Prav.

TABLE OF CONTENTS

LIST OF TABLES

LIST OF FIGURES

ABBREVIATIONS

ω-Aga.....ω-Agatoxin
ATP.....Adenosine trisphosphate
cAMP.....Cyclic 3',5-adenosine monophosphate
BSA.....Albumin, Bovine
Ca^{2+}.....Calcium
$[Ca^{2+}]_i$.....Intracellular calcium
CNS.....Central nervous system
CsAc.....Caesium acetate
CsAsp.....Caesium aspartate
CS1.....Anti $G\alpha_s$ antiserum
ω-CTx.....ω-Conotoxin
DAG.....Diacyl glycerol
cDNA.....complementary DNA
DNA.....Deoxyribonucleic acid
DRG.....Dorsal Root Ganglion
EGTA.....Ethylene glycol-bis
.....(ß-aminoethylether N,N,N',N')-tetraacetic acid
FITC.....Fluoroscein isothiocyanate
FTX.....Funnel web spider toxin
GABA.....γ-aminobutyric acid
GAR.....Goat-anti-rabbit
GDP.....Guanosine diphosphate
G protein.....Guanine nucleotide binding protein
Gα.....G protein α subunit
Gß.....G protein ß subunit
Gßγ.....G protein ßγ subunits
Gpp(NH)p.....5'-guanylimidodiphosphate
GTP.....Guanosine triphosphate
GTPγS.....Guanosine 5'-O(3-thio)triphosphate
5-HT.....5-Hydroxytryptamine
HEPES.....(N-[2-Hydroxyethyl]piperazine-
.....N'-[2-ethanesulphonic acid])
HVA.....High Voltage Activated
I_{Ba}.....Barium current \ Calcium channel current
IgG.....Immunoglobulin G
IP_3.....Inositol trisphosphate
LVA.....Low voltage activated
DL-Lysine.....DL-2,6,Diaminhexanoic acid monohydrochloride
NA.....Noradrenaline
NGF.....Nerve growth factor
OC1.....Anti-$G\alpha_o$ (C-terminal) antiserum
OC2.....Anti-$G\alpha_o$ (C-terminal) antiserum
ON1.....Anti-$G\alpha_o$ (N-terminal) antiserum
PCR.....Polymerase chain reaction
PKA.....Protein Kinase A
PKC.....Protein Kinase C
PLA_2.....Phospholipase A_2
PLC.....Phospholipase C
PTX.....Pertussis toxin
RNA.....Ribonucleic acid
mRNA.....messenger RNA
SG1.....Anti-$G\alpha_i$ (C-terminal) antiserum
TEA.....Tetraethylammonium
TRIS.....2-Amino-2-(hydroxymethyl)-1,3-propanediol
Triton X100.....*iso*-octylphenoxypolyethoxyethanol
TTX.....Tetrodotoxin

CHAPTER ONE

INTRODUCTION

1:1 NEUROMODULATION

Neurones are specialised cells that utilize the electrochemical gradient across their plasma membrane to transduce information. Neuronal membranes establish an electrochemical gradient by energy dependent pumps that pass sodium ions out and potassium ions into the cells, this is maintained by the membrane's impermeability to sodium ions. Current flows along electrochemical gradients through transmembrane proteins which transiently open in response to changes of voltage across the membrane or receptor activation. These selective pores in the membrane are known as ion channels.

Neurones transduce signals electrically, as action potentials which are composed of a rapid sodium ion influx, depolarising the neuronal membrane, followed by the efflux of potassium ions and membrane hyperpolarisation. Adjoining membrane regions are activated by depolarisation and the signal is transduced. The message carried by the neurone is encoded within the frequency of these action potentials and the electrical activity generally has a final output of neurotransmitter release (Katz, 1969). Neurotransmitters are chemical compounds released in high concentrations from specialised neuronal structures called synapses. Neurotransmitters range from simple molecules like adenosine trisphosphate (ATP) to complex peptides such as Neuropeptide Y (Rang & Dale, 1987). Neurotransmitters activate specific receptors on the target postsynaptic cell and possibly the presynaptic terminal.

The first stage of neuromodulation occurs during development when neurones differentiate into particular cell types which then are organised for the appropriate inputs and target. How the correct innervation is achieved at a particular density is not completely understood but it is known to be determined by trophic factors released from the target and the activity of the developing neurones (Purves, 1989). Once the framework of the nervous system is established it must then grow with the organism, accommodate injury and adapt.

The ongoing modulation of electrical activity, neurotransmitter release and receptor activation in neurones, governs the transduction of a signal through that particular neuronal circuit. These are the most subtle levels of neuromodulation and are the basis of many neural responses such as adaptation, learning and memory. In order to investigate these types of neuromodulation much work has focussed on the periphery of the CNS. The special senses translate external signals into action potentials that are carried to the brain and have receptors specifically designed to respond to a changing signal, thereby, extracting relevant information and filtering out or adapting to static irrelevant stimuli (Barlow, 1987). The ability of a neuronal signal to be modulated en route, following receptor activation was first realised in the somatosensory system. It was noted clinically that the perception of pain (nociception) could be modified by stimulation of somatosensory fibres near the site of injury or the state of mind of the patient. This phenomenon of antinociception was hypothesised to be due to peripheral or central neurones acting on the transmitting fibre carrying the pain signal and inhibiting the release of neurotransmitter or by hyperpolarising the target neurone of the transmitting fibre (Melzack and Wall, 1965). Presynaptic inhibition was thought to occur by depolarisation of the primary afferent neurone due to local release of neurotransmitter from neighbouring neurones and increasing the chloride conductance of the presynaptic membrane (for review see Nicoll and Alger, 1979). Prior to this hypothesis, inhibition in the nervous system was thought to be by the action of inhibitory fibres post-synaptically. The presynaptic component of the gate theory has been investigated in sensory neurones.

1:2 DORSAL ROOT GANGLION NEURONES

Dorsal root ganglion (DRG) neurones relay all somatosensory information to the central nervous system (CNS). DRGs are bipolar neurones which have receptors in the periphery and a synaptic connection centrally. They have a wide variety of peripheral receptors corresponding to the area of innervation, and centrally they are known to release the neurotransmitters glutamate and substance P (Iggo, 1987). In the adult, DRGs can be divided into three groups based on the conduction velocity of their fibres. These values and the corresponding modality that is carried by that fibre type, are shown in Table 1.1. The majority of primary afferent (DRG) inputs into the spinal cord synapse in the dorsal horn, onto neurones which project to the brain and interneurones (Cervero, 1986). Immunocytochemical studies have shown that in addition to glutamate and substance P, there are also inhibitory neurotransmitters present, such as glycine and γ-aminobutyric acid (GABA) in the dorsal horn of the spinal cord. Descending fibre inputs into the dorsal horn release neurotransmitters such as serotonin (5-HT), noradrenaline (NA) and opioid peptides (Hammond, 1988).

Table 1.1 Classification of DRG neurones

Fibre type	Conduction velocity (m/s)	Mean cell size (μm^2)	Modality
Adult rat			
Aα	> 30	> 1000	Proprioceptive
Aß	14 - 30	> 1000	Tactile
Aδ	2.2 - 8	< 1000	Temperature
C	< 1.4	< 1000	Pain
Neonatal rat			
All fibres	< 1.0	< 1000	

In order to study the mechanisms of neuromodulation at the molecular level, DRG neurones have been cultured to facilitate electrophysiological recording and the measurement of neurotransmitter release. The size of an adult rat DRG neurone's cell body roughly correlates with the conduction velocity of their axons and thus their

modality (Harper and Lawson, 1985). Aα- and Aß-type DRGs have large cell bodies with rapidly conducting axons which usually transmit proprioceptive and tactile information. The smaller DRGs are classified as C and Aδ-type and have slower conducting axons that usually transmit pain and thermal information.
Acutely isolated DRGs from an adult rat have a variety of cell sizes which presumably reflects the different groups seen in vivo (Scroggs and Fox, 1992). DRGs cultured from embryonic and neonatal rats originate from immature ganglia, the extent of myelination that determines the conduction velocity and characterises the cell type is not fully developed (Fulton, 1987). DRGs cultured at this stage of development originate from slowly conducting neurones and provide a good model of C-type sensory neurones in vitro. If the incoming fibres, interneurones and descending neurones are acting presynaptically on DRGs, then neurotransmitter inhibition of neurotransmitter release would be expected to be reproduced in culture. Cultured DRGs have been shown to release substance P in response to an electrically evoked depolarisation and this is inhibited by the addition of NA or GABA to the medium (Holz *et al.*1989). Neurotransmitter regulation of neurotransmitter release has been shown in a wide variety of neuronal cell types (for review see Miller, 1990). These results support the original gate theory that signal transduction modulation is also presynaptic.

1:3 NEUROTRANSMITTER RELEASE AND CALCIUM

Neurotransmitters are packaged and released from nerve terminals. The invasion of an action potential into a nerve terminal and its depolarisation leads to the release of neurotransmitter which acts on the target. This was first investigated in the neuromuscular junction.
Neurotransmitter release was shown to act on a receptor which depolarised the muscle, the release of neurotransmitter was dependent on the influx of calcium and in the absence of terminal depolarisations miniature electrical changes could be recorded in the muscle end plate (Katz, 1967). The idea of neurotransmitters being stored

and released as discrete quanta was predicted and the steep relationship with extracellular calcium was established (Dodge and Rahamimoff, 1967). It is now known that neurotransmitters are stored in synaptic vesicles (for review see Südhof and Jahn, 1991) and are released on influx of extracellular calcium (Llinás *et al.*1981; Zucker and Haydon, 1988; Augustine *et al.*1991).

The nervous system has essentially two levels of neurotransmission; one fast producing immediate electrical changes in the post-synaptic neurone and the other slow, acting indirectly and stimulating second messenger systems (for review see Strange, 1988). These levels of transmission are not exclusive to the neurotransmitter released but to the type of receptor activated. Receptors grouped functionally this way have been confirmed using molecular biological analysis; one group of receptors forms an ion conducting pore which opens on activation and the other group act by transducing the signal to intracellular proteins (for reviews see (Olsen and Tobin, 1990; Findlay and Eliopoulos, 1990). Neuronal circuits are mostly polysynaptic and therefore have multiple levels of communication; "fast" receptors may act in an excitatory or inhibitory fashion depending on the ion species the receptor ion/channel conducts and "slow" receptors in a modulatory fashion by activating intracellular mechanisms.
Receptors are not only located in the postsynpatic neurone but also presynaptically where they can modulate the response of the synaptic terminal and therefore neurotransmitter release (Kalsner, 1990).
Specific areas of the presynaptic terminal have been shown to have active zones which are characterised by an increased density of calcium channels, synaptic vesicles and corresponding cytoskeleton (Pumplin *et al.*1981; Hirokawa *et al.*1989). The release of neurotransmitter is dependent on the availability of synaptic vesicles for release and the influx of calcium (Mulkey and Zucker, 1991). The amount of calcium influx depends on the number, the probability of opening and the conductance of the calcium channels in the active zone, responding to the change in membrane potential

from depolarisation.

1:4 CALCIUM CHANNELS

The concentration of cytosolic free calcium is important for control of many cellular responses. Cytosolic free calcium can be increased by influx across the plasma membrane or release from internal stores (for review see Tsien and Tsien, 1990). There is a large concentration gradient of calcium across the neuronal membrane (10^6), the calcium ions can be selectively conducted through transmembrane protein channels that are voltage-dependent and are activated in response to membrane depolarisation. The movement of current carried by calcium across the membrane during an action potential was first shown in the crayfish muscle (Fatt and Ginsborg, 1958). This "calcium spike" was enhanced by the presence of potassium channel blockers slowing the repolarising phase of the action potential. The total calcium channel current has now been divided up into specific groups of voltage dependent calcium channels (VOCCs) and their classification depends on the method of characterisation.

1.4.1 Biophysical identification of calcium channels

VOCC currents are now mostly studied with the patch clamp technique (Hamill *et al.*1981). This technique uses a fire polished glass pipette lowered onto the neuronal plasma membrane and suction is applied to produce a high resistance seal. This is known as cell attached configuration of the patch clamp technique. Any charge movement under the pipette can be recorded by means of an amplifier. Further application of suction in the cell attached configuration ruptures the membrane under the patch pipette and a low resistance contact is created between the patch pipette and the inside of the cell, this configuration is known as the whole cell configuration of the patch clamp technique. The flow of current across the whole plasma membrane can then be accurately recorded and the voltage of the cell controlled.

Two other patch clamp configurations can be obtained from the cell attached configuration and involve the excision of patches of neuronal membrane. The configurations differ in which side of the excised patch of plasma membrane faces away from the pipette and is in contact with the medium. In the cell attached and the latter configurations, current flow through single channels can be recorded.

The VOCC current is recorded in isolation by blocking the fast depolarising current from sodium influx with tetrodotoxin (TTX). Extracellular sodium can also be replaced with choline to minimize TTX-insensitive sodium currents which can also contaminate the current flowing through calcium channels (Kostyuk *et al.*1981). Potassium currents can be blocked by tetraethylammonium (TEA) and barium in the extracellular medium and caesium in the patch pipette. Calcium can be replaced with barium in the extracellular medium, barium can pass through calcium channels and therefore can be used as a charge carrier through calcium channels. Using barium has several advantages, calcium inactivation of calcium channels and the activation of second messenger systems, enzymes and ion channels sensitive to calcium are reduced using barium as the charge carrier. The conductance of barium ions through calcium channels is greater than for calcium ions.

Using the patch clamp technique of recording, calcium channels have been defined operationally by their activation and inactivation rates, calcium-dependent inactivation, sensitivity to specific holding potentials and the conductance through single calcium channels (Reuter, 1983; Carbone and Lux, 1984; Nowycky *et al.*1985; Fox *et al.*1987). The calcium channels were originally divided into three groups which were named according to their biophysical characteristics; "L" for long lasting, "T" for transient and "N" for not being L or T. These three channel subtypes can be divided into two groups based on the voltage step required for activation.

Low voltage activated (LVA) calcium channels (T-type) are transiently activated with small depolarisations (more positive than -50mV) from hyperpolarised potentials (-90mV) whilst high voltage activated (HVA) calcium channel (N- and L-type) currents are activated with depolarisation steps to larger step potentials (more postive than -20mV) than are required for the LVA calcium channel current. The HVA and the LVA calcium channel currents have therefore been isolated by specific holding potentials and test steps (Carbone and Lux, 1984; Nowycky *et al.*1985; Fox *et al.*1987). The specific identification of the N- and the L-type calcium channels on biophysical grounds is more complicated than originally realised. The channel voltage dependence and inactivation kinetics of the N- and L-type calcium channels have been shown to overlap (Aosaki and Kasai, 1989; Plummer *et al.*1989).

1.4.2 Pharmacological identification of calcium channels

The contribution of a specific calcium channel subtype in the calcium channel current can be evaluated using calcium channel antagonists. At low concentrations the calcium channel antagonists are highly specific inhibitors of particular biophysically defined calcium channel subtypes. This selectivity is lost as the concentration is increased. The inorganic ion nickel selectively inhibits LVA calcium channel current whilst HVA calcium channel current are more selectively blocked by the metal ions gadolinium, lanthanum and cadmium. Now a wide range of organic compounds are known to inhibit calcium channel currents and the most selective of these inhibit HVA calcium channels.

Originally the only synthetic blockers available were the 1,4-dihydropyridines (DHPs). The development of this class of calcium channel antagonist has shown that they are selective for L-type calcium channels along with phenylalkylamines and the benzothiazepines (Triggle *et*

*al.*1991). The HVA calcium channel current in the heart is carried exclusively by L-type calcium channels which are particularly sensitive to this group of calcium channel antagonists and they are used clinically for treatment of angina.

Pharmacological investigations of calcium channels developed further with the discovery of toxins from the venom of a piscivorous cone snails, Conus Geographus and Conus Magus (Olivera *et al.*1985). There are more than 300 species of venomous snails from the Conus genus. Their venom contains three groups of toxins, α, μ and ω-conotoxins which block nicotinic acetylcholine receptors, sodium and calcium channels respectively (for review see Gray and Olivera, 1988).

ω-conotoxin-GVIA (ω-CTx-GVIA) is a small peptide of 27 amino acids and is one of the many peptides in the l-conotoxin fraction of the venom which can now be synthesized. The application of ω-CTx-GVIA to biophysically defined calcium channels was seen to inhibit both the N- and L-type calcium channels in the HVA calcium channel current (Fox *et al.*1987). The selective inhibition of this conopeptide for N- and L-type calcium channels was for some time unclear (for review see Sher and Clementi, 1991).

Conopeptides have been labelled in agreement with the paper of Hillyard et al.(1992), ω-CTx represents conotoxin from the group ω, the letters G and M represent the species geographus and magus respectively and the following Roman numerals and letters define the specific peptide. ω-CTX-MVIIA is also thought to block N-type calcium channels, this inhibition however is readily reversible unlike ω-CTx-GVIA. ω-CTx-MVIIC has recently been synthesized, this toxin was not purified and characterized from the venom but the amino acid sequence was deduced by molecular biological techniques. ω-CTx-MVIIC also blocks N-type calcium channel current and in addition another current type which is insensitive to ω-CTx-GVIA and DHP antagonists (see below).

Calcium channel toxins have been found in the venom of the spider, Agelenopsis aperta. The polyamine funnel web spider toxin (FTX) was shown to be a particularly effective inhibitor of HVA calcium channel currents in Purkinje cells which are insensitive to ω-CTx-GVIA and DHP antagonists, this novel VOCC was therefore designated P-type for Purkinje cells (Llinás *et al.*1989).
This venom has been divided into four classes of channel-specific toxins (Olivera *et al.*1991) and the specific component which blocks the P-type channel has now been identified as ω-Aga-IVA (Mintz *et al.*1992a). ω-Aga-IVA is a small peptide comprised of 48 amino acids. Another fraction of the venom, ω-Aga-IIIA which is a 96 amino acid peptide has been shown to inhibit both the N- and L-type calcium channels (Mintz *et al.*1991), whilst ω-Aga-IA has been shown to block both low and high voltage activated calcium currents (Adams *et al.*1989)

In most neurones the HVA calcium channel current is carried by a heterogeneous population of calcium channels and the percentage carried by each calcium channel subtype can be investigated with calcium channel antagonists. If calcium channel antagonists are selective for a particular calcium channel then the proportion of the total calcium channel current can be evaluated by their application, providing the toxin completely blocks the channel. Using a combination of the HVA calcium channel antagonist, nitrendipine, ω-CTx-GVIA and ω-Aga-IVA, most of the HVA calcium channel current has been shown to be carried by L-, N- and P-type calcium channels (Mintz *et al.*1992a).

ω-CTx-MVIIC has been shown to partially block P-type current in Purkinje cells at relatively high concentrations and ω-CTx-GVIA resistant calcium currents in hippocampal CA1 pyramidal cells. ω-CTx-MVIIC does not compete with ω-CTx-GVIA or ω-Aga-IVA binding to synaptosomal membranes and therefore is binding to a unique site(s) but not necessarily a unique channel (Hillyard *et al.*1992). The remaining HVA calcium channel current that is insensitive to DHP antagonist, ω-CTx-GVIA and ω-Aga-IVA, can be partially blocked by ω-CTx-MVIIC. This current may possibly be carried by another still unclassified HVA calcium channel subtype.

Unlike the HVA calcium channel antagonists described above there are no equivalent selective antagonists for the LVA calcium channel current. The most selective LVA calcium channel current antagonist is thought to be amiloride (Tang *et al.*1988), however, this selectivity has not been seen by others (for review see Akaike, 1991). High concentrations of ω-CTx-GVIA and DHP antagonists have also been shown to partially inhibit the T-type calcium channel (for review see Hess, 1990; Scott *et al.*1991).

1.4.3 Molecular biological identification of calcium channels

The biophysical and pharmacological classification of calcium channel subtypes has recently been supported by molecular biological techniques. The sequence of the complementary deoxyribonucleic acid (cDNA) has been deduced for some calcium channel subunits and this information has made it possible to compare the predicted primary structure of calcium channels subunits. In some cases, the messenger ribonucleic acid (mRNA) of the calcium channel subunit have been introduced into non-neuronal cells, the encoded proteins have been successfully expressed and a calcium channel current recorded.

The first VOCC to be purified was the DHP-sensitive calcium channel which is found in high concentrations in transverse tubules of skeletal muscle (Curtis and Catterall, 1984). The DHP binding protein once characterised was shown to consist of four subunits (α_1,$\alpha_2\delta$,ß,γ) of specific molecular weight (for reviews see (Campbell *et al.*1988; Snutch and Reiner, 1992). The sequence of L-type calcium channel α_1-subunit DNA was the first to have the sequence identified, i.e.cloned (for reviews see (Birnbaumer *et al.*1991; Snutch and Reiner, 1992). The stable transformation of the α_1-subunit into cells with the α_1-subunit cDNA, produced cells which expressed DHP-sensitive, voltage-gated calcium channels. This indicated that the minimum structure for these channels was at most an α_1ßγ complex and possibly an α_1-subunit alone (Perez-Reyes *et al.*1989).
Isolation and characterization of rat brain cDNA has shown that they are homologous to the DHP-sensitive calcium channel α_1-subunits of heart and skeletal muscle. They were originally grouped into four distinct classes A-D (Snutch *et al.*1990). The class C and D both share around 75% amino acid identity with the rabbit skeletal muscle calcium channel and the class C clone shares 97% amino acid identity with the rabbit cardiac calcium channel. The rat brain classes A and B are more distantly related to the DHP-binding calcium channels (47-64% amino acid identity) and share 51 and 55% amino acid identity with classes C and D respectively. A new distinct calcium channel clone has recently been isolated and has been placed in a new class E which has most amino acid identity with the A and B calcium channel clones (Soong and Snutch, 1992). This diversity of channel subtypes has been shown with polymerase chain reaction (PCR) to result from the expression of distinct genes which have been grouped 1-5 (Perez-Reyes *et al.*1990). Amplification of synthesized DNA with the PCR technique has also shown the number of possible calcium channel subtypes that could be generated from alternative splicing of one gene.

The primary structure of two rabbit brain calcium channels have also been identified by cloning and sequencing isolated cDNA and both have similar structural features to rat brain calcium channels (Mori *et al.*1991; Niidome *et al.*1992). Also a number of calcium channels have been identified from the marine ray, *Discopyge ommata*, with cDNA that are homologous to the rat brain calcium channel clones (Horne *et al.*1992; Horne *et al.*1993).
I have divided up the molecular biological classification of the calcium channel α_1 subunits into groups with the calcium channel antagonists. The rationale for this grouping comes from preliminary results which indicate that there is a high degree of selective binding to calcium channel proteins expressed in cells from specific calcium channel clones. The expression of specific calcium channel proteins and the calcium channel currents recorded have also been shown to be selectively inhibited by calcium channel antagonists.

1.4.3.1 DHP binding calcium channel α_1 subunits

The DHP binding α_1 subunits were the first to be expressed and the calcium channel current recorded. In murine L cells, stable expression of skeletal muscle calcium channel α_1 subunit alone generated voltage-sensitive, high threshold L-type calcium channel currents that were DHP-sensitive and blocked by cadmium. The activation kinetics, however, were 100 times slower than skeletal muscle calcium channel currents. Co-expression of the ß subunit together with the α_1 subunit in cell lines expressed calcium channel currents with kinetics similar to those found in skeletal muscle cells (Lacerda *et al.*1991; Varadi *et al.*1991).
DHP-sensitive (L-type) calcium channels are found in skeletal muscle, cardiac muscle, neuroendocrine and neuronal cell types. The DHP-sensitive calcium channel cDNA in the heart and the brain have been grouped as C and D or 2 and 3 for the Snutch and Perez-Reyes classifications respectively (Snutch *et al.*1990; Perez-Reyes *et al.*1990).

In an attempt to evaluate the proportion of the C clone expressed in cells and therefore the proportion of calcium channel current carried by the C clone α_1 subunit, RNA oligonuceotides were generated which bind specifically to RNA that encodes the calcium channel C clone. The oligonucleotide was incubated with the RNA extracted from heart or rat brain before injection and expression in Xenopus oocytes. The complex formed is unable to be translated into a protein. This antisense oligonucleotide technique has been shown to block the expression of heart L-type calcium channels in the Xenopus oocyte and almost fully inhibits the expression of calcium channel currents in Xenopus oocytes injected with rat brain mRNA (Snutch *et al*.1990).
The latter result does not fit with the pharmacological findings in neurones where the majority of HVA calcium channel current is not selectively inhibited by DHP antagonists (Mintz *et al*.1992). Also the brain calcium channels expressed in Xenopus oocytes from rat brain mRNA injection have previously been shown to be totally insensitive to DHP antagonists in contrast to calcium channel current expressed from heart mRNA injection (Leonard *et al*.1987).
The disparity may be due the calcium channel C clone encoding calcium channel α_1 subunits which are then modulated by different polypeptides in the cells of the brain and the heart. The difference may also result from the insensitivity of the antisense oligonucleotide technique itself (Snutch *et al*.1991).

The other putative L-type calcium channel clone, α_1D, has been co-expressed with the $ß_2$ and α_{2b} subunits, isolated from the human brain, in Xenopus oocytes. Co-expression with the $ß_2$ subunit is obligatory for channel activity, whereas the α_{2b} subunit appears also to play an accessory

role of potentiating expression (Williams *et al.*1992). The expressed calcium channel is sensitive to DHP agonist and antagonists and was also reversibly blocked by a high concentration of ω-CTx-GVIA (10-15μM). Reversible inhibition of L-type calcium channels has been previously reported in sensory neurones (Aosaki and Kasai, 1989).

1.4.3.2 ω-CTx-GVIA binding calcium channel α_1 subunit

The rat brain calcium channel gene cDNA of class B has been generated and encodes the full sequence of a distinct calcium channel α_1 subunit. Polyclonal antiserum generated against a peptide unique to part of this sequence has been shown to selectively immunoprecipitate high affinity ^{125}I-labeled ω-CTx-GVIA binding sites from labelled forebrain membranes of the rat. In contrast, polyclonal antiserum raised against a unique peptide sequence of the rat brain C clone did not immunoprecipitate ω-CTx-GVIA but the DHP antagonist, [H^3]-PN200-110 (Dubel *et al.*1992). The ω-CTx-GVIA receptor has been immunoprecipitated by a monoclonal antibody which was raised against the ß-subunit of the skeletal muscle DHP receptor (McEnery *et al.*1991; Sakamoto and Campbell, 1991). The ω-CTx-GVIA binding channel is thought to be a multi-subunit complex, including components homologous to the skeletal muscle L-type calcium channel. The rat brain B clone has a limited distribution and is only found in the nervous system and neuronally derived cell lines, like N-type calcium channels. The primary structure of the human neuronal calcium channel α_{1B} subunits has been deduced and has been co-expressed with human neuronal $ß_2$ and α_{2b} subunits in mammalian human embryonic kidney (HEK) HEK293 cells. This recombinant channel was irreversibly blocked by ω-CTx-GVIA and was insensitive to DHP antagonists (Williams *et al.*1992). Co-expression of the $ß_2$ subunit was necessary for N-type channel activity, whereas the α_{2b} subunit appeared to modulate the expression of the channel. These results indicate that the calcium channel B clone that specifically binds and is inhibited by the conopeptide, ω-

CTx-GVIA, is most probably the N-type calcium channel. This result is powerful support for the pharmacological isolation of calcium channel subtypes with toxins and a reminder of the shortcoming of defining channel types on biophysical grounds alone.

1.4.3.3 FTX binding calcium channel α_1 subunit

Injection and subsequent expression of the rabbit brain calcium channel α_1-subunit cDNA (BI) in Xenopus oocytes produces a HVA calcium channel current insensitive both to the DHP antagonist, nifedipine and ω-CTx-GVIA. The BI calcium channel α_1-subunit is inhibited by the funnel web spider venom. These results indicate that this is possibly a P-type channel. This is supported by the near loss in mRNA expression of BI in mice with Purkinje cell degeneration and in granule cells in the cerebellum of Weaver mice (Mori *et al.*1991). Mori et al. also showed that the calcium channel activity of the BI α_1-subunit was dramatically increased by co-expression of the α_2 and ß subunits which are known to be associated with the DHP receptor. Recently the expression of BI in oocytes has been shown to be inhibited 50% by ω-CTx-MVIIC (0.5μM) whereas the expressed calcium channels were only partly blocked with ω-Aga-IVA (200nM) (Sather *et al.*1992). ω-Aga-IVA inhibition has been shown to have no overlap with ω-CTx-GVIA and nitrendipine inhibition of calcium channel currents (Mintz *et al.*1992a; Mintz *et al.*1992b). In addition the binding of [^{125}I] ω-Aga-IVA was not significantly inhibited by ω-CTx-GVIA, ω-Aga-1A and ω-Aga-IIIA (Adams *et al.*1992). The inability of ω-Aga-IVA to inhibit the expressed BI calcium channel indicates it is probably not the P-type calcium channel but some other unclassified HVA calcium channel. Calcium channels expressed by the BI clone are almost completely blocked by the Neurex conopeptide, SNX-260 (0.5μM) (Sather *et al.*1992). SNX-260 is the iodinated form of ω-CTx-MVIIC. This indicates the power of calcium channel identification by pharmacological means. Many more ω-conopeptides have been isolated and synthesized and have yet to be screened for calcium channel specificity (Hillyard,D.R.-Neurex, personal communication).

Most of the toxins that have been screened from the funnel web spider and the Conus species selectively inhibit DHP-insensitive calcium channel currents. Recently, a novel snake polypeptide toxin has been isolated from the black mamba snake, *Dendroaspis polyepsis polyepsis*, that is reported to specifically inhibit the nimodipine sensitive, L-type calcium channel current in rat dendate granule neurones (Niesen *et al.*1992).

1.4.3.4 Undefined calcium channels

There are a number of calcium channel α_1 subunits which have been cloned but not yet expressed. The homology of their sequence and the distribution of expression levels give some indication of which calcium channel subtype they may belong. The rat brain calcium channel clone A has been shown to be expressed in all regions of the CNS but most prominently in the cerebellum (Starr *et al.*1991). The calcium channel A clone cDNA sequence is mostly homologous with the calcium channel B clone sequence (Snutch *et al.*1990). Since the calcium channel clone B has been expressed and is selectively inhibited by ω-CTx-GVIA (N-type), then the calcium channel clone A may possibly encode the P-type or BI calcium channel.

A novel calcium channel α_1 subunit amino acid sequence has been deduced in the rabbit brain by cloning and sequencing isolated cDNA (Niidome *et al.*1992). The predicted calcium channel primary sequence is more closely related to BI than the skeletal muscle L-type calcium channel. This calcium channel clone (BII) has been shown to be distributed predominantly in the brain and is most abundant in the cerebral cortex, hippocampus and corpus striatum. The distribution of BII correlates well with ω-CTX-GVIA binding (Takemura *et al.*1989). BII from the rabbit brain may therefore be equivalent to the calcium channel B clone identified from the rat brain (Snutch *et al.*1990) which is homologous to the expressed human calcium channel α_{1B-1} (Williams *et al.*1992).

The class E calcium channel α_1 clone has recently been isolated from the rat brain. It is expressed throughout the brain and is most abundant in the hippocampus (Soong and Snutch, 1992). The deduced primary structure of the class E protein is most closely related to the brain class A and B α_1 subunits.
If the calcium channel A clone encodes the P-type calcium channel α_1 subunit, which is still unclear, then the calcium channel E clone might encode a similar calcium channel type to BI.

A comprehensive review of calcium channel clone sequences and the predicted calcium channel α_1 subunit amino acid sequences is not yet available but it is clear that there are at least four HVA calcium channels in neurones. The calcium channel type which is insensitive to DHP antagonist, ω-CTx-GVIA and ω-Aga-IVA may possibly be encoded by the calcium channel clones BI and/or E. The pharmacological and molecular biological classification of HVA calcium channels has been summarised on table 1.2. The unclassified HVA calcium channel (BI and/or E calcium channel clones) I have labelled O for other.

The marine ray calcium channel clone doe-2 is most similar to the skeletal and cardiac muscle calcium channel α_1 cDNA (1-3 of the Perez-Reyes classification). Whilst the calcium channel clones doe-1 and doe-4 are more similar to the subfamily of non-L-type calcium channels (groups 4 and 5). The homology of calcium channel α_1 cDNA between mammals and mammals to the marine ray indicate that calcium channel genes have been well preserved during evolution (Horne *et al.*1992; Horne *et al.*1993).
There is no primary structure yet available for the LVA, T-type calcium channel. It may be possible that this channel could be derived from alternative splicing of one of the other cloned α_1 subunits or it may be evolutionarily distinct from the DHP binding calcium channels (Snutch and Reiner, 1992).

The brain B, D and BI calcium channel α_1 subunit clones have been expressed and calcium channel currents recorded. The co-expression of their complementary subunits are required for high levels of calcium channel expression with the appropiate kinetics.
The selective inhibition of cloned calcium channel currents to specific calcium channel antagonists supports the selectivity that these antagonists exert on biophysically defined calcium channel currents in neuronal tissue.

The reversible inhibition by ω-CTx-GVIA of the human brain D clone may result from co-expression of the calcium channel α_1D subunit with the same accessory subunits ($ß_2$ and α_{2b}) as the calcium channel α_1B subunit which is irreversibly inhibited by ω-CTx-GVIA. Reversible inhibition of L-type calcium channels by ω-CTx-GVIA has previously been shown in sensory neurones (Aosaki and Kasai, 1989). This indicates that expression of calcium channels in ovo or transfection into endothelial cells also seem to mimic the diverse pharmacological calcium channel antagonist profiles recorded in CNS neurones.

The crossover of biophysical and pharmacological characteristics of calcium channels might exist as a result of the heterogeneity of the subunits in the calcium channel multimeric structure. It has been proposed that multiple calcium channel subtypes may exist from the combination of accessory subunits with a particular calcium channel α_1 subunit (Williams *et al.*1992). In addition distinct calcium channels can also be generated by alternative splicing of a single gene. The calcium channel clone classes B,C and D have been shown to have two splice variants (Williams *et al.*1992; Snutch *et al.*1991; Williams *et al.*1992). These may be producing channels which are also differentially expressed in the mammalian CNS.
The amino acid sequences of the calcium channel α_1 subunits,

predict sites for phosphorylation by specific enzymes. The second messenger activation of intracellular enzymes can theoretically act at these sites to possibly modulate channel open probabilities and conductance. This will be covered in section 1.5.4.

1.4.4 Functional identification of calcium channels

The functional distinction of calcium channels relate to the biophysical characteristics of that subtype.

LVA (T-type) calcium channels are as permeable to calcium ions as HVA calcium channels. The density of LVA calcium channels is significantly reduced during development in sensory neurones whilst in some adult brain cell types, such as hypothalamic and olivary neurones, LVA calcium channels dominate (Kostyuk *et al.*1989). The LVA calcium channel currents have fast inactivation kinetics and are effectively controlled by small membrane potential changes.

LVA calcium channel current has been shown to be responsible for the majority of calcium influx during short duration action potentials in sensory neurones, however, this is dependent on the membrane potential (McCobb and Beam, 1991). The HVA calcium channel current contribution to the total calcium influx increases as the duration of the action potential increases, whilst the LVA calcium channel current contribution remains the same. The specific contribution of LVA calcium channel current in neurotransmitter release is not known because of the lack of specific LVA calcium channel antagonists. LVA calcium channels have been recorded in a wide range of mammalian neurones throughout the brain (Akaike, 1991). The lack of molecular biological information of LVA calcium channels means that there is at present little evidence of LVA calcium channel expression and localisation.

Table 1.2 showing pharmacological and molecular biological classification of HVA calcium channels

Channel subtype	Pharmacological selectivity							Molecular Biological			
	DHP	ω-CTx			ω-Aga						
		GVIA	MVIIA	MVIIC	IA	IIIA	IVA				
	<5μM	<5μM	<5μM	<10μM	10nM	<0.2μM					
L	Yes[a]	No	No	No	Yes[e]	Yes[f]	No	C,D[h]	2,3[l]	Card[m]	doe-2[pq]
N	No	Yes[b]	Yes[c]	Yes[d]	Yes[e]	Yes[f]	No	B[i]	5[l]	BII[n]	doe-4[pq]
P	No	No	NK	Partial[d]	NK	No	Yes[g]	A[j]	NK	NK	
O	No	No	NK	Partial[d]	NK	NK	No	E[k]	4[l]	BI[o]	doe-1[pq]

NK = Not known or not yet determined.

References

a=(Triggle *et al.*1991), b=(Williams *et al.*1992; Dubel *et al.*1992), c=(Gray and Olivera, 1988), d=(Hillyard *et al.*1992), e=(Adams *et al.*1989), f=(Mintz *et al.*1991), g=(Mintz *et al.*1992), h=(Snutch *et al.*1990; Williams *et al.*1992), i=(Snutch *et al.*1990; Williams *et al.*1992), j=(Starr *et al.*1991),k=(Soong and Snutch, 1992),l=(Perez-Reyes *et al.*1991),m=(Mikami *et al.*1989),n=(Niidome *et al.*1992),o=(Mori *et al.*1991; Sather *et al.*1992),p=(Horne *et al.*1992),q=(Horne *et al.*1993).

DHP-sensitive L-type calcium channels are found in their highest density in skeletal and heart muscle (Tanabe *et al.*1987; Mikami *et al.*1989). In the nervous system the L-type calcium channel is thought to be involved in diverse roles such as neuronal development (Silver *et al.*1990; Doherty *et al.*1991) neurosecretion and neurotransmitter release in some systems (Dolphin *et al.*1991; Perney *et al.*1986). The L-type calcium channel may also be involved in signal reinforcement because L-type calcium channel immunoreactivity has been shown clustered at the base of major dendrites in hippocampal pyramidal neurones (Westenbroek *et al.*1990).

The DHP-insensitive HVA calcium channels are predominantly found in the mammalian brain (Dubel *et al.*1992). The ω-Aga-IVA sensitive, P-type calcium channel is found throughout the CNS, with the highest density seen in cerebellar Purkinje neurones (Mintz *et al.*1992a; Llinás *et al.*1992). The release of the excitatory neurotransmitter, glutamate, from rat brain synaptosomes obtained from the frontal cortex, has been shown to be inhibited by ω-Aga-IVA and insensitive to DHP antagonists and ω-CTx-GVIA (Turner *et al.*1992). Glutamate release was also partially sensitive to ω-Aga-IIIA. The influx of $^{45}Ca^{2+}$ in rat brain synaptosomes is not blocked by ω-CTx-GVIA (Lundy *et al.*1991) but inhibition has been demonstrated with P-type calcium channel blockers and the conus peptide ω-CTx-MVIIC (Hillyard *et al.*1992). If synaptosomes produced from the brain are a good presynaptic terminal model, then the majority of calcium influx on depolarisation is being conducted through P-type calcium channels to trigger neurotransmitter release. In some systems the N-type calcium channel has been shown to be solely responsible for calcium influx at presynaptic structures and subsequent neurotransmitter release (Kerr and Yoshikami, 1984; Lipscombe *et al.*1989).

The evidence that calcium channel currents are predominantly via DHP-insensitive calcium channels, has mostly been taken

from neuronal cell bodies and not synaptic terminals. The calcium channels and modulatory mechanisms expressed in the cell body are presumed to be similar to those found at the presynaptic terminal. In the few available synapses, large enough for electrophysiological recording, calcium channel currents have been shown to be DHP-insensitive (Llinás *et al.*1992; Stanley and Goping, 1991).

1:5 MODULATION OF CALCIUM CHANNELS

The modulation of VOCCs in neurones and neuroendocrine cells is important for secretion, cell excitation and patterns of firing in central neurones. The importance of calcium channel modulation depends on the cell type involved and the localisation of action. An action potential invading a synapse would create a voltage change similar to the potential changes evoked experimentally to activate calcium channel currents. The HVA calcium channel currents have been implicated, using calcium channel antagonists in release studies, as being important in neurotransmitter release. HVA calcium channel currents are also easily recorded and sensitive to modulation. For these reasons I shall mostly focus in this section on the modulation of HVA calcium currents which I have grouped into four sections.

1.5.1 Voltage

Voltage changes can open closed channels and may also convert open channels into an inactivated or special closed state which prevents channel opening again in response to a voltage step within a specific time period. Gating mechanisms have been well defined at the single channel level (Hille, 1984) and these phenomena become important in rapid channel activation, such as bursts of firing.
The probability of a group of calcium channels opening will influence the total current flow across the membrane. The open probability (p_O) is related to the total amount of current (I) that will occur in a voltage step as:-

$$I = n.p_O.i.n_t$$

where n is the number of channel activated by the change in voltage, n_t the total number of calcium channels and i the single channel conductance.

If all the HVA calcium channel types are activated by the voltage step then each parameter will have multiple values to represent the respective calcium channels. The relative contribution of each channel type (n) to the total calcium channel current varies between cell types and this has been defined pharmacologically (Mintz *et al.*1992a). The single channel conductances (i) within the HVA calcium channels have been investigated using barium ions as the charge carrier. LVA single calcium channels have the smallest conductances of around 8pS and the HVA, DHP-sensitive calcium channels as large as 25pS, whilst all the DHP-insensitive calcium channel types have single channel conductances in between these values. However, the ability to conduct the divalent cation, calcium, has been shown to be similar for the T-, N- and L-type calcium channels (Kostyuk *et al.*1989).

The open probability and channel gating characteristics depend on the range and frequency of the voltage changes across the channel. Neurotransmitters have also been shown to modulate p_o. The open probability is the most transiently variable factor that determines the total calcium channel current. This will be covered in section 1.6.

Voltage changes have also been shown to recruit a facilitation calcium channel current in chromaffin cells due to a voltage-dependent phosphorylation step (Artalejo *et al.*1992). Voltage changes act on the voltage sensor of the calcium channel to alter the ionic permeability and also seems to change the susceptibility of the channel, or a closely associated protein, to be a substrate for kinases or phosphatases.

1.5.2 Calcium

Calcium ions not only carry positive charge across the membrane during voltage activation but also act specifically on, or modulate, the activity of many intracellular proteins, such as enzymes, synaptic vesicle proteins and ion

channels. It was first noted that injection of a calcium chelator into a cell decreased the rate of inactivation of a calcium current (Hagiwara and Nakajimi, 1966). The local intracellular rise in the calcium concentration passing into the cell on depolarisation was shown to be the cause of the inactivation (Brehm and Eckert, 1978). It was then proposed that this self-limiting mechanism would keep the channel refractory until the internal calcium was reduced. The mechanisms of calcium removal will vary within cell types and will lead to variations in patterns of cell excitation (Blaustein, 1988). The open probability of the channels will depend in part on the intracellular calcium concentration ($[Ca^{2+}]_i$) which in turn depends on the intracellular buffering of the cell and calcium pumping mechanisms out across the plasma membrane or into internal stores. In addition to bulk cytoplasmic $[Ca^{2+}]i$ being able to modulate calcium channels, the influx of calcium through a single channel has been reported to contribute to the inactivation of an adjacent channel (Imredy and Yue, 1992).

1.5.3 Expression

The total number of calcium channels that are expressed in a cell is represented by **n** in the above equation for total current. The proportion of a calcium channel subtype will vary between particular neuronal cell types. Cellular proteins are in a dynamic equilibrium and the level of expression and degradation depend on the level of activity of a particular cell. In the sea slug, Aplysia Californica, Bailey and Chen (1983) showed that the number, size and vesicle number of the sensory neurone active zones were larger in animals showing long-term sensitization than in control animals and smaller in animals showing long-term habituation. This demonstrates that not only the ion channels but the whole synaptic structure is plastic. In single hippocampal neurones, the abundance of mRNA has been shown to change within 30 minutes in response to stimulation (Mackler *et al.*1992). This illustrates how dynamic and responsive protein synthesis can be in neurones.

1.5.4 Neurotransmitter modulation of calcium channel currents

The modulation of calcium influx in sensory neurones by the application of neurotransmitters has been known since the work of Dunlap and Fischbach (1978). The action potential duration decreased on the application of GABA, 5-HT and NA and this provided the first evidence of another mechanism of presynaptic inhibition alongside primary afferent depolarisation. The major inhibitory neurotransmitter, GABA, did not depolarise the neurone by increasing membrane permeability to chloride but was modulating the influx of calcium.

The modulation of cellular excitability by the activation of "slow" receptors is transduced by guanosine trisphosphate (GTP) binding proteins (G proteins).

1.5.4.1 G-proteins

G-proteins that are involved in transmembrane signalling in the CNS of vertebrates are heterotrimeric (α,ß,γ) proteins within the GTPase-superfamily. G proteins transduce sensory, hormonal or neurotransmitter signals to most second messenger systems and some ion channels in every neuronal cell type, and are involved in specific, tightly coupled signalling pathways (for reviews see (Bourne *et al.*1991; Birnbaumer *et al.*1991; Brown, 1991; Dolphin, 1990; Hille, 1992).

Activation of a G-protein coupled receptor catalyses the exchange of bound guanosine diphosphate (GDP) for GTP on the G protein α-subunit (Gα subunit). The GTP bound Gα subunit is active and it is thought to dissociate from the G protein ßγ subunits (Gßγ subunit) and transduce the signal to the appropriate effector. The activated Gα subunit lifetime is self-regulated by its inherent GTPase activity, hydrolysis of GTP to GDP inactivates the Gα subunit and the cycle is completed by reassociation with the Gßγ subunit. The Gα subunits are targets of two bacterial toxins, Cholera and Pertussis toxin. These toxins covalently modify Gα subunits enzymatically by transferring the adenosine diphosphate (ADP)-ribose moiety to two amino acids on the Gα subunit.

Cholera toxin acts to bypass receptor activation and activates the $G\alpha_s$ subunit as well as inhibiting GTPase activity which fixes the $G\alpha_s$ subunit in the activated form. Pertussis toxin (PTX) acts in the opposite way by blocking $G\alpha_i$ and $G\alpha_o$ subunits interacting with the receptor and inactivates the signalling pathway (for review see Dolphin, 1987). Uncoupling of G proteins and receptors with PTX also reduces the affinity of the receptor for the agonist (Asano *et al.*1985). Some of the G-protein coupled receptors, a list of corresponding G-protein(s), their toxin sensitivity and effector system activated are shown in Table 1.3.
There is also evidence that some effectors can also regulate the rate of GTPase activity of the Gα subunit, this is analogous to GTPase activating proteins (GAP) shown for the proto-oncogene product p21ras and other small monomeric GTPases (for review see Kaziro *et al.*1991). Phospholipase C (PLC), cGMP dependent phosphodiesterase (PDE) and stimulated L-type calcium channels have been shown to act like GAPs and increase GTP hydrolysis of the Gα subunit (Arshavsky and Bownds, 1992; Berstein *et al.*1992; Sweeney and Dolphin, 1992).
Receptor transduction via a G protein to an effector is used in many diverse cell types with a wide variety of functions such as the special senses (McLaughlin *et al.*1992), neurosecretion (Haydon *et al.*1991; Scholz and Miller, 1992), neurite outgrowth (Doherty *et al.*1991; Strittmatter *et al.*1990) and cell differentiation (Wang *et al.*1992).
The activation of the G-protein coupled receptor can be amplified because a G-protein can activate more than one effector. The G-protein keeps a memory of receptor activation perpetuating the signal until the bound GTP is hydrolysed. This cascade of activation is most developed in the retina where light activated rhodopsin catalyses the exchange of GDP for GTP on multiple G protein (transducin) molecules. Activated transducin then stimulates multiple cGMP phosphodiesterase which leads to a decrease in cGMP levels in rods, and closure of plasma membrane cation channels which are gated by cGMP (Pugh and Lamb, 1990).
Inherent GTPase activity of the Gα subunit installs a negative feedback into G protein signal transduction system.

In those pathways where the effector has been shown to increases GTP hydrolysis, a highly efficient and responsive transduction system exists.
The Gßγ subunit was originally thought to act as an anchor in the membrane for the Gα subunit. The Gßγ subunit was then shown to activate potassium channels in excised patches of chick embryonic atrial cells (Logothetis *et al.*1987). Later work on potassium channel activation in atrial cells has shown that the activation of the enzyme phospholipase A_2 (PLA_2) could produce metabolites which activate the channel (Kurachi *et al.*1989) and that PLA_2 activity was stimulated by the Gßγ subunit (Kim *et al.*1987). In addition, Gßγ subunits from PTX-sensitive G proteins have also been shown to stimulate the ß2 isoform of phospholipase C in the COS-1 and COS-7 cell lines (Camps *et al.*1992; Katz *et al.*1992). Gßγ subunits have also been proposed to act as a common heterodimer in the plasma membrane which could couple Gα subunits from an opposing G-protein systems and reduce their transduction (Linden and Delahunty, 1989). Most recently Gß subunit subtypes have been shown to specifically couple not only to a particular Gα subunit in transmembrane signalling but also to a specific receptor (Kleuss *et al.*1992). The idea of a common, passive Gßγ subunit, which anchors the Gα subunit to the membrane, is too simple. It now seems that G protein transduction pathways are highly specific and tailored precisely to specific receptor and effector subtypes.

Several second messenger systems have been identified, activated by specific G proteins, that modulate calcium channels. I have separated the second messenger systems into four groups, none of these pathways are mutually exclusive and most of the enzymes are sensitive to $[Ca^{2+}]_i$.

1.5.4.2 Cyclic Nucleotides

The first G-protein to be discovered was in the cyclic 3',5-adenosine monophosphate (cAMP) system. The $G\alpha_s$ subunit acts on the enzyme adenylyl cyclase (ACase) and elevates the intracellular concentration of cAMP ($[cAMP]_i$) whilst $G\alpha_i$ inhibits ACase and decreased $[cAMP]_i$. The Gα subunits were labelled s and i because they stimulate and inhibit ACase respectively (for review see Gilman, 1987)). This cyclic nucleotide is required for the maintenance of HVA calcium channel currents and the prevention of rundown especially in excised patches (Doroschenko *et al.*1982; Kostyuk *et al.*1988). cAMP is thought to act through cAMP-dependent-protein kinase A (PKA) and phosphorylation of the calcium channels. L-type calcium channels have been shown to require phosphorylation to be active (Hartzell *et al.*1991). Another cyclic nucleotide (cGMP) has been shown to modulate calcium currents directly, acting through a cGMP-dependent protein kinase, to increase the calcium channel current and the sensitivity to neurotransmitter (Paupardin-Tritsch *et al.*1986). Also the cation channels in photo- and olfactory receptors have been shown to be gated directly by cGMP and cAMP respectively (Matthews, 1991).

1.5.4.3 Phospholipase C and Ins(1,4,5) trisphosphate and Diacylglycerol.

There are large number of receptor activated pathways in the nervous system which are coupled to inositol phospholipid metabolism. Receptor stimulation activates the enzyme phospholipase C (PLC), this enzyme then hydrolyses phosphatidylinositol (4,5)-bisphosphate to the immediate products of d-myo-inositol (1,4,5)-trisphosphate (IP_3) and sn(1,2)-diacylglycerol (DAG). DAG activates the enzyme protein kinase C (PKC) and its actions are discussed below. IP_3 activates receptor-channels on the endoplasmic reticulum which release stored intracellular calcium (for reviews see (Nahorski, 1988; Berridge and Irvine, 1989).

Table 1.3 Showing a summary of G-protein coupled receptor pathways described in the text of chapter one.

Receptor	G-protein	Toxin sensitivity	Effectors	Signalling pathway
Adrenaline,histamine ACTH,glucagon + others	$G\alpha_s$[a]	Cholera[f] toxin	ACase Ca^{2+} channels	↑ cAMP ↑ Ca^{2+} current
Odorants	$G\alpha_{olf}$[a]	Cholera[f] toxin	ACase	↑ cAMP
Photons	$G\alpha_{t1+2}$[a]	PTX [f]	cGMP phosphodiesterase	↓ cGMP
NA,prostaglandin, opiates + many peptides	$G\alpha_{i1-3}$[a]	PTX[f]	ACase PLC PLA_2 K^+ channels	↓ cAMP ↑ IP_3,DAG,$[Ca^{2+}]_i$ Arachidonic acid (AA) release Membrane polarisation
NA,opiates,neuropeptide Y, GABA,5-HT,acetylcholine, adenosine,somatostatin + others	$G\alpha_{o1+2}$[b]	PTX[f]	PLC Ca^{2+} channels	↑ IP_3,DAG,$[Ca^{2+}]_i$ ↓ Ca2+ influx
Acetycholine	$G\alpha_q$[c] $G\beta\gamma$[d] $G\beta\gamma$[e]	- PTX -	PLC PLA_2	↑ IP_3,DAG,$[Ca^{2+}]_i$ AA release ↑ K^+ efflux

The table was created from the following reviews and research papers:- a=(Gilman, 1987; Bourne *et al.*1991; Hille, 1992),b=(Kleuss *et al.*1991; Asano *et al.*1992),c=(Gutowski *et al.*1991; Berstein *et al.*1992; Taylor *et al.*1991),d=(Katz *et al.*1992; Markram *et al.*1992),e=(Kim *et al.*1987),f=(Dolphin, 1987).

Using the nystatin-perforated patch pipette, as opposed to diffusion of the cell with calcium buffers in the patch electrode during whole cell recording, receptor activated IP_3 production and subsequent calcium mobilisation has been shown to inhibit the calcium currents in pituitary tumour cells (Kramer *et al.*1991). IP_3 has also been shown to act directly on the calcium channel current in cerebellar granule neurones. This response is independent of the receptor-channel on the endoplasmic reticulum, the release of intracellular calcium or a change in the calcium buffering of the cell (De Waard *et al.*1992).

1.5.4.4 Protein Kinase C

The production of DAG from inositol phospholipid breakdown by PLC activates the membrane bound enzyme PKC; this then acts on the calcium currents in some systems. Activation of the PKC by phorbol esters or oleoylacetylglycerol (OAG) was initially shown to inhibit the calcium current (Rane and Dunlap, 1986), also negative results exist where these compounds fail to inhibit the calcium current in other cell types (Docherty and McFadzean, 1989; Dolphin *et al.*1989; Wanke *et al.*1987). There is also evidence that the DAG analogue, OAG can act on calcium currents directly and is unaffected by application of PKC inhibitors (Hockberger *et al.*1989).

In Aplysia, phorbol esters and intracellular injection of purified PKC has led to the enhancement of the calcium current (DeRiemer *et al.*1987). The mechanism of PKC in these cells was to unmask a calcium channel with a higher unitary conductance than was seen in the control cell (Strong *et al.*1987).

1.5.4.5 Phospholipase A_2 and arachadonic acid

The initial evidence of this second messenger system acting on calcium channels came from FMRFamide action in Aplysia. Production of arachidonic acid by FMRFamide stimulation of PLA_2, produced a decrease in the calcium current and an increase in the potassium current (Piomelli *et al.*1987). Activation of receptors linked to PLA_2 and arachidonic acid production have been shown in the CNS (for review see Axelrod *et al.*1988)) and it has been proposed that arachidonic acid may modulate synaptic transmission by feeding back across the synaptic cleft to receptors on the pre-synaptic terminal (Dumuis *et al.*1988; Herrero *et al.*1992).

In DRG neurones elevation of cAMP, IP_3 production, phorbol ester stimulation of PKC and application of arachidonic acid directly onto DRG neurones were without effect on HVA calcium channel currents (Dolphin *et al.*1989). The modulation of calcium channel current was therefore thought to be by direct or indirect modulation by a G protein.

1:6 DIRECT MODULATION OF CALCIUM CHANNELS BY G-PROTEINS

The direct G-protein modulation of ion channels has been proposed for three groups of G-proteins, $G\alpha_o$, $G\alpha_s$ and $G\alpha_i$. The ability of a G-protein to modulate an ion channel directly offers a tightly coupled rapidly reversible and potentially powerful mechanism. At active zones where calcium influx is crucial for neurosecretion, this type of mechanism would be an efficient, economic and precise method for control of neuronal signalling.

1.6.1 Introduction

The inhibitory action of adenosine on glutamate release from cerebellar granule neurones was shown to be reduced by preincubation with PTX (Dolphin and Prestwich, 1985). A G protein was then postulated to be involved in coupling the receptor to the inhibition of the calcium influx and therefore neurotransmitter release (Holz *et al.*1989). The modulation of VOCCs by the neurotransmitters, noradrenaline and GABA, was then shown to be mimicked by intracellular perfusion with guanine nucleotides. Both of these effects were reduced with pre-incubation with PTX, suggesting the involvement of a G-protein (Holz *et al.*1986; Scott and Dolphin, 1986). PTX, ADP-ribosylates the G-proteins, $G\alpha_i$ and $G\alpha_o$, with $G\alpha_o$ being the major substrate in bovine brain membranes (Neer *et al.*1984; Sternweis and Robishaw, 1984). Using specific antibodies raised against these two G-proteins, $G\alpha_o$ was shown to be immunochemically distinct from $G\alpha_i$ and that it was a highly conserved protein. $G\alpha_o$ was shown to be distributed throughout the brain with particularly high concentrations in the forebrain. The concentration of $G\alpha_o$ in cerebral cortex was shown to be 5 times that of the $G\alpha_i$, but unlike $G\alpha_i$ its function was at that point unknown (Gierschik *et al.*1986).

In sensory neurones noradrenaline inhibited the calcium channel current recorded in the whole cell configuration of the patch clamp technique. In contrast, recording of calcium currents in the cell-attached mode of the patch clamp technique showed that noradrenaline application to the cell only affected the calcium current outside the area of the patch. The action of cAMP was ruled out and NA was therefore thought to operate through a tight receptor-channel coupling (Forscher *et al.*1986). This was also shown with the activation of the $GABA_B$ receptor by the agonist baclofen (ß-p-chlorophenyl GABA) (Green and Cottrell, 1988).

1.6.2 GTPγS infusion from the patch pipette and voltage-dependent G protein coupling to calcium channels

In the whole cell configuration of the patch clamp technique, the intracellular saline of the pipette exchanges with the cell cytoplasm. In order to investigate if direct activation of G proteins could mimic the application of neurotransmitter, the non-hydrolysable GTP analogues, guanosine 5'-O-3'thiotriphosphate (GTPγS) or guanylyl-imidodiphosphate (Gpp(NH)p), have been included in the patch pipette. These GTP analogues exchange from the patch pipette to the cell and when GDP coupled to the Gα subunit is exchanged for GTP, GTPγS or Gpp(NH)p can also bind and the Gα subunit is irreversibly activated. Infusion of GTPγS or Gpp(NH)p into neurones reduces the calcium channel current amplitude (Dolphin and Scott, 1987; Toselli *et al.*1989; Schofield, 1991; Elmslie *et al.*1990), potentiates neurotransmitter application and converts reversible neurotransmitter inhibition into one that is irreversible (McFadzean and Docherty, 1989; Lester and Jahr, 1990; Bley and Tsien, 1990). Infusion with GTPγS also slows the rate of current activation and this has been shown in some systems to be PTX sensitive (Dolphin and Scott, 1987; Toselli *et al.*1989) and in insensitive in others (Hescheler *et al.*1988).

Neurotransmitter inhibition of the calcium channel current has been shown to be voltage dependent, that is the calcium channels gating is shifted to more positive potentials in the presence of neurotransmitter (Grassi and Lux, 1989; Kasai and Aosaki, 1989; Regan *et al.*1991; Penington *et al.*1991; Kasai, 1992). Voltage-indepenent mechanisms of neurotransmitter inhibition of the calcium channel current have also been reported (Beech *et al.*1992). The modulation of the calcium channel current by GTPγS has also been shown to be voltage dependent (Scott and Dolphin, 1990; Marchetti and Robello, 1989). The inhibitory action of neurotransmitters and GTPγS has been shown to be relieved, in a rapid and reversible manner, by a conditioning prepulse

before a voltage step. The Gα subunit coupling to the calcium channel has been proposed to be voltage-dependent and the prepulse is thought to transiently uncouple the two proteins (Grassi and Lux, 1989; Plummer *et al.*1989; Elmslie *et al.*1990).
Negative evidence also exists where preincubation with PTX has been shown to be unable to block G protein modulation of the calcium channel current (Wanke *et al.*1987; Song *et al.*1989; Hescheler *et al.*1988; Bley and Tsien, 1990; Beech *et al.*1992). This may indicate that a PTX-insensitive G protein is involved or it may depend on the amount of precoupling between receptor and inactive G protein in a particular system, as PTX prevents receptor-G protein coupling. In addition, a prepulse has been shown unable to relieve muscarinic and $GABA_B$ inhibition of the calcium channel currents in adult DRGs (Formenti and Sansone, 1991). Also a prepulse has been shown to stimulate baclofen inhibited calcium channel currents to a similar proportion as control calcium channel currents in DRGs (Tatebayashi and Ogata, 1992).

Most experimental findings have indicated that a PTX-sensitive G protein, G_i or G_o, are involved in calcium channel modulation in central neurones. The G-protein, $G\alpha_i$, has three subtypes $G\alpha_i1$-3 which couple receptors to membrane bound enzymes, potassium and calcium channels (for review see Bourne *et al.*1991). Four G_o-type proteins have been purified and characterised in bovine brain (Inanobe *et al.*1990). So far only two $G\alpha_o$ subunits have been shown functionally, these two $G\alpha_o$ subunits, $G\alpha_o1$ and $G\alpha_o2$, differ most in their C-terminal region (Hsu *et al.*1990) and have been shown to be activated independently (Kleuss *et al.*1991).

The various methods used to evaluate which G protein is involved in calcium channel modulation will be discussed in the section 1.7.

1.6.3 G protein stimulation of calcium channels

Another G protein which has been shown to couple to calcium channels is $G\alpha_s$. $G\alpha_s$ stimulates the voltage-dependent, DHP-sensitive calcium channel directly in heart and skeletal muscle. $G\alpha_s$ also acts indirectly by stimulating ACase, elevates $[cAMP]_i$ and activates PKA which phosphorylates the L-type calcium channel (Birnbaumer *et al.*1991). The DHP binding calcium channel subunit can be immunoprecipitated with the $G\alpha_s$ and the Gß subunits of G_s (Hamilton *et al.*1991).

In rat nodose neurones the peptide CGRP has been shown to increase the HVA calcium channel current (Wiley *et al.*1992). Based on the biophysical characteristics of the calcium channel current recorded Wiley et al. believe that CGRP is enhancing primarily the N-type calcium current. The action of CGRP was not via $G\alpha_s$ however because it was abolished by pre-incubation with PTX.

1.6.4 G protein modulation of potassium channels

$G\alpha_o$ has been shown to stimulate inwardly rectifying potassium channels in cell-free membrane patches of hippocampal pyramidal neurones (VanDongen *et al.*1988) and $G\alpha_i$ has been shown to similarly activate an inwardly rectifying potassium channel in atrial cells (Yatani *et al.*1988). The dopamine D2 receptor has been shown to activate two types of potassium currents in anterior pituitary cells via $G\alpha_{i3}$ (Lledo *et al.*1992).

Many G protein subtypes mediate the activation and inhibition of a wide variety of potassium channel subtypes both directly and indirectly (for review see Brown, 1990)).

1:7 METHODS OF INVESTIGATING G-PROTEIN MODULATION OF CALCIUM CHANNELS

The PTX-sensitive G-protein involved in peptide inhibition of the calcium channel subunit was first investigated in NG108-15, neuroblastoma X glioma cells. Calcium channel current inhibition by D-Ala^2,D-Leu^5-enkephalin (DADLE) in NG108-15 cells was blocked by pre-incubation with PTX. Inhibition by DADLE was then restored by intracellular exchange of purified G proteins, G_i or G_o, from the patch pipette. The $G\alpha_o$ subunit was shown to restore the DADLE inhibition of the calcium channel current, the $G\alpha_i$ subunit was also effective at 10 times greater concentration in the patch pipette (Hescheler *et al.*1987). Purified $G\alpha_o$ was seen to be as effective as the heterotrimeric G_o and the inclusion of $G\beta\gamma$ at 200 times greater concentrations than G_o, was unable to restore the DADLE inhibition of the calcium channel current. Similarly (Toselli *et al.*1989) showed that acetycholine inhibition of the calcium channel current in hippocampal neurones, pretreated with PTX, could be restored by intracellular infusion with G_o and to a lesser extent G_i.

Using a similar protocol of intracellular infusion of G proteins, the action of Neuropeptide Y was shown to be mediated by G_o in rat sensory neurones (Ewald *et al.*1988). Using $G\alpha$ subunits expressed in *Escherichia coli*, (Linder *et al.*1990) showed that the recombinant proteins, $G\alpha_o$, $G\alpha_i1$ and $G\alpha_i3$ were equally able to restore neuropeptide Y inhibition in PTX treated DRGs. Also intracellular infusion of the activated $G\alpha_i$ subunit was shown to be most effective in restoring neurotransmitter inhibition of the calcium channel current in guinea-pig submucosal neurones (Surprenant *et al.*1990).

Intracellular exchange of a high concentration of exogenous $G\alpha$ subunits into neurones following PTX treatment have provided no clear indication of which PTX sensitive G protein subtype is involved in calcium channel modulation.

Direct G protein transduction can also be studied if an endogenous G protein is selectively removed from the transduction pathway. Antibodies have been generated against the C-terminal of the two PTX-sensitive Gα subunits, $G\alpha_o$ and $G\alpha_i$ (McFadzean *et al.*1989). The anti-G_i antiserum recognised $G\alpha_i1$, $G\alpha_i2$ and transducin whilst the anti-G_o antiserum only recognises $G\alpha_o$. The C-terminal of the Gα subunit is thought to be the site that couples to the receptor (Masters *et al.*1988; Heideman and Bourne, 1990); antibody binding to this site therefore prevents the specific G protein receptor interaction and blocks signal transduction through that system.
The antisera were injected into NG 108-15 cells at a dilution that was shown to be active in blocking opioid peptide mediated inhibition of adenylyl cyclase (McKenzie *et al.*1988). Elevation of cAMP alone did not inhibit the calcium current. Only the antiserum raised against $G\alpha_o$ was able to significantly protect against noradrenaline inhibition of the calcium current (McFadzean *et al.*1989).

1:8 AIMS AND OBJECTIVES

The aim of this study was to establish the particular G-protein involved in $GABA_B$ modulation of the HVA calcium channel current in cultured DRGs.

The objectives were to:-

a) Record calcium channel currents from acutely replated cultured DRGs of the rat.
b) Establish the characteristics of the calcium channel currents in acutely replated DRGs and whether they could be inhibited by (-)-baclofen and GTPγS.
c) Introduce antibodies into acutely replated DRGs.
d) Evaluate using anti-G protein antibodies, the Gα subtype involved in modulation of HVA calcium channel currents, in acutely replated DRGs.
e) Establish which calcium channel type was being modulated by the G protein.
f) Using anti-G protein antibodies and immunocytochemistry establish the localisation of the particular G proteins.

Some of the results described in this thesis have been published.

A.S.Menon-Johansson and A.C.Dolphin (1992). Inhibition of $GABA_B$ modulation of calcium channel currents in cultured rat dorsal root ganglion neurones by loading replated cells with anti-G protein antibodies. J. Physiol., 452,177P.

CHAPTER TWO
MATERIALS AND METHODS

CHAPTER 2: MATERIALS AND METHODS

2.1 CELL PREPARATION

2.1.1 Dorsal Root Ganglion neurones

Two, two day old rats (Wistar or Sprague Dawley) yield approximately 10^5 cells.

2.1.1.1 Coverslip preparation

Sterile coverslips (22 x 22 mm) were incubated overnight in polyornithine (0.25mg/ml), washed in sterile water and then dried. Each coverslip was then placed in a 35mm diameter culture dish. Incubation with laminin was done prior to the dissection.

2.1.1.2 Dissection

The neonatal rat was decapitated, using a large pair of scissors. The vertebral column was exposed and removed by cutting through the skin, above the spinal cord, in the rostro-caudal direction and then through the muscle along both sides of the column, using fine pointed scissors. The column was then washed with sterile phosphate buffered saline (PBS) and placed in a large (85mm) Petri dish containing PBS. Next, the dorsal surface of the column was removed by inserting one tip of a pair of fine spring-loaded scissors into the rostral end of the spinal cord and cutting down to the caudal end on both sides just above the transverse processes. On completion of both sides, the dorsal vertebral surface of the spinal cord can be pulled away, leaving the ganglia exposed bilaterally in the intervertebral foraminae. Using a dissection microscope the ganglia were removed by pulling from behind with fine forceps. The roots on the ganglia were also removed with fine forceps before the ganglia were collected in a small (35mm) Petri dish containing F14+HS medium. Approximately 35-40 ganglia were obtained per column.

2.1.1.3 Dissociation of ganglia

Ganglia were transferred to F14+HS medium containing 0.125% collagenase and incubated for 13 minutes (37°C). They were then washed three times in approximately 3 mls of PBS prior to incubation in PBS containing 0.25% trypsin for 6 minutes (37°C). Following the enzyme treatment, DRGs were washed three times with 5 mls of F14+HS medium. The ganglia were then mixed thoroughly with 160 kunits/ml of DNAase in F14+HS for 2 minutes prior to trituration (10-15 times). Then 1.0ml of F14+HS was added to give the final volume of 2.0mls. A fire polished Pasteur pipette, with a slightly reduced bore at the end, was used for medium transfer and trituration.

2.1.1.4 Final plating

Polyornithine coated coverslips were incubated (37°C) for two hours with 200µl of Laminin (1.0µg/ml). The cover slips were then washed with 300µl of F14+HS medium before plating out the cells. Nerve growth factor (NGF) was added to the cell suspension (10ng/dish). The cell suspension was then equally distributed between the ten pre-coated and washed coverslips from the incubator.

After two hours in the incubator the cells adhered to the coverslip and then were topped up with 1.5mls F14+HS medium with NGF (15ng/dish).

Approximately 30 hours later the cells were fed by replacing 1.0ml of the F14+HS medium with 1.0ml of defined medium plus NGF (10ng/dish). Cells were fed every 2-3 days by the same procedure.

2.1.2 THE REPLATING PROCEDURE

Cells were used on day 3/4 of culture. A fire-polished Pasteur pipette (as for trituration) was used for the replating procedure. All the medium in the culture dish was removed and a specific volume (200µl) was returned to the cells. Macromolecules in specific experiments were diluted in this volume (see 2.2.3 Replating medium). This solution was drawn up and then ejected over the coverslip (approximately 10 times) whilst rotating the culture dish. The progress was monitored with a low power phase contrast microscope. This cell suspension was then removed and plated onto a dried polyornithine coated coverslip and placed in the incubator for one hour before use.

2:2 SOLUTIONS, DRUGS AND METHODS OF APPLICATION

2.2.1 CULTURE REAGENTS FOR DRGs

Ham's nutrient mixture F-14 (modified) medium was made up from powder into a stock of 10X concentration with distilled and de-ionized water, filtered (0.2µm) in sterile conditions, aliquoted and stored at -20°C. Components of F14 plus horse serum (HS) and F14 defined media are described in Tables 2.1 and 2.2. Other reagents used in the cell preparation are shown in Table 2.3

2.2.2 RECORDING MEDIA AND DRUG APPLICATION

2.2.2.1 Extracellular recording media

Constituents of all media used are given in Table 2.4. The pH was adjusted to 7.4 with NaOH (2M) (or TRIS base (1M) for the sodium free medium). The volume was then made up (-1.0ml) with de-ionised distilled water and the osmolarity set to 315 mosmols with sucrose. The medium was filter-sterilised and 50.0mls aliquots were stored at -20°C.
On the day of use the extracellular medium was thawed and tetrodotoxin and barium chloride (the charge carrier) were added as in Table 2.4. The medium was kept on ice, a warmed (21°C) volume (900µl) was added to the coverslip of cells in the microscope chamber and was replaced every 30 minutes or following each drug application.

2.2.2.2 Extracellular drug application

Drugs described in Table 2.5 were dissolved in each new aliquot of extracellular medium on the day of use and were applied to the cells by gravity assisted perfusion from a wide bore drug pipette (tip diameter approximately 10μm) placed maximally 100μm from the cell. Low pressure ejection was only applied when microperfusion was not visible on the closed circuit television (CCTV) monitor, see figure 2.1. Extracellular saline was ejected onto cells as a control, the pressure ejector was set to 200mmHg with a pulse width of 0.5 seconds, these control conditions had a negligible effect on the peak current (-3.7 ± 5.3%, n=7).The control ejection value includes 3 cells where the extracellular saline was continuously ejected. Neither continuous ejection or pulses of drug application effected the calcium channel current recorded. When microperfusion was not visible drugs were applied with the pressure ejector set on continuous ejection (70mmHg). Drug application is denoted by a bar drawn on the current time graphs in chapter 3.

Nicardipine, Nifedipine and BayK 8644 are light sensitive compounds. Therefore all stock concentrations were made and the compounds applied in conditions of low level illumination from a sodium lamp.

Table 2.1 Showing components of F14 with Horse Serum (HS) culture medium

F14 + HS

Reagent	Source	Stock concentration	V(ml)/ W(mg)	Final concentration
F14	Imperial	10X stock	10.0ml	
Heat inactivated (HS)	Gibco		10.0ml	10.0%
Glutamine	Flow	200mM	1.0ml	2.0mM
Penicillin+Streptomycin	Flow	5000(IU)+ 5000(µg/ml)	1.0ml	50IU+ 50µg/ml
$NaHCO_3$	Sigma	Salt	120.0mg	14.3mM

V: Volume of stock required for 100ml of medium
W: Weight of salt required for 100ml of medium

All culture medium volumes are made up with de-ionized distilled water; filter-sterilised and refrigerated (kept no longer than 21 days).

Table 2.2 Showing components of Defined F14 medium

Defined Medium

Reagent	Source	Stock concentration	V/2(ml/µl) W/2(mg)	Final concentration
F14	Imperial	10X stock	5.0ml	
Glutamine	Flow	200mM	0.5ml	2.0mM
Penicillin+Streptomycin	Flow	5000(IU)+ 5000(µg/ml)	0.5ml	50IU+ 50µg/ml
$NaHCO_3$	Sigma	Salt	60.0mg	14.3mM
Insulin	Sigma	1mg/ml, in water	0.25ml	4.0µgs/ml
Transferrin	Sigma	25mg/ml,in water	10.0µl	5.0µgs/ml
Progesterone	Sigma	1mM, in ethanol	10.0µl	20.0nM
Putrescine	Sigma	0.504M, in water	10.0µl	0.1mM
Selenium	Sigma	150µM, in water	10.0µl	30.0nM

V/2: Volume of stock required for 50ml of medium
W/2: Weight of salt required for 50ml of medium

Table 2.3 Showing sources and concentrations of other reagents used in DRG cell culture

Reagent	Source	Stock concentration	Final concentration	Additional information
Poly-L-ornithine	Sigma	25mg/ml in sterile water	0.25mg/ml in sterile water	Stock 100µl aliquots stored at -20°C
Laminin	Sigma	0.1mg/ml in PBS	1.0µg/ml in PBS	Stock 10µl aliquots stored at -70°C
Collagenase	Sigma	1.25% in sterile water	0.125% in F14 + HS medium	Stock 120µl aliquots stored at -20°C
Trypsin	Sigma	2.5% in PBS	0.25% in PBS	Stock 120µl aliquots stored at -20°C
DNAase	Sigma	1600 kunits/ml in PBS	160 kunits/ml in F14+HS	Stock 120µl aliquots stored at -20°C
NGF	A.M.Davies (St.George's Hospital Medical Sch. London)	1µg/ml in F14	13.2ng/ml day 1 then day 2 6ng/ml in culture medium	Stock 500µl aliquots stored at -20°C.

Table 2.4 Showing constituents of the extracellular bathing mediums

		Solution A		Solution B	
Reagent	Stock concentration in water (M)	5V(mls)	Final concentration	5V(mls)	Final concentration
NaCl	2.0 M	35.0	140 mM	-	-
TEA Br	1.0 M	10.0	20 mM	80.0	160 mM
KCl	1.0 M	1.5	3 mM	1.5	3 mM
$MgCl_2$	0.5 M	1.0	1 mM	1.0	1 mM
$NaHCO_3$	0.25 M	2.0	1 mM	2.0	1 mM
HEPES	1.0 M	5.0	10 mM	5.0	10 mM
Glucose	1.0 M	2.0	4 mM	2.0	4mM
		V/2(µls)		V/2(µls)	
TTX	0.5 mM	100.0	1.0 µM	50.0	0.5 µM
$BaCl_2$	1.0 M	125.0	2.5 mM	125.0	2.5 mM

5V : Volume of stock required for 500 ml of medium
V/2 : Volume of stock required for 50 ml of medium
Salts were obtained from both BDH and Sigma

Table 2.5 Showing additions to the extracellular recording medium of drugs applied by low pressure ejection.

Drug	Final concentration	Source	Stock concentration	Additional information
(-)-Baclofen	10/25/50/100 200 µM	Boehringer Mannheim	10.0 mM	Stock in water Stored at -20°C
-CTX (GVIA)	1.0 µM	Sigma	500.0 µM	Stock in water. Aliquots of 10µl. Stored at -20°C.
Nicardipine	1.0 µM	Syntex Laboratories	10.0 mM	Stock in water. Stored at -20°C.
Nifedipine	1.0 µM	Sigma	10.0 mM	Stock in 70% ethanol Stored at -20°C.
BayK 8644	1.0 µM	Research Biochemicals Inc.	10.0 mM	Stock in 70% ethanol Stored at -20°C.

2.2.2.3 Intracellular recording media and drug application

The constituents of the two intracellular recording media used are shown in Table 2.6. The intracellular salines have been named from their major components of caesium acetate (CsAc) and caesium aspartate (CsAsp). The pH was set with CsOH to 7.2 and the osmolarity adjusted up to 310 mosmol with sucrose. The medium was then filter-sterilised, aliquoted and stored at -20°C. Adenosine trisphosphate (ATP) was added on ice to 20.0mls of cooled intracellular recording medium, filter-sterilised and then aliquoted out into 0.5ml fractions and stored at -20°C. One was used each experimental day. When required GTPγS was added to a fraction of the intracellular recording media to be used that day, see Table 2.6.

2.2.3 Replating medium

Cells were replated in their culture medium, which consisted of approximately 30% F14+HS and 70% defined medium. Macromolecules to be loaded into the cells were diluted into this medium (200µl) at various concentrations. If the cells were kept longer than 60-90 minutes the remainder (1300µl) of the original culture medium was replaced. The reagents and dilutions used in the replating media are shown in table 2.7. The protein weights of non-immune serum and the antisera were calculated using the Bicinchoninic acid protein assay reagent (Pierce) with a microtiter plate reader (Dynatech MR5000).

Table 2.6 Showing constituents used in CsAc and CsAsp patch pipette solutions, and the modifications used.

		CsAc		CsAsp	
Reagent	Stock concentration in water	2.5V (mls)	Final concentration	2.5V (mls)	Final concentration
CsAc	1.0M	35.0	140 mM	-	-
CsAsp	0.5M	-	-	70.0	140 mM
EGTA	1.0M	0.275	1.1 mM	0.275	1.1 mM
$MgCl_2$	0.5M	1.0	2.0 mM	1.0	2.0 mM
$CaCl_2$	0.1M	0.250	0.1 mM	0.250	0.1 mM
ATP	0.1M	*	2.0 mM	*	2.0 mM
HEPES	1.0M	2.5	10.0 mM	2.5	10.0 mM

* = ATP was added to each aliquot separately (see text).

2.5V : Volume required of stock for 250 mls of medium.

Drug	Final Concentration	Source	Stock Concentration	Additional Information
GTPyS	10 - 200 µM	Boehringer Mannheim	10.0 mM	Stock diluted in patch solution on day of experiment. Stock in water. Stored at -20°C

Table 2.7 Showing macromolecules dissolved in replating medium

Macromolecule	Final Concentration	Source	Stock Concentration	Additional Information
Non-specific Rabbit (IgG) Immunoglobulin	0.04-5.0 mg/ml of IgG powder + 1:25 -1:200 of stock	Sigma	Lyophilised powder + Stock solution at 1mg/ml	Stock in water Stored at -20°C
Non-specific rabbit serum (SER)	Dilutions of 1:100 - 1:25 (≡ 0.61 - 2.4 mg/ml)	Jackson immunochemical reagents	Undiluted	In 8.0µl aliquots Stored at -70°C
Anti-$G\alpha_o$ antiserum (OC1\OC2) (ON1 1:50)	Dilutions of 1:100 - 1:25 (≡ 0.61 - 2.4 mg/ml for OC2)	G.Milligan (University Glasgow)	Undiluted	Freeze dried serum reconstituted with water. 8.0µl aliquots Stored at -70°C
Anti-$G\alpha_i$ antiserum (SG1)	Dilutions of 1:50 - 1:25 (≡ 0.56 - 1.1 mg/ml)	G.Milligan	Undiluted	Freeze dried serum reconstituted with water. 8.0µl aliquots Stored at -70°C
Anti-$G\alpha_o$ antiserum	Dilutions of 1:50.	G.Milligan	Undiluted	Freeze dried serum reconstituted with water. 8.0µl aliquots Stored at -70°C.
G_o alpha subunit C-terminal 11mer peptide (P_o)	Dilutions of 1:25 (≡10.0 µg/ml)	N.Berrow (made here R.F.H.S.M)	$2mgml^{-1}$ stock	Amino acid sequence as used by G.Milligan for raising OC1 and OC2 plus extra cysteine Sequence = ANNLRGCGLYC Stored as 10µl aliquots at -70°C.

The changes in optical density from the reaction of the serum protein with the protein assay reagents were then compared to standard dilutions of bovine serum albumin (BSA).

2:3 ELECTROPHYSIOLOGICAL RECORDINGS

Whole cell voltage clamp recordings (Hamill et al, 1981), were made with an Axoclamp-2A switching amplifier. Coverslips were placed on the stage of an inverted Nikon microscope and the cells were viewed at 300x magnification with Hoffman modulation contrast optics.

2.3.1 Patch electrode preparation

Patch electrodes were made from borosilicate glass tubing (0.8-1.0mm bore diameter) on a Brown-Flaming micropipette puller (Sutter Instruments Co). Once filled with the appropriate patch solution, electrodes had a resistance of 2-5MΩ.

2.3.2 Basic protocol

The pipette was lowered into the extracellular bathing medium above the chosen cell. First the input offset was set to zero, and then hyperpolarising current pulses (100pA for 100ms at 1Hz) were initiated. The bridge circuit was balanced and provided a measure of the pipette resistance. In the direct current clamp (DCC) mode the capacitance of the pipette was neutralized with the amplifier set to pass 2nA steps (1Hz, 100ms duration) and the waveform was adjusted on the monitoring oscilloscope (see figure 2.1, the top oscilloscope was used to adjust the settling characteristics of the pipette).

The amplifier was then switched back to the bridge circuit and the pipette was lowered onto the centre of the cell body; as contact was made with the cell the apparent pipette resistance increased. A small amount of suction was applied by a syringe attached to the pipette holder by plastic tubing and this resulted in a large increase in the seal resistance between the pipette and the cell membrane.

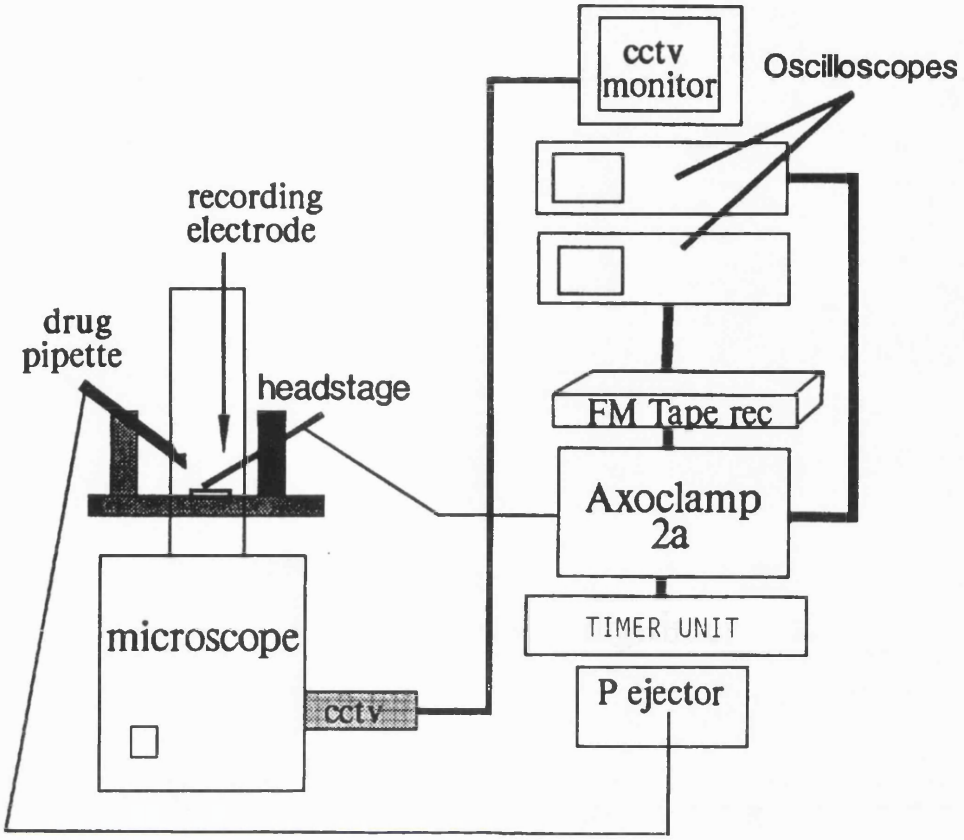

Figure 2.1 Showing the main components of the electrophysiological recording equipment

Usually a GigaOhm resistance seal developed within 60 seconds. At this point the amplifier was switched to discontinuous single electrode voltage clamp (dSEVC) mode in which the amplifier switches between sampling and current injection modes at a frequency that can be set (15-22kHz for replated DRGs). 30mV Hyperpolarising voltage steps (1Hz, 100ms duration) were then applied while the gain of the holding circuit was increased so that the voltage waveform became square and the waveform on the monitoring oscilloscope showed that sampling of the membrane voltage occurred at a point when the voltage transients had decayed sufficiently. Further increases in the gain were possible with the imposition of small amounts of phase lag.

In cells where membrane rupture had not occurred spontaneously or in which space clamp was not adequate by this stage, small amount of extra suction and transient increases in the phase lag were applied. Using these procedures the whole cell configuration of the patch clamp technique and optimum space clamp conditions were obtained.

2.3.3 Experimental protocol

In all the experiments, the holding potential of the cell was set at -80mV and all test steps were applied for 100ms duration. On achieving the whole cell configuration, the step potential which produced the maximum inward calcium channel current was found and this potential step was applied at 0.033Hz. Each test step was accompanied by three hyperpolarising steps of -30mV to determine the leak current. The peak amplitude of the current increased steadily to a plateau, normally within 240-300 seconds, in all of the cells.

Drug application or current voltage relationships were only carried out when the maximum current amplitude had been achieved and three consecutive currents of equal size and kinetics had been recorded.
The trigger pulse was initiated by a timer unit which then activated the amplifier and marked the FM tape. Pre-pulse stimulation prior to the test steps were gated by the timer unit and the battery driven prepulse generator fed directly into the amplifier (this circuit is not included in figure 2.1). Both the timer unit and the prepulse generator were made in house (Medical engineering, St.George's Hospital Medical School).

Current voltage relationships were recorded by giving a series of -20mV hyperpolarising steps (10 at 1Hz) and then applying a test potential every 10 seconds. Once the test steps were complete the same number of hyperpolarising steps were again applied.

2.3.4 Cell capacitance

Cell capacitance cannot be directly measured with the Axoclamp-2A amplifier so after each recording, where possible, the amplifier was switched to DCC mode and the cell was depolarised to a steady potential of +50mV. Stable records were not possible at more hyperpolarised potentials.

Current steps of 50pA were then injected (0.2Hz, 100ms). This method was taken from the thesis of Dr H.A.Pearson, University of London.
The passive resistive and capacitative characteristics of the cell membrane cause the voltage of the cell membrane to change in an exponential manner to square-wave current injection. The relationship between voltage change over time is given by;

$$V(t) = Vmax\ (1-e^{-t/\tau})$$

where V(t) is the voltage change over time t, Vmax is the maximum potential change reached and τ is the time constant for charging the cell membrane.

The time constant, τ, is related to the capacitance (C) and the resistance (R) of the cell by;

$$\tau = RC$$

R was calculated by dividing Vmax with the amplitude of the current pulse, and having fitted an single exponential curve to the voltage change to give τ, C can be obtained. The test step was approximately 10 times longer than one time constant so the membrane charging was more than 99.95% complete when values of the change in voltage were measured. The baseline values, amplitude of current step (B - A) and voltage response (D - C) were calculated from an average of 50 points within a sampling area. These areas are shown by the boxes drawn on figure 2.2.

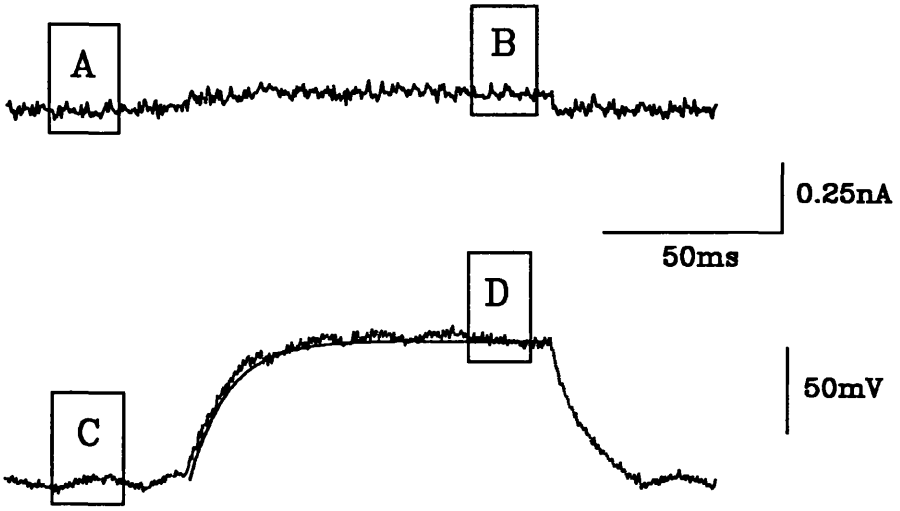

Figure 2.2 Shows the method of calculating the capacitance of a cell

The estimated capacitance was also calculated from the cell diameter. Assuming the cell approximated to a sphere, the surface area was then calculated. Neuronal membranes have a capacitance of 10^{-14} F/μm^2, therefore the estimated capacitance value is the surface area (μm^2) multiplied by 10^{-14}. The mean calculated capacitance was 17.7 ± 2.2 pF and this was similar to the estimated value of 18.0 ± 0.9pF, n=15. The current density has therefore been calculated throughout by dividing the peak current by the estimated surface area (pA/μm^2).

2.3.5 Data acquisition

All the current and voltage traces were recorded directly onto magnetic tape (19.05cm/s) with a Racal Store 4D FM recorder. Each procedure was accompanied by a simultaneous voice recording. The tape recording was calibrated by a calibration step from by the amplifier (10mV, 1nA).

2.4 DATA ANALYSIS

All recordings were captured on computer using the Voltage Clamp Analysis program (VCAN) written and supplied by Dr J. Dempster, Strathclyde University. The analogue signals on the tape were sampled (2.6 kHz) from the A-D converter (CED 1401). Each set of leak and test steps were grouped and then leak subtracted. The leak subtracted data were then analysed using the VCAN software. The time to peak was measured manually whilst the peak and sustained current values were averages of 4 and 20 points respectively. These files were saved and later sorted on a spreadsheet (Quattro).

Specific current records were saved to files for collation and analysed using Sigmaplot (Jandel Scientific). All the current records and figures shown in chapters 3 and 4 were taken from leak subtracted records. The effect of drug applications were calculated as a percentage by the equation:-

$$\text{Effect (\%)} = ((A - B) / A) \times 100$$

where A is the control current and B the current value during drug application, see figure 2.3. In chapter 3 the effect of drug application was also measured isochronally, the time point was set for the peak value of the control current before drug application, this is shown by the vertical line in figure 2.3. In figure 2.3 the peak current value of the current inhibited by the drug (B) is similar to the isochronal measurement.

The peak and sustained current values have been labelled **Ip** and **Is** respectively, throughout chapter 3 and 4.

The peak current values have been plotted against time to illustrate the effect of drug application. Leak subtracted current traces corresponding to time points on the peak current/time graph are also shown as a further illustration of the effect of drug application. The mean ± standard error of the mean (S.E.M.) effect of drug application are represented as bar charts.

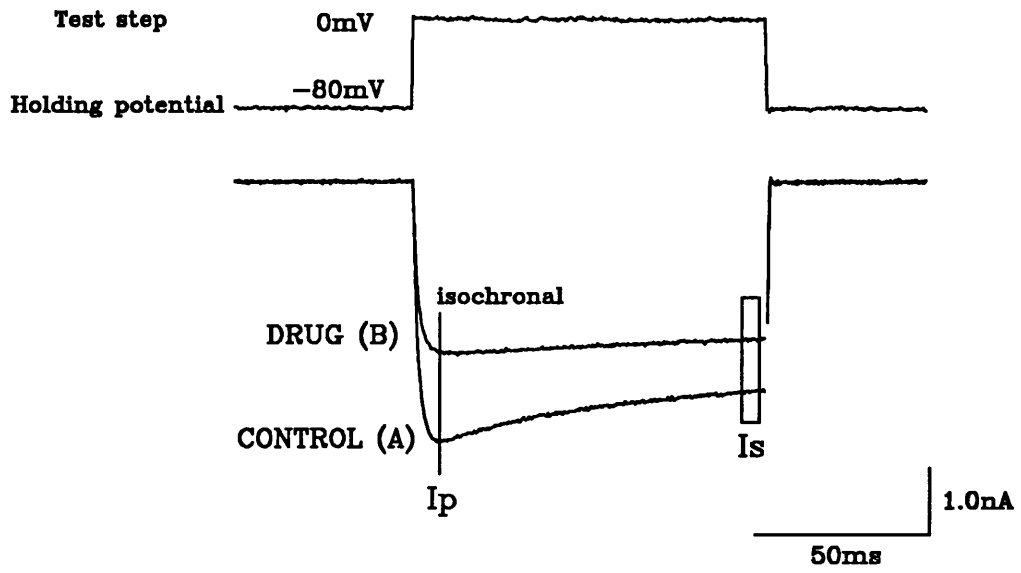

Figure 2.3 Shows the specific points recorded of the current traces evoked by a voltage step.

Current activation (and voltage activation in figure 2.2) was fitted with a single exponential equation:-

$$y(t) = ss + A \times \exp(-t/\tau_1)$$

When the rate of current activation was sufficiently slowed a double exponential curve could be fitted:-

$$y(t) = ss + (A \times \exp(-t/\tau_1) + (B \times \exp(-t/\tau_2))$$

where **ss** is the steady state in both equation, **A** and **B** in the double exponential equation are the proportional amounts of the two components of current with the time constants τ_1 and τ_2 respectively. The proportion of the slow current component in the double exponential curve fit is given by B/A+B. At time infinity, the steady state is the sum of A and B.

Statistical tests applied will be described at the point of use. Statistical significance $p<0.05$ is represented as a single asterisk (*) and data which is statistically significant at $p<0.01$, as two (**).

2:5 IMMUNOCYTOCHEMICAL TECHNIQUES

2.5.1 Immunocytochemistry media

This technique I have developed from the protocols of Dr M.S.Fazeli and Dr T.Cowen (personal communication). The following solutions were required:-

1) Tris Buffered Saline (TBS) = Tris salt (20mM), NaCl (0.9%) and Sodium Azide (0.1%). pH set at 7.3.

2) Paraformaldehyde (4%) made up in TBS.

3) Triton X100 (0.2%) made up in TBS.

4) Serum Wash A = Goat serum (20%), BSA (4%) and (DL)-Lysine (0.1%) made up with TBS.

   Serum Wash B = Donkey serum (5%), Sheep serum (5%), BSA (4%) and (DL)-Lysine (0.1%) made up with TBS. (Serum wash B was only used with the monoclonal antibody.)

5) Diluent = Serum wash A or B (50%) plus (DL)-Lysine (0.05%) made up with TBS.

All the compounds listed were purchased from Sigma except for the donkey and sheep sera which were purchased from Jackson immunochemical reagents.
Each solution was filter-sterilized and stored at 0-4^{o}C for a maximum of 21 days..

2.5.2 Antibodies

All antibodies used were incubated on the cells in the diluent. All the primary staining and secondary antibodies are described on Table 2.8.

2.5.3 Immunocytochemistry procedure

Coverslips of cells are removed from the culture dishes and placed on raised platforms in a humidified box. All volumes used were 200µl. Steps 5 and 6 of this procedure were not required in the antibody loading experiments (see chapter 4)

(1) Wash 3 X 5 minutes with TBS.
(2) Fix with Paraformaldehyde, for 30 minutes at room temp.
(3) Wash 3 X 5 minutes TBS ± 0.2% Triton X100.
(4) Wash 3 X 5 minutes Serum wash.
(5) Incubate with the antibody(s), overnight at 4°C.
(6) Wash 4 X 5 minutes Serum wash.
(7) Incubate with secondary antibody(s), 120 minutes, at 4°C.
(8) Wash 5 X 5 minutes with TBS.
(9) Mount coverslips on glass slide with citifluor (PBS and glycerol).
(10) View - see section 2.6.

2:6 CONFOCAL MICROSCOPY

All immunocytochemistry results were viewed with both conventional fluorescence and confocal microscopy. The advantage of confocal microscopy is that the fluorescent image is strictly limited to what is in focus at a set depth in the specimen. Confocal microscopy thereby provides a highly selective system for imaging and data acquisition.

2.6.1 Equipment

The MRC-600 series laser scanning confocal imaging system (Bio Rad) was used with a Krypton/Argon multi line laser (15mwatt) and an Olympus upright microscope. All computer software was provided by Bio Rad. The image was first viewed by conventional fluorescence microscopy to select the area of analysis. Laser illumination of the specimen was passed through a filter specific for the fluorochrome fluoroscein isothiocyanate (FITC) at 494-520nm, the second channel was left clear for phase contrast imaging.

2.6.2 Data acquisition

All confocal images taken were sections across the specimen in the X and Y plane at set intervals of height through the whole depth (Z plane) of the specimen. Each complete XY plane scan (frame, 768 x 512 pixels) for each Z level was taken seven times and then the sum was divided by seven to give the mean image. After fluorescent images were completed, a phase contrast image was taken. The scan system was at 1 Frame/sec and the image was digitised and stored on an optical disc cartridge.

2.6.3 Data analysis

The data were displayed as single XY frames at specific Z levels or as a sum of all the frames in a single projection. All of the rabbit antibodies were stained with goat anti-rabbit conjugated to FITC. Fluorochrome excitation was recorded with a photomultiplier and these images are displayed in red. As the intensity of the immunoreactivity increases the image becomes brighter (red to yellow). The immunofluorescence of the secondary antibody, sheep anti-mouse conjugated to FITC, I have shown in green.
The gain of the photomultiplier, recording the fluorescent image, was set just below the level required to image non-immune serum. Therefore all immunoreactivity shown for the antisera raised against specific peptides represents specific immunoreactivity. The confocal microscope images shown in chapter 4 and 5 have been taken directly from the video monitor of the computer with a Nikon FX-800 camera and Kodak 200 ASA colour film.

Table 2.8 Showing antibodies used for immunocytochemistry

Antibody	Final Concentration	Source Stock	Additional Concentration	Information
Non-specific rabbit serum (SER)	Dilutions of 1:1000 - 1:2000 (≡ 61 - 30 µg/ml)	Jackson immunochemical reagents	Undiluted	In 8.0µl aliquots Stored at -70°C
Anti-$G\alpha_o$ antiserum (OC1/OC2)	Dilutions of 1:1000 - 1:2000 (≡ 61 - 30 µg/ml)	G.Milligan	Undiluted	Freeze dried serum reconstituted with water. 8.0µl aliquots Stored at -70°C
Anti-$G\alpha_i$ antiserum (SG1)	Dilutions of 1:500 - 1:2000 (≡ 56 - 14 µg/ml)	G.Milligan	Undiluted	As above.
Anti-$G\alpha_o$ antiserum	Dilution of 1:2000.	G.Milligan	Undiluted	As above.
Anti-$G\alpha_s$ antiserum	Dilution of 1:2000.	G.Milligan	Undiluted	As above.
Anti-Neurofilament 68 (monoclonal)	Dilution of 1:2000.	Sigma	Undiluted	Aliquots of 10µl.. Stored at -20°C.
Goat anti Rabbit IGG conjugated with FITC	Dilution of 1:40	Sigma	Undiluted	Aliquots of 25.0µl Stored at -20°C
Sheep anti Mouse IGG conjugated with FITC	Dilution of 1:40	Jackson immunochemical reagents	Undiluted	Aliquots of 20µl Stored at -20°C

CHAPTER THREE
RESULTS I

3.1 High voltage activated calcium channel currents in acutely replated DRGs: their pharmacology and modulation by G-protein activation.

3.1.1 INTRODUCTION

Neurotransmitter modulation of calcium channel currents in DRGs has been known since the work of Dunlap and Fishbach (1978). DRGs have been a common model to study the phenomena of calcium channel modulation because they can be readily dissected and easily cultured. Also the original work of calcium channel characterisation at the biophysical and pharmacological level was investigated in cultured DRG neurones. The focus of my thesis was directed towards the involvement of G proteins in calcium channel modulation and therefore my characterisation of the calcium channel current in acutely replated DRGs was mainly an extension of the wealth of data already available for DRGs.

3.2 RESULTS

3.2.1 Acutely replated DRG's

Immediately after enzymatic and mechanical dissociation, DRGs adhere to the polyornithine/laminin coated coverslips and after six hours plating they begin to put out extensive neurites. Figure 3.1 shows a DRG after twelve hours in culture. Electrophysiological recording of calcium channel currents (I_{Ba}) from unreplated cells in the first week of culture is complicated because of the early growth of extensive neurites that makes good space clamp extremely difficult (>90% of cells could not be adequately clamped). Acutely replating DRGs within the first week of culture provides a cell body with little or no neurites, see figure 3.2.

Replated DRGs recorded within 90 minutes of the replating procedure have ideal space clamp. After that time neurite outgrowth starts to impair the space clamp in these cells. All replated cells were therefore recorded from within 90 minutes of the replating preparation, these cells are termed acutely replated DRGs.

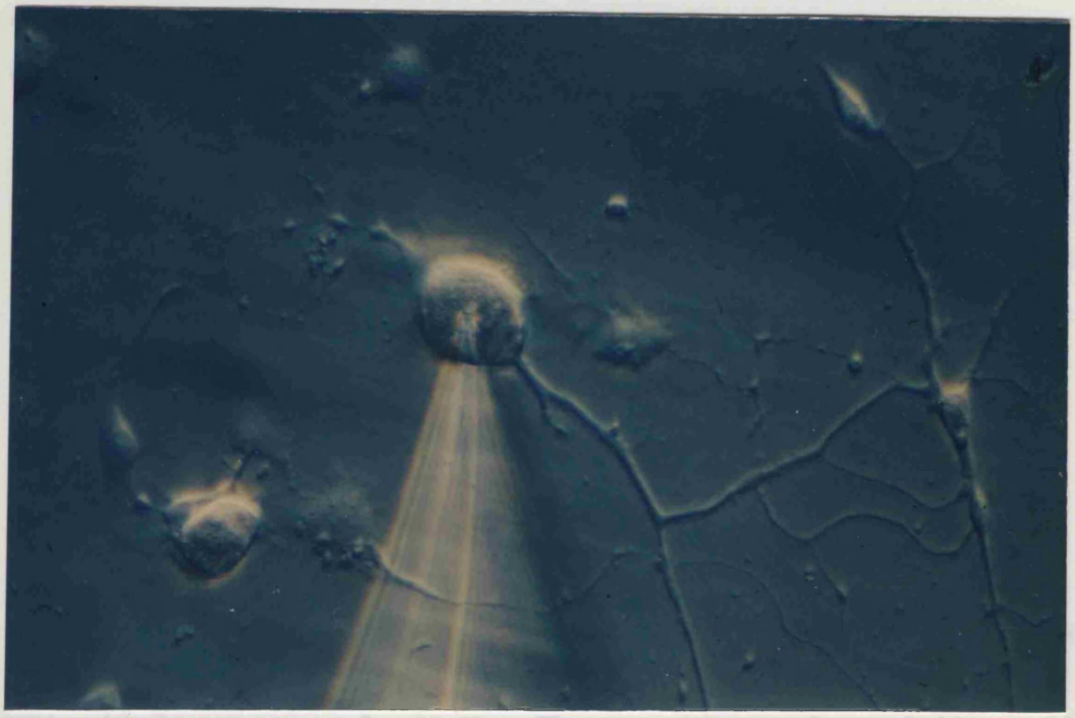

Figure 3.1 Picture of an unreplated DRG viewed by Hoffman modulation contrast optics.
Shows an unreplated DRG with neurites and a patch pipette above it. The cell diameter is 40μm.

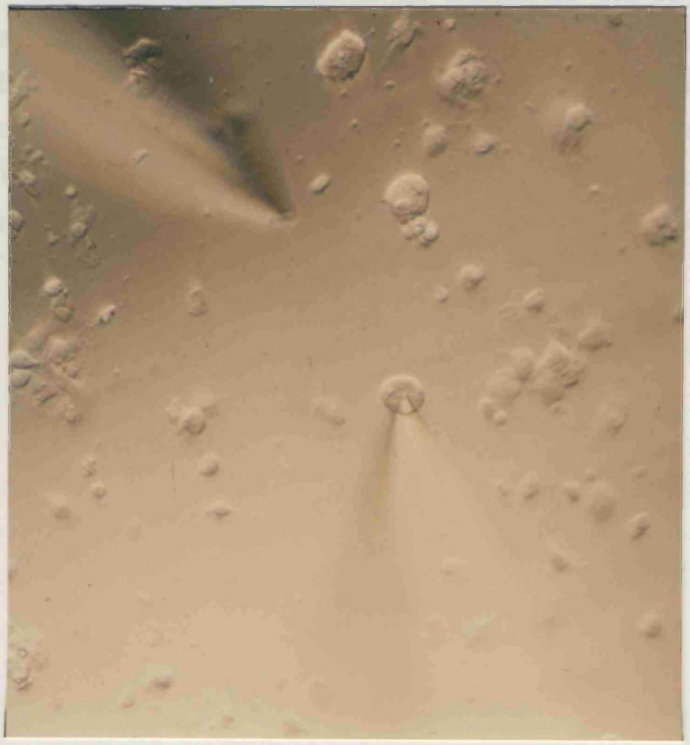

Figure 3.2 Picture of acutely replated DRGs viewed by Hoffman modulation contrast optics.
Shows acutely replated DRGs after one hour in the incubator, a patch pipette is above a 25μm diameter cell, the drug pipette, above, is 100μm from the cell.

3.2.2 High voltage activated calcium channel currents.

The characteristics and modulation by G-protein activation of high and low voltage activated calcium channel currents (I_{Ba}) have been well characterised for unreplated DRGs (Dolphin and Scott, 1987).

HVA calcium channel currents that predominate in DRGs are easy to record. I have therefore focused specifically on the HVA calcium channel current. HVA calcium channel currents were activated by step depolarisations to around 0mV from a holding potential of -80mV. Figure 3.3 A shows a current voltage relationship for an acutely replated DRG. In this particular example a LVA calcium channel current activated at -60mV and the HVA calcium channel current at -20mV and peaked at -5mV. Step depolarisations to more positive potentials decreases the activated current until it reverses in this example at +30mV. The average null potential was around +45mV. The negative value of the null potential compared to the calculated reversal potential for barium conduction through calcium channels is thought to result from an outward movement of caesium through the calcium channels (Scott *et al*, 1991).

The current traces of HVA current activation from steps -20 to -5mV are shown in figure 3.3 B. The maximum current (1.45 ± 0.19nA, mean ± S.E.M., n=17 for the caesium acetate (CsAc) intracellular saline showed 28.4 ± 1.5% inactivation during the test step.

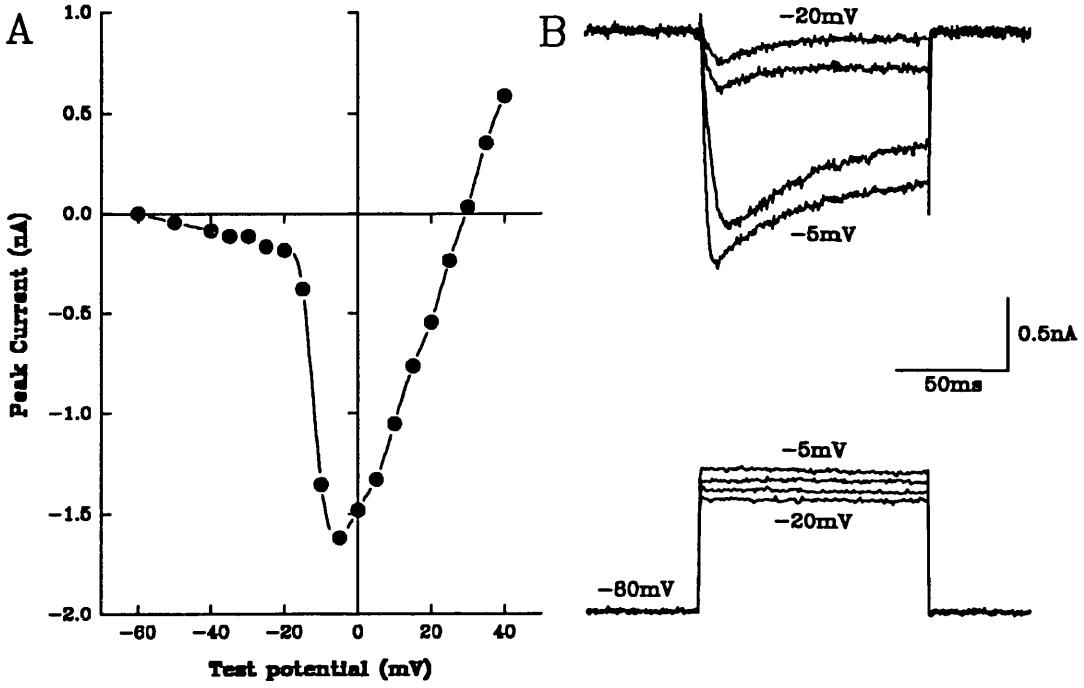

Figure 3.3 The HVA calcium channel current in an acutely replated DRG.
A, the current voltage relationship for a cell held at -80mV. Test steps were applied for 100ms.
B, shows current traces during step potentials that mostly activate the current with the corresponding voltage traces shown below.

3.2.3 The action of 1,4-dihydropyridines on the HVA calcium channel current.

3.2.3.1 The effect of nicardipine application on the HVA calcium channel currents in acutely replated DRGs.

The effect of the 1,4-dihydropyridine (DHP) antagonist, nicardipine, application over time is shown in figure 3.4A. The peak calcium channel current (I_{Ba}) is plotted against time and illustrates the small and reversible action of nicardipine. This nicardipine action on the current records are shown in figure 3.4B. No change in current kinetics was seen following nicardipine application.

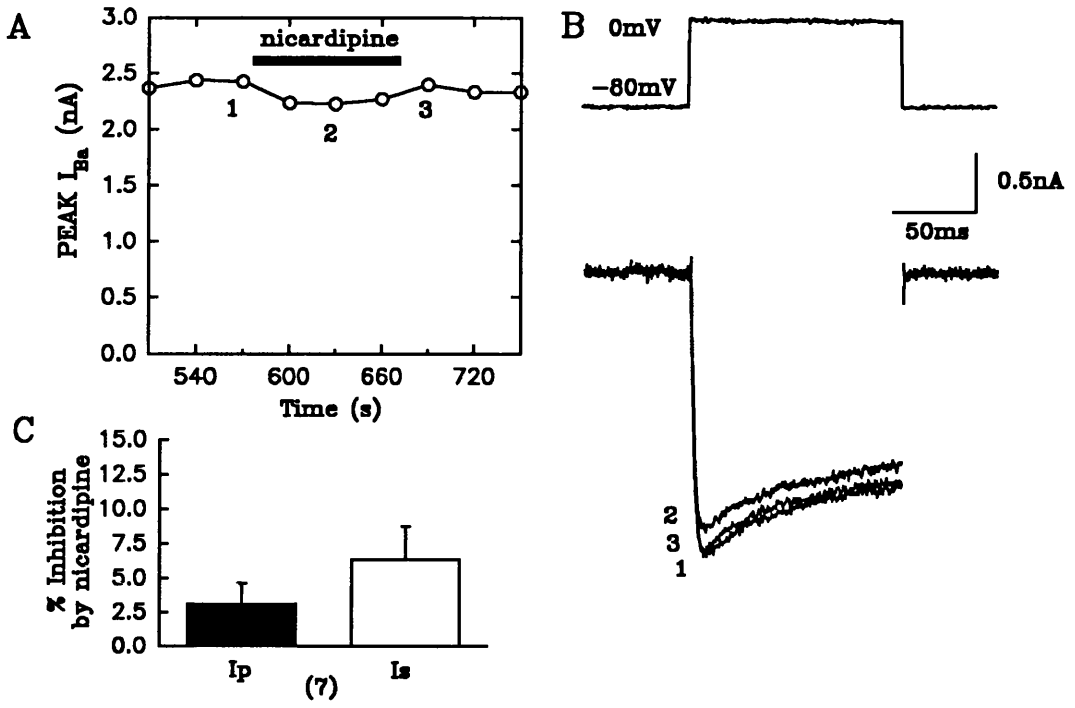

Figure 3.4 The action of nicardipine on the HVA calcium channel current.
A, a graph of the peak I_{Ba} versus time illustrating the action of nicardipine (1μM). Drug application is denoted by the filled bar.
B, shows the maximum nicardipine action on the current records. The numbered traces correspond to the points in graph A.
C, shows the maximum action of nicardipine on the peak (Ip) and sustained (Is) current components of the HVA I_{Ba}.

The mean value of the maximum action of nicardipine on the peak and sustained components of current are shown in figure 3.4C. The peak current was inhibited by 3.1 ± 1.6% and the sustained current by 6.3 ± 2.4%, n=7.

3.2.3.2 The effect of nifedipine application on the HVA calcium channel current in acutely replated DRGs.

The DHP antagonist nifedipine (1μM) was as ineffective as nicardipine. In a total of three cells the application of nifedipine on the peak HVA I_{Ba} was without effect (1.1 ± 4.8%) whilst the sustained component of the current was inhibited 4.4 ± 2.6%.

3.2.3.3 The effect of (±)-BayK 8644 application on the HVA calcium channel current in acutely replated DRGs.

The effect of the DHP agonist (±)-BayK 8644, of which the (-) isomer is active and the (+) isomer is a poor agonist, on acutely replated DRGs can be divided into two groups. In one group of cells the peak current was stimulated 25.94 ± 6.21% and the sustained current component by 26.39 ± 8.4% (n=3).

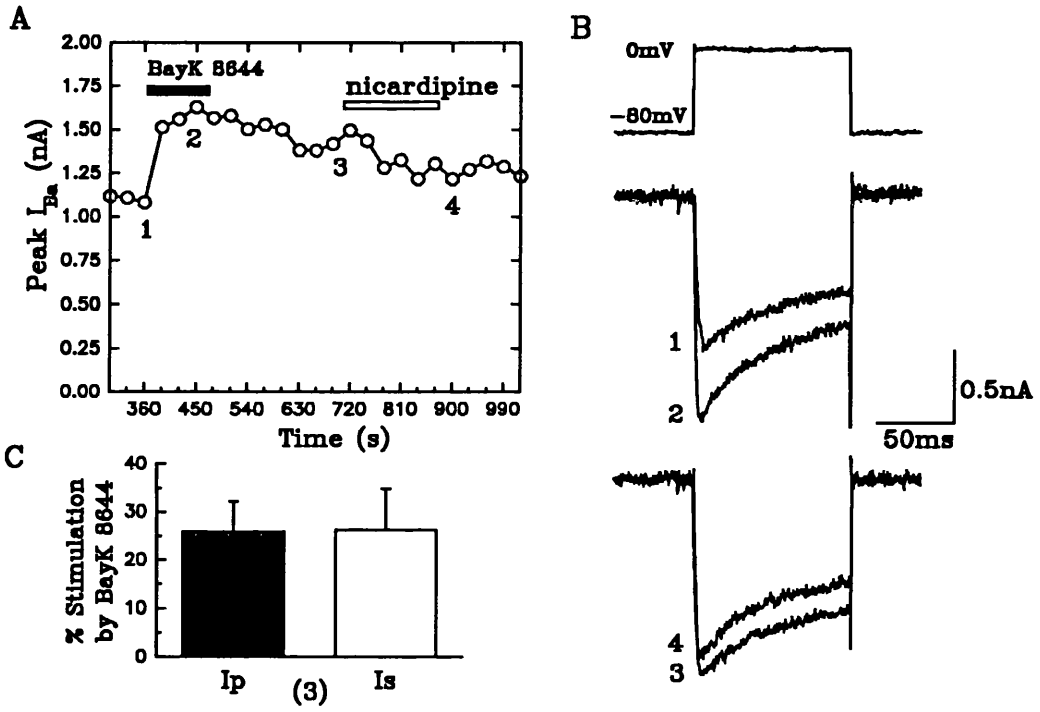

Figure 3.5 Shows the stimulating action of (±)-BayK 8644 on the HVA calcium channel current in acutely replated DRGs.
A, shows a graph of the peak I_{Ba} versus time. (±)-BayK 8644 (1μM) application is denoted by the filled bar. The stimulated current in this example is reduced by application of nicardipine (10μM) and this is denoted by the open bar.
B, shows the current traces of the numbered points in graph A. The control current (1) is stimulated by BayK 8644 application (2). The partially recovered current (3) is inhibited by nicardipine (4).
C, shows the mean effect of (±)-BayK 8644 on the three cells that were stimulated. The number of cells are shown in parenthesis.

In the other group of acutely replated DRGs the peak current was inhibited by 16.75 ± 2.2% and the sustained current

component by 20.46 ± 4.2% (n=4) with (±)-BayK 8644. In the latter group of cells, (±)-BayK 8644 appeared to have a biphasic action, a small stimulation (1.82 ± 0.63%) which was then followed by the inhibition of the calcium channel current. The stimulatory and inhibitory action of (±)-BayK 8644 are illustrated in figures 3.5 and 3.6 respectively.

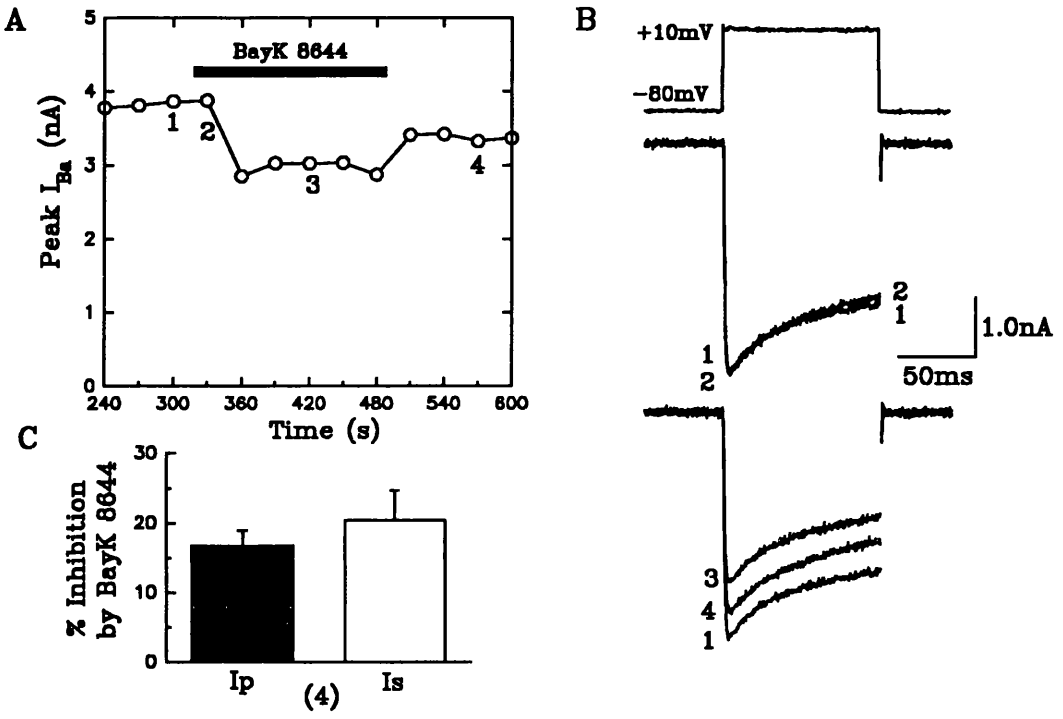

Figure 3.6 Shows the inhibitory action of (±)-BayK 8644 on the HVA calcium channel current in acutely replated DRGs.
A, shows a graph of peak I_{Ba} versus time. (±)-BayK 8644 (1μM) application is denoted by the filled bar.
B, shows the current traces of the numbered points in graph A. The control current (1) is slightly stimulated after 30 seconds application of (±)-BayK 8644 (2). The control current (1) is shown again below with the maximum inhibition by (±)-BayK 8644 (3) and the recovery (4).
C, shows the mean effect of (±)-BayK 8644 in the inhibited group of cells. The number of cells are shown in parenthesis.

The mean effect of (±)-BayK 8644 action in both groups (n=7) was that the peak I_{Ba} was stimulated +1.55 ± 9.01% whilst the sustained component has a mean inhibition of -0.38 ± 10.23%.

3.2.4 The action of ω-Conotoxin-GVIA on the HVA calcium channel current.

The pronounced and irreversible effect of ω-CTx-GVIA (1μM) on the peak I_{Ba} over time is shown in figure 3.7A. The maximum inhibition by ω-CTx-GVIA in this example occurred after 180 seconds. The current traces of the control and the maximum inhibition by ω-CTx-GVIA are both shown in figure 3.7B.

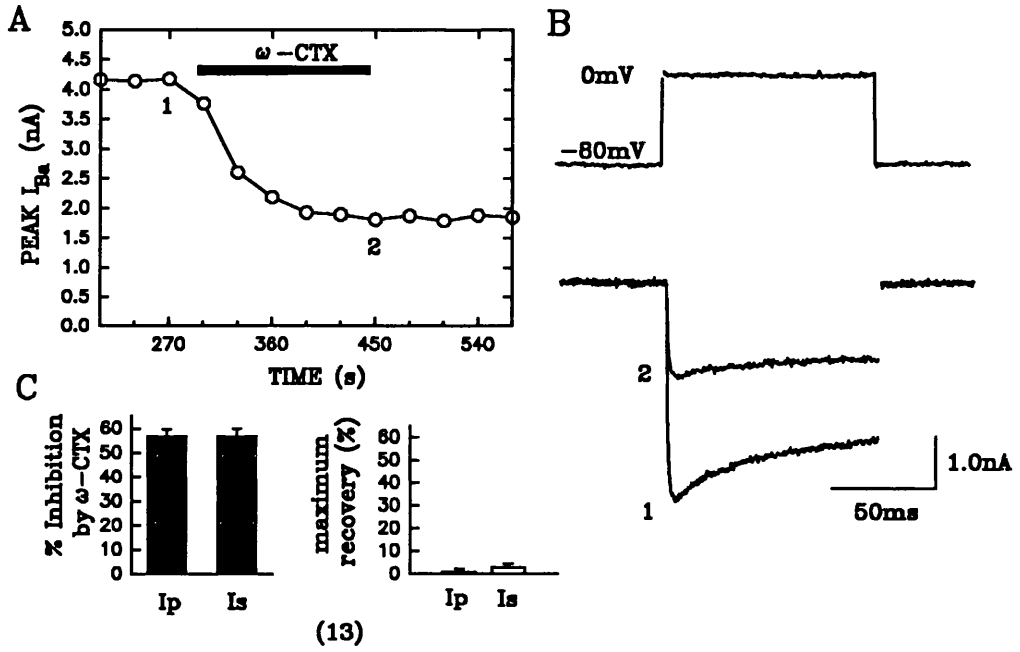

Figure 3.7 The action of ω-Conotoxin-GVIA on the HVA calcium channel current.

A, a graph of the peak I_{Ba} versus time, illustrating the action of ω-CTx-GVIA (1μM), application is denoted by the filled bar.

B, shows the current traces of the control and the maximum inhibition by ω-CTx-GVIA, both current traces correspond to the numbered points in the graph.

C, shows the mean value of the maximum action of ω-CTx-GVIA and the maximum recovery for the peak and sustained HVA I_{Ba}. The number of cells are shown in parenthesis.

The peak and sustained currents were similarly inhibited by ω-CTx-GVIA (1μM) by 56.85 ± 2.73% and 56.18 ± 2.91% respectively, (n=13). The effect of ω-CTx-GVIA was irreversible. The maximum recovery seen for the peak and sustained current was 0.8 ± 1.5% and 2.8 ± 1.7% respectively. These results are shown in figure 3.7C.

ω-CTx-GVIA and the DHP antagonists nicardipine and nifedipine were the only calcium channel antagonists used on the acutely replated DRGs. There was negligible effect of DHP antagonists in acutely replated DRGs and approximately 40% of the calcium channel current was insensitive to ω-CTx-GVIA. This finding is in agreement with Mintz et al. (1992a) who have shown that 41% of the calcium channel current remains in acutely dissociated DRGs following DHP antagonist and ω-CTx-GVIA application.
The remaining ω-CTx-GVIA and DHP antagonist insensitive current was shown to be inhibited 23% by the P-type calcium channel antagonist ω-Aga-IVA. The final 18% of the HVA calcium channel current was insensitive to all three calcium channel antagonists. The remaining calcium channel current in acutely replated DRGs may well represent the P and other types of yet unidentified calcium channels.

3.2.5 The dose response relationship of (-)-baclofen application on the peak HVA calcium channel current.

The maximum percentage inhibition of the peak calcium channel current ± standard deviation over a range of baclofen concentrations are shown in figure 3.8. The dose response curve was fitted assuming the Hill coefficient was equal to one. The maximum response was calculated as 41% and the EC_{50} was 14μM for (-)-baclofen.

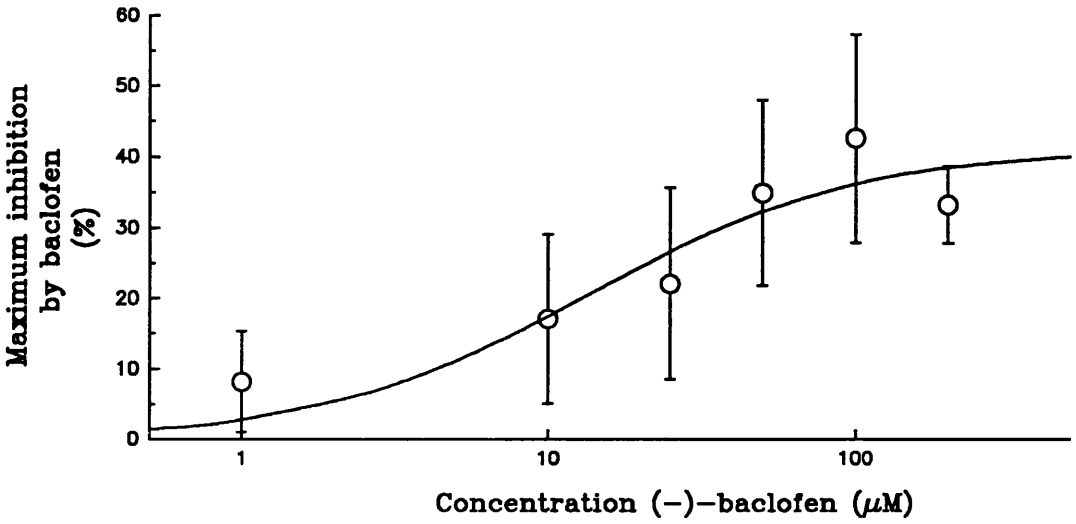

Figure 3.8 The dose response of (-)-baclofen application on the peak HVA calcium channel current.
Shows the maximum percentage inhibition of the peak calcium channel current ± standard deviation over a range of baclofen concentrations. The Hill equation was fitted to the points, assuming the Hill coefficient was equal to one. The computer fit is shown by the line through the points.

The dose response curve was plotted with the standard deviation as opposed to the standard error of the mean so as to remove the bias because of the different number of recorded current inhibitions at each concentration. The values of maximum inhibition of the peak I_{Ba} over a range of concentrations are shown in the table 3.1.

Table 3.1 Shows the mean inhibition of the peak HVA calcium channel current over a range of baclofen concentrations.

Concentration (μM)	mean % inhibition	standard deviation	number
1	8.16	7.18	4
10	17.08	12.0	4
25	22.06	13.57	7
50	34.89	13.01	20
100	42.59	14.71	8
200	33.22	5.39	3

3.2.6 The action of (-)-baclofen on the HVA calcium channel current.

The reversible inhibition of the peak HVA I_{Ba} by baclofen (50μM) over time is shown in figure 3.9A. The current traces showing the control and maximally inhibited current by baclofen are shown in figure 3.9B. The mean percentage inhibition by baclofen of the peak current was 30.67 ± 5.41% and this was similar to the inhibition calculated isochronally for each cell of 33.92 ± 5.95%, n=7. The sustained current component was inhibited by baclofen application, 22.35 ± 4.90%. An example of the time point for the isochronal measurement is shown in figure 3.9B. The isochronal value was calculated because baclofen in addition to inhibiting the current amplitude also slowed the rate of current activation. If the time to peak increases then the amount of inhibition by baclofen in the initial portion of the current will be greater than the peak current value calculated within the test step. In this group of seven cells, the time taken to attain the peak current increased from 7.91 ± 0.57ms to 36.55 ± 13.76ms with baclofen application. The rate of current activation was dramatically slowed, that is the time to peak was greater than 50ms, in three of the seven cells. The non-significant increase in time to peak in this study, of 28ms, meant that the isochronal measurement for percentage inhibition was 3.25% greater than the peak current measurement.

The number of current traces that had dramatically slowed activation rates with baclofen application (3/7) was greater than kinetic changes that occurred in a later control (serum-second study) group (7/20), see table 4.1. Even with a greater proportion of current traces with slowed activation rates the isochronal measurement in this study group is negligibly larger than the peak current

measurement. The reason for the similarity of percentage inhibition and the isochronal measurement is illustrated on figure 3.9B. The current recorded during baclofen application (2) has an initial, rapidly activating phase that occurs within the isochronal point (marked by the vertical line). It is then followed by a slowly activating phase in which the current amplitude increases partially to a peak current value after 20ms from the beginning of the test step.
All later values showing baclofen inhibition are of the peak and not the isochronal current measurement because there was little difference in the calculated values of inhibition. The time to peak are given in later experiments to provide an indication of the change in the rate of current activation with baclofen application.

To test if the inhibition by baclofen was voltage dependent a 10ms prepulse to +90mV was given to the cell 20ms before the test step, this is shown in figure 3.9B. The percentage relief of baclofen inhibition by a prepulse varied considerably between cells, the range of relief was from 6.9 to 92.3% in this study. The prepulse uncouples G protein modulation of the calcium channels and the subsequent amount of current that can be recruited by the test step increases. The mean percentage relief of baclofen inhibition by a +90mV prepulse was 33.93 ± 11.68% and 33.11 ± 5.96% for the peak and isochronal calculations respectively. The similarity between the prepulse effect on the peak and isochronal measurements indicates that the majority of the effect of the prepulse occurs in the initial portion of the test step and that the peak current measurement can adequately record this effect regardless of the change in kinetics of current activation in these cells. Both the peak and isochronal values of the percentage relief of baclofen inhibition by a prepulse were significantly greater than that seen for the sustained current component ($p<0.01$), this is shown in figure 3.9 C.

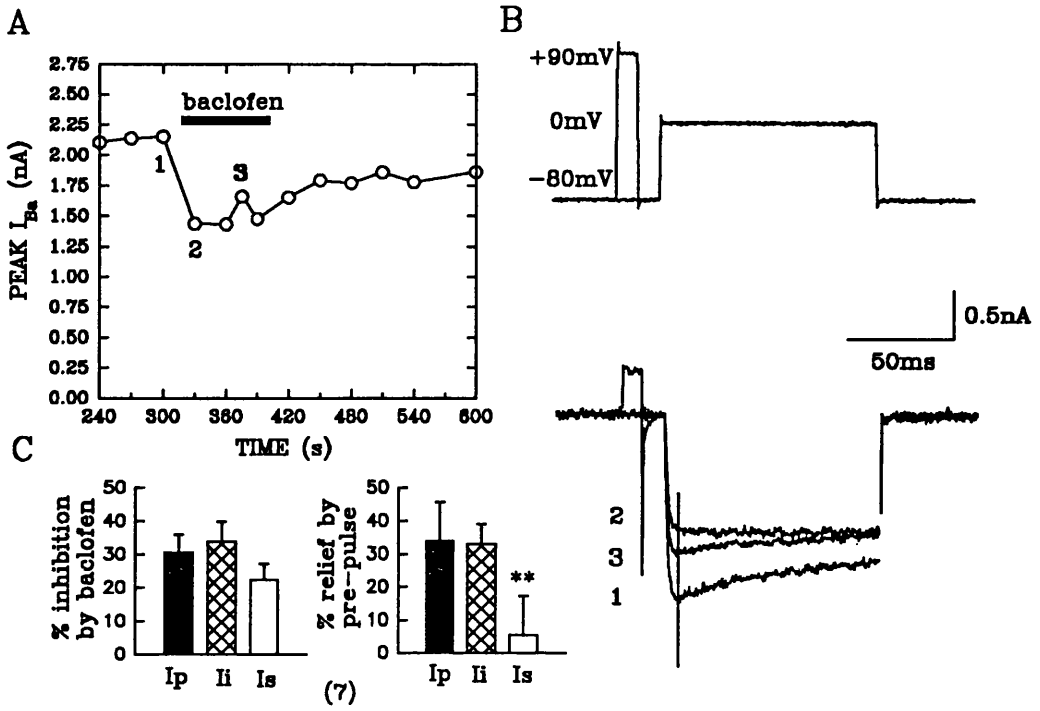

Figure 3.9 Shows the action of (-)-baclofen on the HVA calcium channel current.
A, shows a graph of peak I_{Ba} versus time illustrating the reversible inhibition by baclofen (50μM). Drug application is denoted by the filled bar. The effect of a prepulse to +90mV for 10ms given to the cell 20ms before the test step is labelled 3.
B, shows the current traces of the control (1) and the maximum inhibition by baclofen (2). Application of a prepulse increases the current amplitude and the rate of current activation (3).
C, shows the mean percentage inhibition by baclofen and the percentage relief of baclofen inhibition by the prepulse for the peak, isochronal (Ii) and the sustained current. The statistical significance ($p<0.01$) is represented by two asterisks. The number of cells are in parenthesis.

The time to peak for the test step following the prepulse was 8.52 ± 0.75ms which is similar to the time to peak before baclofen application (cf. 7.91 ± 0.57ms).

3.2.7 The action of GTPγS on the HVA calcium channel current.

In order to bypass $GABA_B$ receptor stimulation by baclofen and subsequent G protein activation, GTPγS was included in the patch pipette. The infusion of GTPγS into the cell activates G proteins as GTPγS binds to the Gα subunit during the basal exchange of GDP for GTP.

The effect of intracellular infusion of GTPγS (10μM) on peak I_{Ba} over time is shown in figure 3.10A. The current increases steadily for the first 210 seconds from rupturing the membrane and attaining the whole cell configuration of the patch clamp technique. This may represent both the intracellular infusion of caesium blocking outward potassium channels and the phosphorylation of calcium channels over time. There is 2mM ATP in the patch pipette.
After 210 seconds the current steadily decreases in amplitude. The rate of current decrease is increased by application of baclofen (50μM) and then a plateau is reached. Further application of baclofen has little effect. Increasing the concentration of GTPγS in the patch pipette increases the rate of GTPγS action.

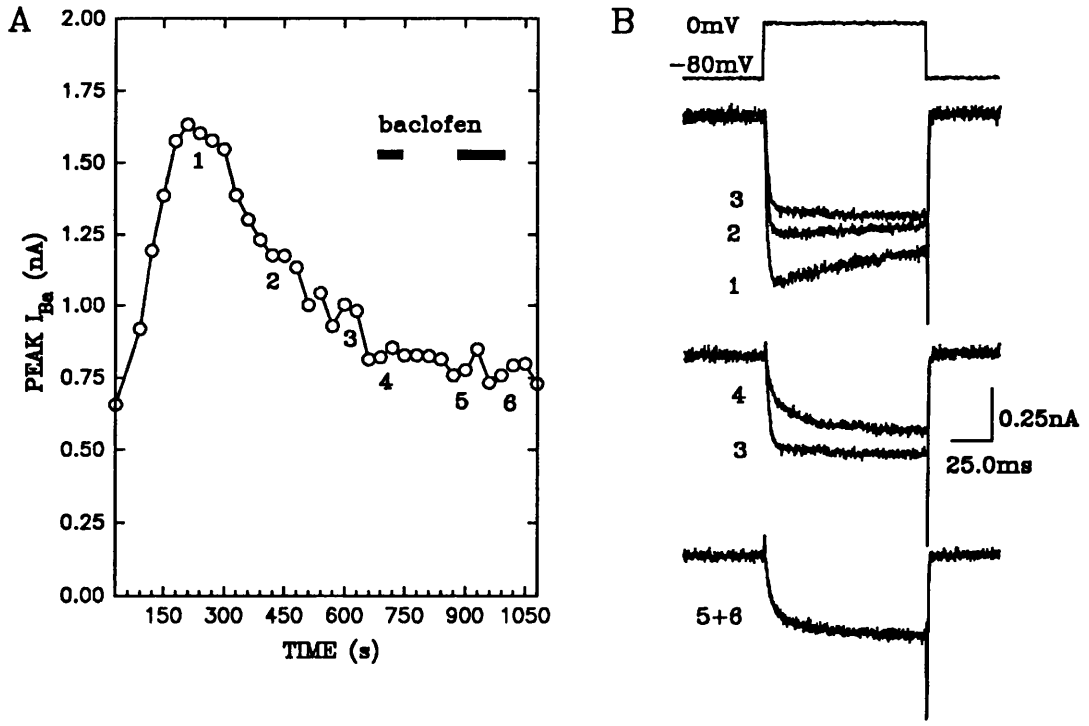

Figure 3.10 The action of GTPγS on the HVA calcium channel current.
A, a graph of peak HVA I_{Ba} versus time for a cell infused with GTPγS (10μM). Baclofen (50μM) application is denoted by the filled bars.
B, shows the current traces which correspond to the numbered points in the graph.

The decrease of current amplitude and slowing of the kinetics of activation were independent of the concentration of GTPγS in the patch pipette (10-200μM). The rate of full GTPγS action increased with increasing concentrations of GTPγS in the patch pipette, see table 3.2.

Table 3.2 Shows the time taken for full GTPγS action, the time to peak current and the sustained current values for three concentrations of GTPγS in the patch pipette.

Concentration of GTPγS	Time to full GTPγS effect (s)	Time to peak (ms)	Sustained current (nA)	n
200μM	317 ± 38	82.9 ± 6.9	1.0 ± 0.2	7
50μM	405	76.4	0.8	2
10μM	645	59.9	0.7	2

GTPγS irreversibly activates all Gα subunits and the minimum concentration used of 10μM was still sufficient to produce the maximum response. Baclofen application activates the $GABA_B$ receptor which then catalyses the exchange of GDP for GTP on the Gα subunit. This in turn increases the rate of GTPγS binding to the Gα subunit and the subsequent rate of the effect on the calcium channel currents. GTPγS action is potentiated in these cells because the cell cytoplasm exchanges with the intracellular saline in the patch pipette which does not contain GTP.

The current traces in figure 3.10B show the maximum current attained and the progress of GTPγS action where the current amplitude declines and the rate of current activation slows. Application of baclofen further reduces the current amplitude and the slowing of the kinetics as it potentiates the rate of GTPγS action. The second application of baclofen is ineffective indicating that the Gα subunits are fully activated. When higher concentrations of GTPγS (50-200μM) and three stable consecutive modulated currents were recorded, the application of baclofen (50μM) produced a mean inhibition of 2.6 ± 3.2% (n=5) for the sustained current component.

This result indicates that the basal exchange of GDP for GTP on the Gα subunit is sufficiently fast to produce the full GTPγS modulation of the current, within 300 seconds for 200μM GTPγS, without agonist stimulation of the G protein coupled receptor.

The rate of current activation decreases over time with GTPγS infusion to such an extent that in some cells a double exponential can be fitted to the current trace. This is shown in figure 3.11B. The number of current traces which can be fitted with a double exponential increases over time. The double exponential equation fitted was:-

$$y(t) = ss + (A \times \exp(-t/\tau_1) + (B \times \exp(-t/\tau_2))$$

where **ss** is the steady state and **A** and **B** are the proportional amounts of the two components of current with the time constants τ_1 and τ_2 respectively. The proportion of the slow current component in the double exponential curve fit is given by B/A+B.
The maximum number of current traces that could be fitted with a double exponential in a group of 18 cells was 12 and this was recorded at 300 seconds from the beginning of cell infusion, see figure 3.11 C. The largest mean contribution of the slow component (B/A+B) was 0.27 ± 0.06 after 270 seconds of infusion with GTPγS. The relative contribution of the slow component at this time point ranged from 0 to 0.73. The mean time constants of current activation for the fast and slow current components were τ_1=2.19 ± 0.33 ms and τ_2= 37.62 ± 7.48ms respectively, n=18.

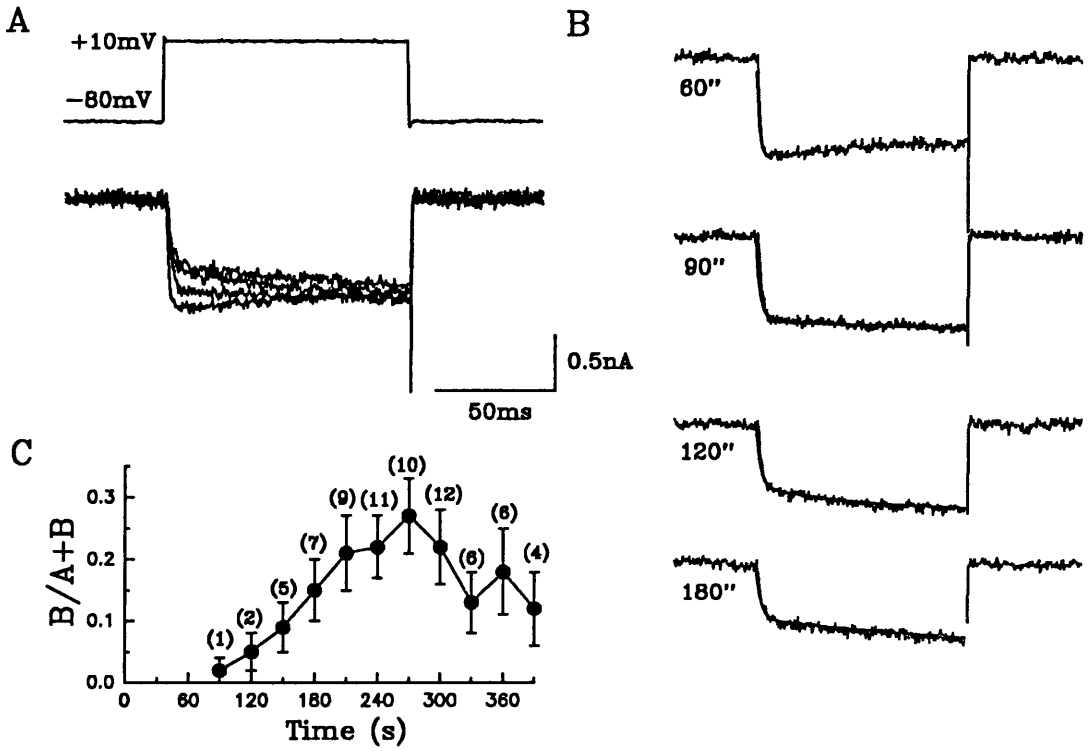

Figure 3.11 Shows curve fitting to current traces of an acutely replated DRG infused with GTPγS.

A, shows the reduction in amplitude and the rate of current activation over time in a cell infused with GTPγS (200μM).

B, shows the fitting of a single and double exponential curve to the four current traces shown together in A. The rate of current activation was only sufficiently slowed in the current traces recorded after 90 seconds from the onset of membrane rupture and recording.

C, shows the increase in the relative contribution of the slow component over time (n=18). The number of current traces at each time point that could be fitted with a double exponential are indicated above each point in parentheses.

The slow rate of current activation is thought to represent the voltage-dependent dissociation of the activated G protein from the calcium channel over the test step. As the proportion of G protein coupled calcium channels decreases, in a voltage-dependent manner during the test step, the current amplitude increases.

The ability to fit a double exponential was complicated by the kinetics of some current traces and the extent that the current amplitude decreased with GTPγS in the patch pipette. An example of the kinetics of a current trace modulated with GTPγS that is unable to be fitted with a double exponential over the whole test step is shown in figure 3.13A. The rate of current activation is decreased with GTPγS infusion but the current begins to inactivate after 50ms within the test step. The steep reduction in the number of cells included in the B/A+B graph after 300 seconds (figure 3.11C) is due to the application of agonists or prepulses.
Another indicator of the action of GTPγS is to compare the change of the time to peak against time. The mean time to peak values for two groups of cells with or without GTPγS in the patch pipette are shown in figure 3.12. The time to peak steadily increases over time for the cells infused with GTPγS, the mean time to peak is greater than 50ms after 210 seconds from the onset of whole cell recording.

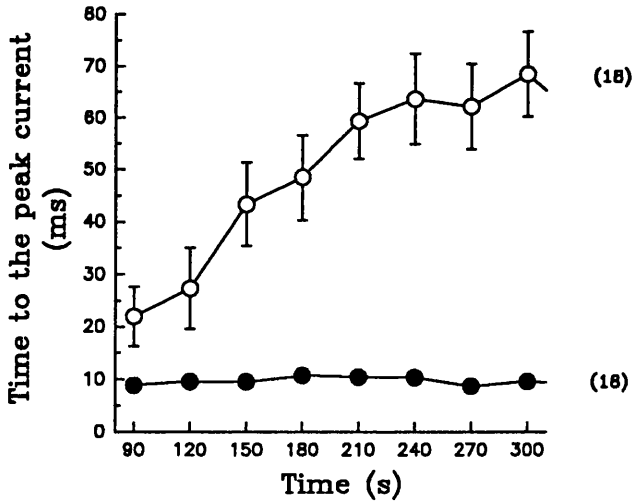

Figure 3.12 Shows the change in the time to peak against time in cells with or without $GTP_{\gamma}S$ in the patch pipette.
The mean time to peak values changing over time for cells with and without GTPγS in the patch pipette are shown by open and filled circles respectively. The standard error of the mean bars are occluded by the size of the filled symbol in the control. The number of cells are given in parentheses.

3.2.8 The action of a prepulse on control and GTPγS modulated HVA calcium channel currents.

The modulation of the calcium channel current by intracellular infusion with GTPγS was also been shown to be voltage-dependent. Once three stable consecutive records were recorded in a cell infused with GTPγS a 10ms prepulse to +90mV, given 20ms before the test step, was applied to a cell; this is shown in figure 3.13A. The prepulse rapidly and reversibly increased the current amplitude and the rate of current activation. The current trace following the prepulse shows the extent of recovery. Both the current amplitude and kinetics are the same in the recovery as the control in this example. The extent of the relief of the block of current amplitude is related to the time from the end of the prepulse to the beginning of the test step. Figure 3.13B shows the percentage relief of GTPγS modulation in another cell against the time interval between the prepulse and the test step. The rate of GTPγS action to slow the kinetics of current activation was so rapid in acutely replated DRGs that no initial isochronal peak current times could be estimated in these cells before GTPγS began to have its effect. Since the mean time to peak in cells without GTPγS in the patch pipette is 8.23 ± 0.40ms (n=20) and current traces were sampled at 0.39ms intervals, 8.19ms was chosen as the nearest time point for analysis. The percentage relief of GTPγS modulation by the prepulse was measured at 8.19ms from the onset of the test step and for the sustained current component. The percentage relief of current modulation by GTPγS with a prepulse was significantly greater for the initial portion of the current than the sustained current component of the test step.

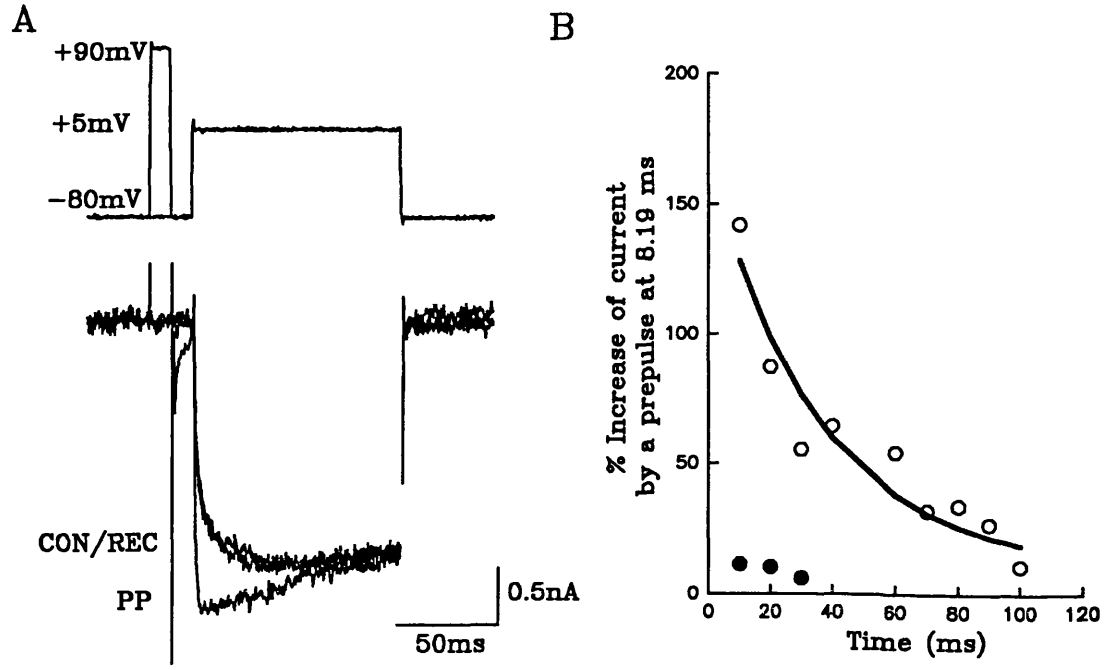

Figure 3.13 Shows the effect of a prepulse on GTPγS modulation of the HVA calcium channel current.
A, shows the effect of a 10ms prepulse to +90mV given 20ms before the test step. The control and recovery records are superimposed and are labelled CON/REC, the current trace following the prepulse is labelled PP.
B, shows the percentage increase in the amplitude of the current in a cell infused with GTPγS at 8.19ms (hollow circles) and the sustained current component (filled circles) against the time interval between the prepulse and the test step. The prepulse of +90mV was applied for 10ms. The data at 8.19ms can be fitted to a single-exponential decay with τ = 34.81ms.

The percentage increase of current amplitude by a prepulse at 8.19ms in GTPγS infused acutely replated DRGs was 93.27 ± 11.74%, n=15. The maximum current size recorded in this group of cells before GTPγS modulation was 1.5 ± 0.3nA. The current amplitude was reduced with GTPγS infusion to 0.60 ± 0.11nA and this was transiently increased to 1.11 ±. 0.18nA following a prepulse. The current amplitude following the prepulse rapidly returned to the GTPγS modulated level. The mean current amplitude for the recovery was 8.82 ± 8.45% less than the GTPγS modulated current amplitude before the

prepulse. The current amplitude in control cells was unaffected by application of a prepulse, the percentage change in current amplitude with and following the prepulse was 0.6 ± 1.3% and -2.1 ± 1.5% respectively. These results are shown in figure 3.14A.
The rate of reblocking by GTPγS is indicated from the result in figure 3.13B. The percentage relief of the GTPγS block by a prepulse to +90mV decreased as the duration between the prepulse and the test step increased and this could be fitted to a single-exponential decay, τ=34.81ms. This recovery from the prepulse is distinctive from the voltage-dependent facilitation current in chromaffin cells which requires more than 50 seconds to recover (Artalejo *et al.*1992).

The effect of a prepulse on GTPγS modulated calcium channel current is illustrated by the equation:-

$$\xrightarrow{-\delta V} \qquad C + G \underset{k_2}{\overset{k_1}{\rightleftharpoons}} CG \qquad \xleftarrow{+\delta V}$$

C represents the closed calcium channel and G the Gα subunit. The calcium channel is unable to open in response to a voltage step when it is coupled to the Gα subunit (CG). The rate constant k_1, represents reblocking of the calcium channels by the G protein and the rate constant k_2, voltage dependent unblocking. Figure 3.13B showed that the time for an e fold reblock of the calcium channel current following a prepulse to +90mV was τ=34.81ms. The time spent at the hyperpolarised holding potential (-80mV) is illustrated by the arrow labelled -δV. The rate constant k_1 is equal to $1/\tau$ and is $0.029ms^{-1}$.

This is a similar value to one reported by Grassi and Lux (1989) of $0.03ms^{-1}$.

The dissociation of the G protein from the calcium channel in a voltage-dependent manner (during the voltage step or the prepulse) is denoted by the arrow marked +δV. The time for the unblock of G protein modulation is given by the slow component of current activation in GTPγS infused cells, an e fold increase in current activation was τ=37.62ms, see section 3.6. The rate constant k_2 was therefore $0.027ms^{-1}$. This was considerably slower than the value derived by Grassi and Lux of $0.11ms^{-1}$ and probably reflects the methods of calculation. Grassi and Lux calculated k_2 by the application of a +40mV increase in membrane potential during a test step to 0mV. However, the time constant of current activation, in acutely replated DRGs infused with GTPγS, was taken during an average test step of 0mV from a holding potential of -80mV. The rate constant of G protein dissociation from calcium channels has been shown to increase with membrane potential (see figure 4D (Kasai, 1992). Therefore the disparity of my calculation to that of Grassi and Lux has probably resulted from the different membrane potential changes evoked.

The prepulse also increases the rate of current activation, the time to peak for the control, prepulse and recovery in acutely replated DRGs with the CsAsp intracellular saline ± GTPγS is shown on figure 3.14B. In GTPγS infused cells the time to peak reduced from 69.56 ± 5.41ms to 13.58 ± 4.58ms with a prepulse which then fully recovered to 70.03 ± 6.26ms in the following current trace (n=15).

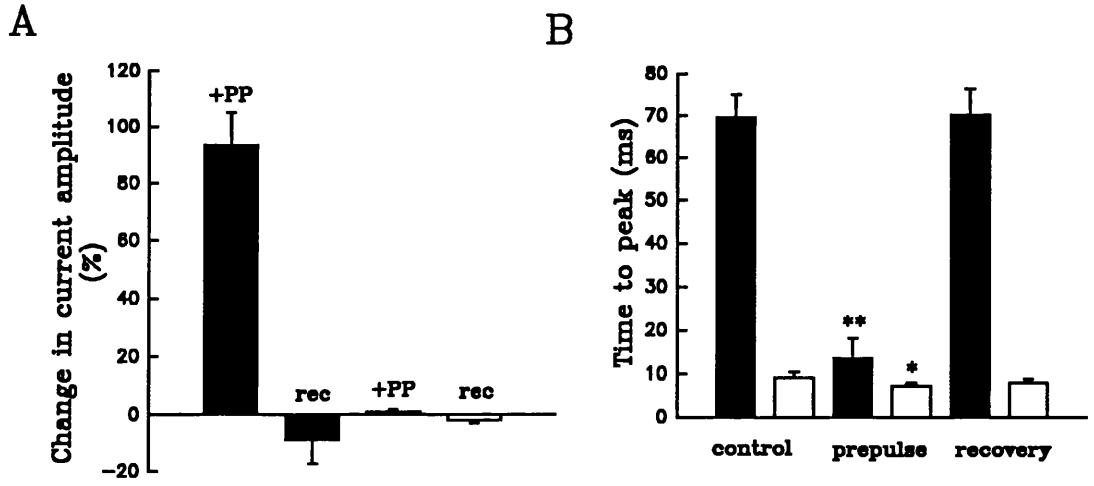

Figure 3.14 The percentage change in current amplitude and time to peak with a prepulse in cells with or without GTPγS in the patch pipette.
A, shows the percentage effect of a 10ms prepulse to +90mV, given 20ms before the test step on the current amplitude for cells with or without GTPγS (10-200μM) in the patch pipette. The current values were measured at 8.19ms into the test step. The bar labelled rec for each group shows the immediate after-effect of such a prepulse.
B, shows the time to peak before, during and after the prepulse recorded from cells with or without GTPγS in the patch pipette. The asterisk represents statistical significance ($p<0.05$) and two asterisks ($p<0.01$). Intracellular saline with GTPγS are shown by the filled bars (n=15) and without GTPγS (n=9) the open bars.

A similar trend was seen in cell with no GTPγS in the patch pipette, the time to peak again was reduced from 9.01 ± 1.37ms to 7.06 ± 0.83ms with a prepulse and then recovered to 7.88 ± 0.89ms (n=9).

3.2.9 The effect of repeated applications of baclofen on the HVA calcium channel current.

The effect of two applications of baclofen (50μM) over time is shown in figure 3.15A. The current traces showing the control and the maximum baclofen inhibition for the two applications are shown in figure 3.15B. The inhibition of the peak current by baclofen was reduced in the second application. The maximum effect of baclofen on the peak and sustained components of the current in the first application is shown in figure 3.15C. The inhibition was 30.22 ± 3.45% and 20.80 ± 2.59% for the peak and sustained current components respectively. The second application of baclofen (II) inhibited the peak current by 15.96 ± 2.45% and the sustained current by 16.80 ± 2.66%, n=7.

The inhibition of the peak current was significantly less in the second application ($p<0.01$, paired Student's t-test). The inability to reproduce a similar response with a second application of baclofen correlates with the idea put forward in 3.1.7. that exchange of the cell cytoplasm with the patch pipette solution is depleting the basal concentration of GTP and therefore reduces the effect of a further application of baclofen. This effect is not seen however in unreplated cells with the same intracellular saline that includes 2mM ATP (A.C.Dolphin, personal communication). The acutely replated DRGs may therefore have been depleted of the enzyme nucleoside diphosphate kinase which can generate GTP from ATP. The cells may have also been depleted of intracellular GDP. There is a non-significant inverse correlation between the time of cell infusion and the maximum inhibition produced by the first 50μM baclofen application ($r=-0.6827$, $p=0.09$, $n=7$).

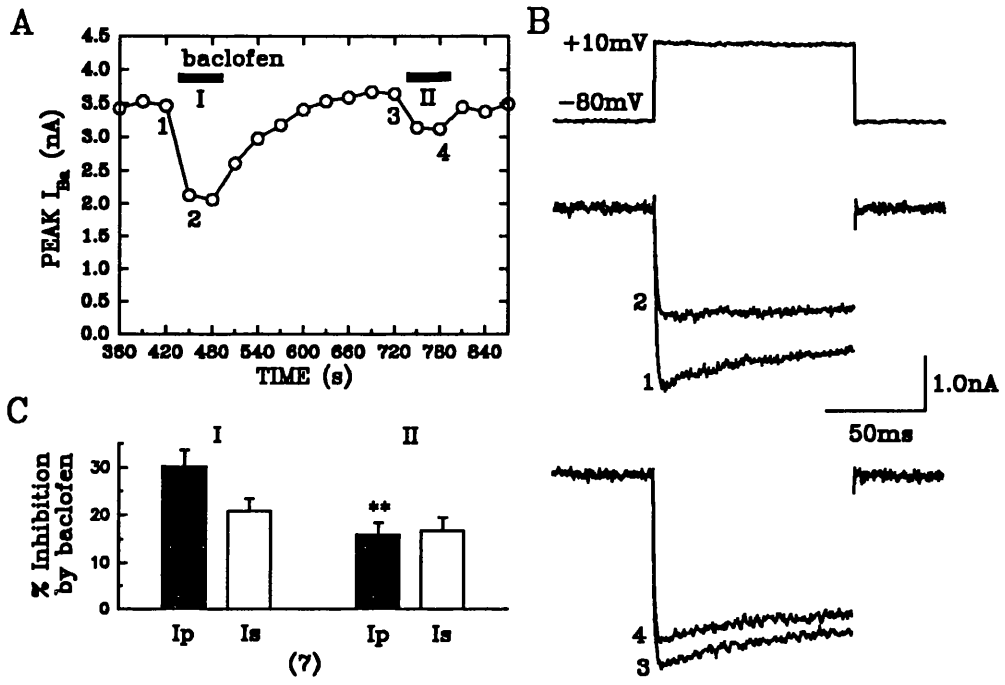

Figure 3.15 The effect of repeated applications of baclofen on the HVA calcium channel current.
A, a graph of peak HVA I_{Ba} versus time illustrating the effect of two applications of baclofen (50μM), denoted by the filled bars.
B, shows the leak subtracted current traces of the control (1 and 3) and the maximum baclofen inhibition (2 and 4), which correspond to the numbered records in the graph.
C, shows the maximum effect of baclofen on the peak and sustained components of the current for both applications. The significantly smaller inhibition of the peak current by the second application of baclofen is represented by the two asterisks ($p<0.01$).

3.2.10 The action of baclofen on HVA calcium channel currents inhibited by ω-CTx-GVIA.

The next set of experiments attempted to establish if the ω-CTx-GVIA sensitive or insensitive calcium channel currents were being modulated by baclofen application.
The application of ω-CTx-GVIA (1μM) and baclofen (50μM) and their effect on the peak calcium channel current over time is shown in figure 3.16A. The current traces showing the control current, the irreversible inhibition by ω-CTx-GVIA and the maximal inhibition by baclofen are shown in figure 3.16B. The mean values of the maximum inhibition by ω-CTx-GVIA for the peak and sustained current components were 56.87 ± 3.95% and 58.03 ± 3.75% respectively, see figure 3.16C.

Following ω-CTx-GVIA inhibition of the HVA calcium channel current, baclofen had a negligible effect, the peak current was slightly inhibited 3.1 ± 9.2% whilst the sustained current was stimulated 0.6 ± 8.45%, n=7. The large standard error values reflect a slight stimulation in three cells by baclofen.

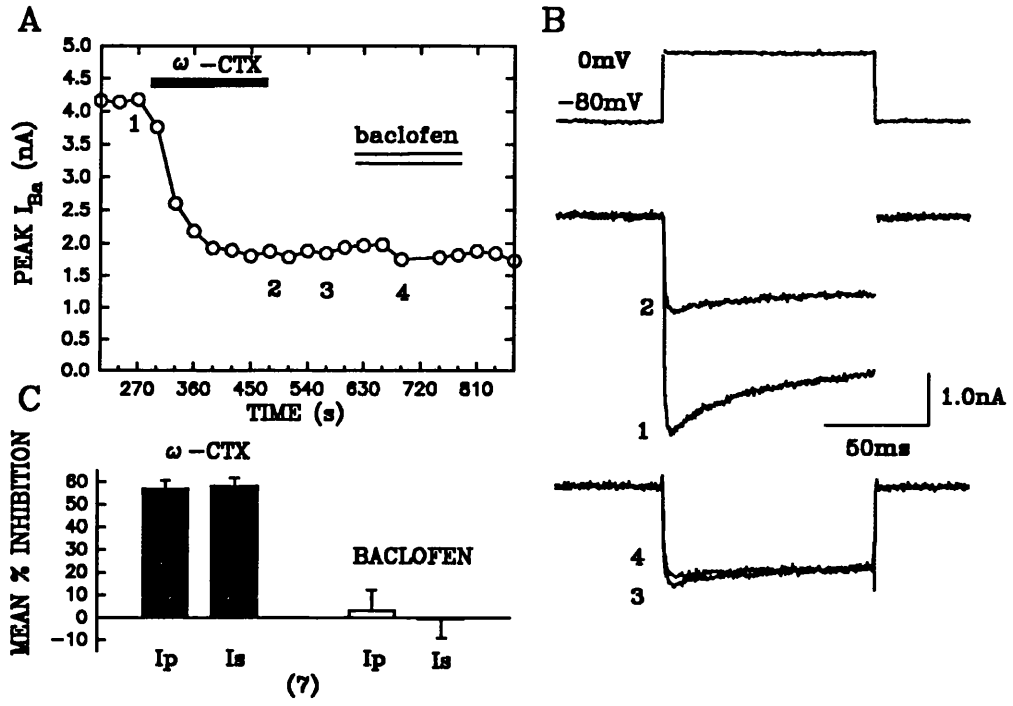

Figure 3.16 The action of baclofen on HVA calcium channel currents inhibited with ω-CTx-GVIA.
A, shows a graph of peak HVA I_{Ba} versus time illustrating the inhibition by ω-CTx-GVIA (1μM) and the application of baclofen (50μM). ω-CTx-GVIA and baclofen application are denoted by the filled and open bars respectively.
B, shows current traces corresponding to the numbered points on the graph A.
C, shows the maximum inhibition by ω-CTx-GVIA and baclofen on the peak and sustained current components. ω-CTx-GVIA and baclofen application are denoted by the filled and open bars respectively.

Baclofen (50μM) normally inhibits control calcium channel currents by 28.4 ± 3.7%, n=18. This result therefore indicates that all the modulation by baclofen is on the N-type calcium channels in these acutely replated DRGs.

3.2.11 The effect of ω-CTx-GVIA on the HVA calcium channel current in cells with GTPγS in the patch pipette.

Since ω-CTx-GVIA application and infusion of acutely replated DRGs with GTPγS (50-200μM) both prevent baclofen inhibition of the calcium channel current, the effect of ω-CTx-GVIA on the HVA I_{Ba} in cells infused with GTPγS was investigated. The effect of GTPγS (50μM) infusion and the subsequent application of ω-CTx-GVIA (1μM) and baclofen (50μM) over time is shown in figure 3.17A. The current traces showing the irreversible inhibitory action of ω-CTx-GVIA (1μM) is shown in figure 3.17B. The application of baclofen and its lack of effect is shown in the lower two current traces.

ω-CTx-GVIA inhibited the peak and sustained calcium channel current components equally in control cells without GTPγS in the patch pipette. Since an accurate isochronal measurement of the time to peak before GTPγS action is unavailable in cells infused with GTPγS I have taken the time point of 8.19ms that was used in the prepulse analysis. The mean values of the maximum inhibition by ω-CTx-GVIA at 8.19ms from the beginning of the step and for the sustained current component were 34.68 ± 8.50% and 46.06 ± 7.42% (n=8) respectively; these results are shown in figure 3.17C. The inhibition by ω-CTx-GVIA was significantly less at 8.19ms compared to the sustained current component ($p<0.05$, paired Student's t-test). Baclofen had a negligible effect and inhibited the peak current by 1.91 ± 2.18%, n=3.

To ensure that the maximum GTPγS effect was being exerted before the application of ω-CTx-GVIA, baclofen (50μM) was applied to the cells. The mean inhibition by ω-CTx-GVIA (1μM) in two cells infused with GTPγS (200μM) after baclofen application was 57.98%, n=2 for the sustained current component. This similar percentage of inhibition indicates that the Gα subunits were maximally activated by GTPγS.

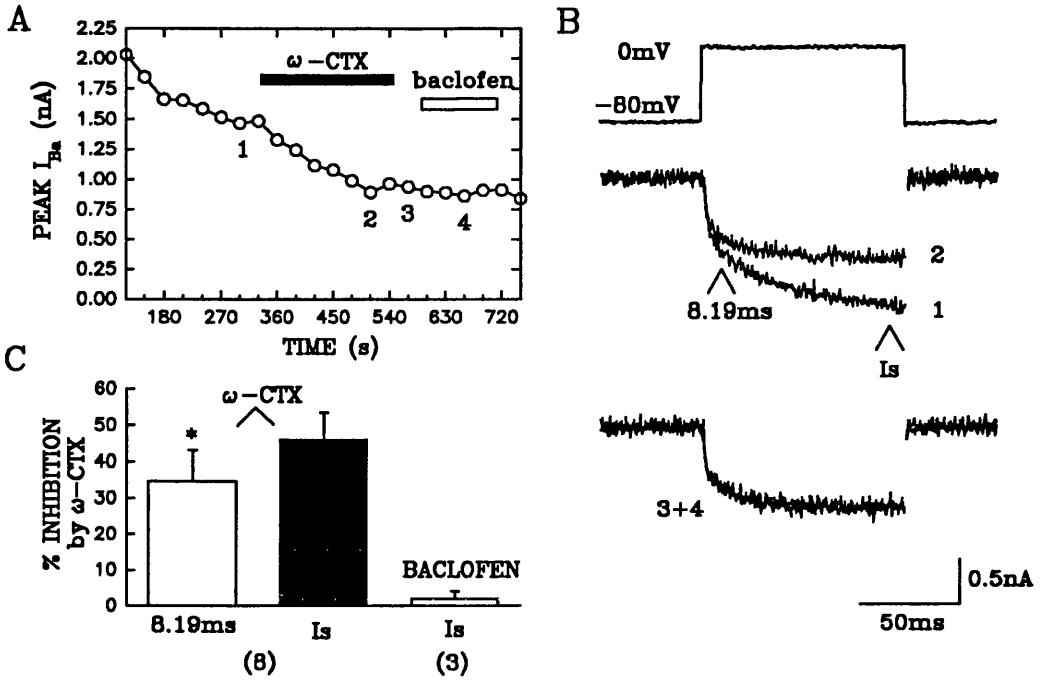

Figure 3.17 The action of ω-CTx-GVIA on the HVA calcium channel current in acutely replated DRGs with GTPγS in the patch pipette.
A, a graph of peak I_{Ba} versus time of a cell infused with GTPγS (50μM), illustrates the action of ω-CTx-GVIA (1μM) and baclofen (50μM). Drug application is represented by a filled bar for ω-CTx-GVIA and an open bar for baclofen.
B, shows the current traces which correspond to the numbered values in graph A.
C, shows the mean values of the maximal inhibition of ω-CTx-GVIA at 8.19ms from the beginning of the step and for the sustained current component. The baclofen effect is shown on the right. The numbers of cells recorded are given in parentheses.

The mean time required for full ω-CTx-GVIA (1μM) action in control and GTPγS infused cells were 168 ± 12.5 (n=13) and 172 ± 28.2 (n=8) seconds respectively.

3.3 DISCUSSION

3.3.1 Summary of observations

1) Large HVA I_{Ba} can be recorded in acutely replated DRGs.
2) The HVA I_{Ba} is only partially inhibited by DHP antagonists whilst over half of the HVA I_{Ba} is irreversibly blocked by ω-CTx-GVIA.
3) Baclofen reversibly inhibits the HVA I_{Ba}. This inhibition can be partly relieved by the application of a prepulse.
4) Infusion of cells with GTPγS reduces the amplitude and slows the rate of current activation, the time to peak significantly increases and it is possible to fit a double exponential to the slowly activating current. The application of baclofen to cells infused with GTPγS increases the rate but not the extent of calcium channel current modulation. The inhibition of current amplitude and slowing of current activation by GTPγS infusion was relieved by a prepulse in a rapid and reversible manner.
5) Prior application of ω-CTx-GVIA to acutely replated DRGs blocks the effect of baclofen application.
6) Cells infused with GTPγS are inhibited by ω-CTx-GVIA to the same extent as control cells but there was significantly less inhibition in the initial part of the test step.

3.3.2 Pharmacological analysis of the HVA calcium channel current.

3.3.2.1 The effect of the DHP agonist and antagonists on the HVA calcium channel current.

The lack of HVA calcium channel currents sensitive to L-type calcium channel antagonists in sensory neurones has previously been reported (Aosaki and Kasai, 1989; Kostyuk *et al.*1988; Kasai, 1992). Also a specific group of acutely dissociated DRGs from adult rats (defined by cell diameter) have been shown to have a similarly small inhibition by DHP

antagonists (Scroggs and Fox, 1992). The action of DHP antagonists in acutely replated DRGs differs from unreplated cells, which have been in culture greater than a week. Previously it has been reported that 5μM nifedipine was able to inhibit the HVA I_{Ba} by 43% (Dolphin and Scott, 1989). The lack of DHP antagonist effect in the present study may be due to the length of time in culture and the replating procedure which involves the removal of neurites. If the L-type calcium channels are located at the neurite base or on the neurites themselves they would be lost on replating. Previously, uneven distribution of L-type calcium channel immunoreactivity has been shown in hippocampal neurones with high density clusters seen at the base of major dendrites (Westenbroek *et al.*1990). It was not possible to accurately record from unreplated DRGs in the first week because of the space clamp difficulties. Therefore the percentage of HVA calcium channel current which is L-type in unreplated DRGs at this time in culture is unknown.

Previously the effect of DHP agonists in unreplated DRGs have been shown to stimulate the HVA calcium channel current by 25 ± 21%. This percentage stimulation is similar to the effect (±)-BayK 8644 had as an 'agonist' in the acutely replated DRGs. The antagonist action of (±)-BayK 8644 had a similar biphasic action as the pure DHP antagonist (-)-(R)-202-791 on the HVA I_{Ba} which has been previously reported (Dolphin and Scott, 1989). The agonist and antagonist action of (±)-BayK 8644 together produced a negligible response. The variability of action may result from the state of calcium channel phosphorylation or the level intracellular Mg^{2+}/ATP, both of which are known to affect DHP agonist action (Hymel *et al.*1988; Dolphin, 1991; Pearson and Dolphin, 1992).

3.3.2.2 The effect of ω-CTx-GVIA on the HVA calcium channel current.

The most recent pharmacological studies have concluded that the N- and not the L-type calcium channels are selectively inhibited by ω-CTx-GVIA (Regan *et al.*1991; Scroggs and Fox, 1991; Plummer *et al.*1991; Cox, 1992). The specificity of ω-CTx-GVIA has also been confirmed using antiserum raised against specific portions of the amino acid sequences of L- and N-type calcium channel $\alpha_1$subunits Only the antiserum raised against the predicted amino acid sequence of the N-type calcium channel immunoprecipitates bound radiolabelled ω-CTx-GVIA in the rat brain (Dubel *et al.*1992). This result is further supported by the selective inhibition of the calcium channel current expressed by the calcium channel B clone in HEK293 cells by ω-CTx-GVIA (Williams *et al.*1992). The calcium channel α_{1B} subunit is thought to be the N-type calcium channel. Based on these results the percentage of HVA I_{Ba} that is irreversibly inhibited by ω-CTx-GVIA in acutely replated DRGs is most probably being carried through N-type calcium channels. This N-type calcium channel current accounts for 57% of the total HVA calcium channel current evoked with test steps from a holding potential of -80mV in acutely replated DRGs.

3.3.2.3 The DHP and ω-CTx-GVIA insensitive HVA calcium channel current in acutely replated DRGs.

DHP antagonists and ω-CTx-GVIA were the only calcium channel antagonists applied to acutely replated DRGs.

In acutely dissociated DRGs from neonatal rats, the HVA calcium channel current has been studied pharmacologically using the DHP antagonist nitrendipine (2-4μM), ω-CTx-GVIA (3-5μM) and ω-Aga-IVA (100-200nM) (Mintz *et al.*1992a). The percentage of current which was insensitive to DHP antagonists and ω-CTx-GVIA was shown to be 39% and differed slightly from a similar investigation in the same laboratory (Regan *et al.*1991). This proportion of DHP antagonist and ω-CTx-GVIA insensitive current is similar to that seen in acutely replated DRGs.

3.3.3 G protein modulation of HVA calcium channel currents in acutely replated DRGs.

3.3.3.1 The effect of (-)-baclofen application.

Baclofen produced variable degrees of inhibition of the HVA I_{Ba} in DRGs which most probably reflects the heterogeneity of the cell types recorded. DRGs were cultured from ganglia dissected from the whole length of the spinal cord. The cell diameter of the acutely replated DRGs recorded ranged from 17-32μm, the average cell diameter was 25μm. Baclofen at 50μM produced a maximum inhibition of the HVA I_{Ba}. The average inhibition was around 30% for the whole investigation, see chapter four.

The application of baclofen increased the time to peak, however, only three of the seven cells in that particular study were dramatically slowed with a time to peak greater than 50ms. This is complemented by the result with GTPγS (200μM) infusion in control cells where only 12 out of the 18 current traces were sufficiently slowed for a double exponential to be fitted. This result contrasts with unreplated DRGs which are always dramatically slowed by application of baclofen and infusion with GTPγS (A.C.Dolphin, personal communication). The initial portion of the test step is more sensitive to baclofen application than the sustained component. Similarly the application of a prepulse and the partial relief of baclofen inhibition is most effective on the initial current component. Only 33% of the baclofen inhibition of the HVA I_{Ba} could be relieved by a 10ms prepulse to +90mV. This shows that the activated G protein acts on and modulates the calcium channel partly in a voltage-dependent manner. In a few acutely replated DRGs, the application of this prepulse protocol completely removed the baclofen inhibition of the HVA I_{Ba}. The effect of a prepulse in cells infused with GTPγS increased the current amplitude 93% and reduced the time to peak significantly to a mean value that is similar to cells that

are not infused with GTPγS. The amplitude of the current relieved by a prepulse in cells infused with GTPγS was however smaller than the maximum current recorded in these cells before the onset of GTPγS action. The duration of the prepulse (10ms) applied to the acutely replated DRGs may have been too short to have revealed the full voltage-dependent coupling of the G-protein and the calcium channels (Kasai, 1992). The relief of baclofen inhibition and GTPγS modulation by a prepulse shown may be an underestimate of the extent of voltage-dependent coupling.
The reason for incomplete relief of baclofen and GTPγS inhibition of the HVA calcium channel current by a prepulse may result from an additional modulation of the calcium channels or the G proteins. The inhibition of the calcium channel current amplitude by GTPγS has been shown to be relieved by inhibition of phosphatase 1 or increasing cAMP-dependent phosphorylation in unreplated DRGs (Dolphin, 1992). The interaction of G proteins with calcium channels is therefore thought to be regulated by phosphorylation. The degree of phosphorylation of the G proteins, calcium channels or both may subsequently affect the voltage-dependent relief of the inhibitory modulation of calcium channels by G proteins.

The G-protein is thought to directly couple to the calcium channel in a voltage-dependent manner (Grassi and Lux, 1989; Kasai, 1992). The prepulse increases the uncoupling of the activated Gα subunits from the calcium channels and therefore provides more calcium channels with a greater probability of opening during the test step. The non-modulated and G-protein coupled calcium channels have previously been described as the 'willing' and 'reluctant' modes respectively (Bean, 1989; Beech *et al.*1992; Kasai, 1992). The 'willing' mode represents calcium channels that respond to a voltage step with a high open probability whilst the 'reluctant' mode represents G protein modulated calcium channels that have a low open probability in

response to a similar voltage step. Recent studies of unitary N-type calcium channel activity has established that there are at least three gating (open probability) modes and transmitter application alters the equilibria between those modes (Delcour and Tsien, 1993). This evidence also supports the willing/reluctant hypothesis but shows that the reluctant mode is probably more complex than previously proposed. The application of a prepulse has been shown to completely relieve neurotransmitter inhibition of calcium channel currents in some systems. The inability of a prepulse to completely relieve G protein modulation of the calcium channel current in acutely replated DRGs, may therefore result from direct action of the G protein on the calcium channel in combination with other enzymes. Dual modulation of the calcium channel current by the G protein ($G\alpha_s$) has previously been shown. $G\alpha_s$ can activate a calcium channel directly and indirectly via the cAMP second messenger pathway system (Birnbaumer *et al.*1991).

3.3.3.2 The effect of GTPγS infusion on the HVA calcium channel current in acutely replated DRGs.

The irreversible activation of Gα subunits by GTPγS infusion and the consequent modulation of HVA I_{Ba} has been extensively studied in sensory neurones (Dolphin and Scott, 1987; Marchetti and Robello, 1989; Lopez and Brown, 1991). The G protein pathway activated by GTPγS and G protein coupled receptors is thought to be similar because of the following:-

The effect of GTPγS to reduce the rate of current activation is comparable to the effect of agonist application but subsequently occludes it. GTPγS infusion initially potentiates the effect of agonist application. Both agonist application and GTPγS infusion inhibition of the calcium channel current are voltage-dependent and sensitive to pre-incubation with PTX.

Intracellular infusion of GTPγS has the ability to activate all Gα subunits but the inhibition of I_{Ba} has been shown in DRGs not to be mediated by second messenger systems (Dolphin

*et al.*1989). Except for nitric oxide, all second messenger pathways are known to be activated by specific G-proteins. The inhibitory modulation of the HVA I_{Ba} by GTPγS infusion, like neurotransmitter modulation can also be relieved by a prepulse. The dramatic recruitment of the current amplitude in GTPγS infused cells by a prepulse was rapid and reversible like the effect of a prepulse on baclofen inhibited HVA I_{Ba} in acutely replated DRGs.

3.3.3.3 The G-protein modulation of the ω-CTx-GVIA sensitive calcium channel current.

The inability of baclofen to inhibit the HVA I_{Ba} after ω-CTx-GVIA application suggests that most of the HVA I_{Ba} in acutely replated DRGs, that are modulated by G protein activation, are N-type calcium channels. Previous studies in other neurones and neuronal cell lines have also shown that N-type calcium channel currents are modulated by G proteins (Aosaki and Kasai, 1989; Lipscombe *et al.*1989; Cox, 1992; Taussig *et al.*1992). In unreplated DRGs the L-type calcium channels are also G-protein effectors (Scott and Dolphin, 1987). L-type calcium channels have also been observed to be modulated by G protein activation in a number of neurosecretory systems (Offermanns *et al.*1991; Schmidt *et al.*1991).

In cells infused with GTPγS the application of baclofen increased the rate and not the extent of GTPγS modulation. Once stable current traces were evoked in acutely replated DRGs infused with GTPγS, the application of baclofen was then without effect. This result indicates that GTPγS infusion is able to maximally activate the same G protein(s) as the $GABA_B$ receptor. Since both ω-CTx-GVIA and GTPγS infusion block further baclofen action, the infusion of cells with GTPγS should affect the application of ω-CTx-GVIA. In GTPγS infused cells this prediction has been confirmed. Significantly less ω-CTx-GVIA inhibition is seen at 8.19ms compared to the sustained current component, whilst in control cells the action of ω-CTx-GVIA is the same for both current components.

This result indicates that:-
a) the N-type calcium channel is the common site of action for both the activated G-protein and ω-CTx-GVIA in acutely replated DRGs,
b) the effect of ω-CTx-GVIA application is greater at the end of the step because a significant proportion of G proteins uncouple from calcium channels in a voltage-dependent manner during the step depolarisation,
c) G-protein modulation of the calcium channel current is independent of ω-CTx-GVIA action because the rate and extent of the maximum inhibition by ω-CTx-GVIA is the same in control and GTPγS infused cells.

3.3.4 Conclusions

Acutely replated DRGs differ from unreplated DRGs in their calcium channel pharmacology and G-protein modulation. The L-type calcium channels are possibly lost as a result of the replating procedure. The G-protein modulation of the HVA I_{Ba} selectively acts on the ω-CTx-GVIA sensitive, N-type calcium channels.
GTPγS modulation of the HVA I_{Ba} is similar to baclofen application. Both are able to slow the rate of current activation and the modulation can be relieved by a prepulse. Baclofen application is ineffective after full GTPγS modulation has occurred and following ω-CTx-GVIA application.
The rate and extent of ω-CTx-GVIA inhibition of the calcium channel current is similar in acutely replated DRGs recorded with or without GTPγS in the patch pipette. Unlike ω-CTx-GVIA action in control cells however there is a significant difference in the inhibition over the voltage step in GTPγS infused acutely replated DRGs. These results indicate that GTPγS activated G proteins acts on the ω-CTx-GVIA sensitive calcium channel and the coupling to the channel is voltage-dependent.

CHAPTER FOUR

RESULTS II

4.1 An investigation of G protein signal transduction in acutely replated DRGs using anti-G-protein antisera.

4.1 Introduction

The PTX-sensitive G protein subtype involved in neurotransmitter modulation of calcium channel currents has been investigated by the infusion of purified Gα subunits from the patch pipette solution into PTX treated neurones. Using this approach both G_o and G_i were shown to restore neurotransmitter inhibition of the calcium channel current in a number of cell types (Hescheler *et al.*1987; Toselli *et al.*1989; Ewald *et al.*1988; Linder *et al.*1990; Surprenant *et al.*1990).

Another method of investigating G protein signal transduction was to use anti-Gα antiserum. Injection of anti-Gα antisera was used to investigate NA inhibition of the calcium current in NG108-15 cells (McFadzean *et al.*1989). Only the anti-$G\alpha_o$ antiserum reduced NA inhibition of the calcium channel current. Using these antisera the aim of this part of my investigation was to establish which PTX sensitive G protein was involved in neurotransmitter modulation of the HVA I_{Ba} in acutely replated DRGs.

4.2. RESULTS

4.2.1 Introduction of non-specific rabbit immunoglobulin into acutely replated DRGs by a modification of scrape loading.

The scrape loading procedure was first fully characterised by McNeil et al. (1984) using a range of fluorescent dextran molecules (40-500kD). They showed that all weights of dextran were able to enter the Swiss 3T3 cells, in a size dependent manner, when the cells were physically removed from the substratum in the presence of the dextran. Replating cells is physically equivalent to the scrape loading procedure and the ability to load antibodies (150kD) was therefore investigated.

DRGs were replated in the presence of non-immune rabbit

immunoglobulin (IgG) at 25µg/ml, and kept at 4°C. After one hour the cells were fixed with Paraformaldehyde (4%) and permeabilised with Triton X100 (0.2%). Using goat anti-rabbit antibodies conjugated to FITC (GAR-IgG-FITC) and fluorescence microscopy the presence of rabbit IgG was visualised. Once the fluorescent image was taken, the cells were then viewed with phase contrast microscopy, see figure 4.1. A range of IgG loading across the group of acutely replated DRGs is seen.

To check that IgG only enters the cell during the replating procedure DRGs were replated without IgG and then incubated at 4°C with IgG (25µg/ml) for one hour. The cells were then fixed, permeabilised and incubated with GAR-IgG-FITC as above, the result is shown in figure 4.2.. No stain is seen indicating that IgG can only enter the cells during the replating procedure. When cells are replated with IgG but not permeabilised with Triton X100 no stain is seen indicating that IgG is only inside the cells (picture not shown).

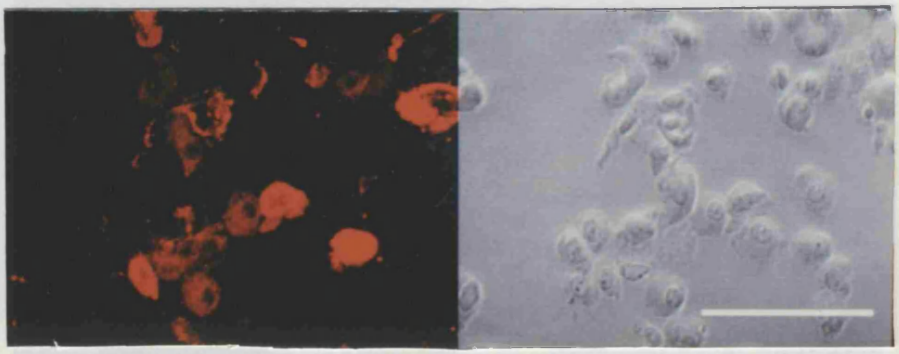

Figure 4.1 shows the introduction of non-specific rabbit immunoglobulin during the replating procedure.
Shows acutely replated DRGs which were replated with IgG (25µg/ml). After one hour at 4°C the cells were washed, fixed, permeabilised and incubated with GAR-IgG-FITC. A range of IgG immunoreactivity can be seen in the fluorescent image on the left (shown in red) and the corresponding phase contrast image is on the right. The scale bar is 100µm.

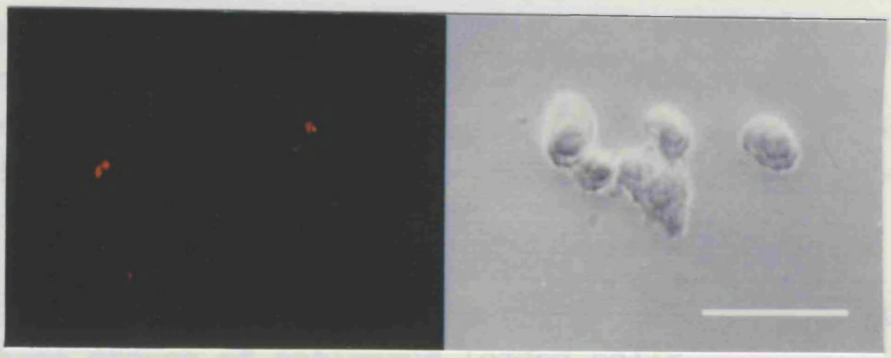

Figure 4.2 Shows that immunoglobulin is only introduced during the replating procedure.
Shows acutely replated DRGs that were replated without IgG. The acutely replated DRGs were then incubated with IgG (25µg/ml) for one hour at 4°C. No IgG immunoreactivity can be seen in the fluorescent image on the left, the corresponding phase contrast image is on the right. IgG only enters the cells during the replating procedure. The scale bar is 100µm.

Figure 4.3 shows unreplated cells that were incubated at 37°C with IgG (25µg/ml). After one hour the cells were treated as the acutely replated DRGs above. No stain was seen indicating that IgG uptake does not occur in unreplated cells.

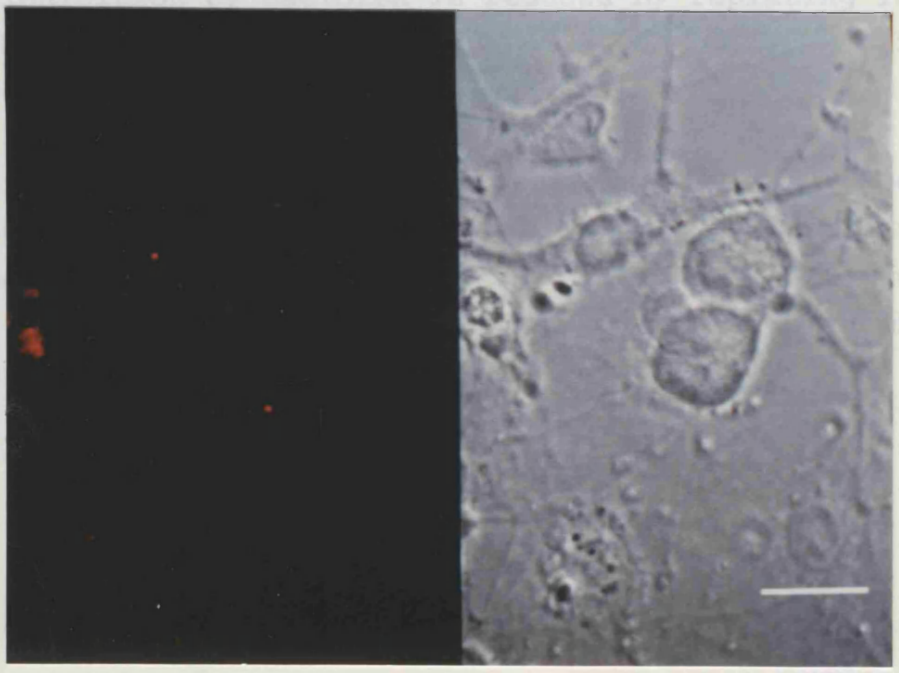

Figure 4.3 Shows unreplated DRGs do not take up non-specific rabbit immunoglobulin.
Shows unreplated cells that were incubated at 37°C with IgG (25µg/ml). After one hour the cells were treated as in figure 4.1. No stain was seen indicating that IgG uptake does not occur in unreplated cells. The scale bar is 50µm.

The loading experiments were done at 4°C because acutely replated DRGs have active endocytosis as they regenerate following the replating procedure. For this reason, if cells are replated without IgG and half an hour later IgG is added at 37°C , the cells strongly stain (picture not shown).

4.2.2 Baclofen inhibition of HVA calcium channel currents in three groups of antiserum loaded cells.

Baclofen modulation of calcium channel currents is reduced by pre-incubation with PTX which ADP-ribosylates the G-proteins $G\alpha_i$ and $G\alpha_o$ (Dolphin and Scott 1987). In order to investigate which one of these G protein subtypes was transducing the $GABA_B$ receptor signal to inhibit calcium channel currents cells were replated with anti-G protein antisera.

The current traces showing maximum inhibition by baclofen (50μM) and recovery in a cell replated in the presence of non-immune rabbit serum at a dilution of 1:50 is shown in figure 4.4A.

This inhibition by baclofen is reduced by replating in the presence of an anti-$G\alpha_o$ antiserum (1:50) which was raised against the C-terminal decapeptide of the $G\alpha_o$ subunit (OC1), this is shown in figure 4.4B.

Baclofen inhibition in a cell replated in the presence of anti-$G\alpha_i$ antiserum (1:50), raised against the C-terminal decapeptide of the $G\alpha_i$ subunit (SG1), is shown in figure 4.4C, the inhibition of the HVA calcium channel current is not affected.

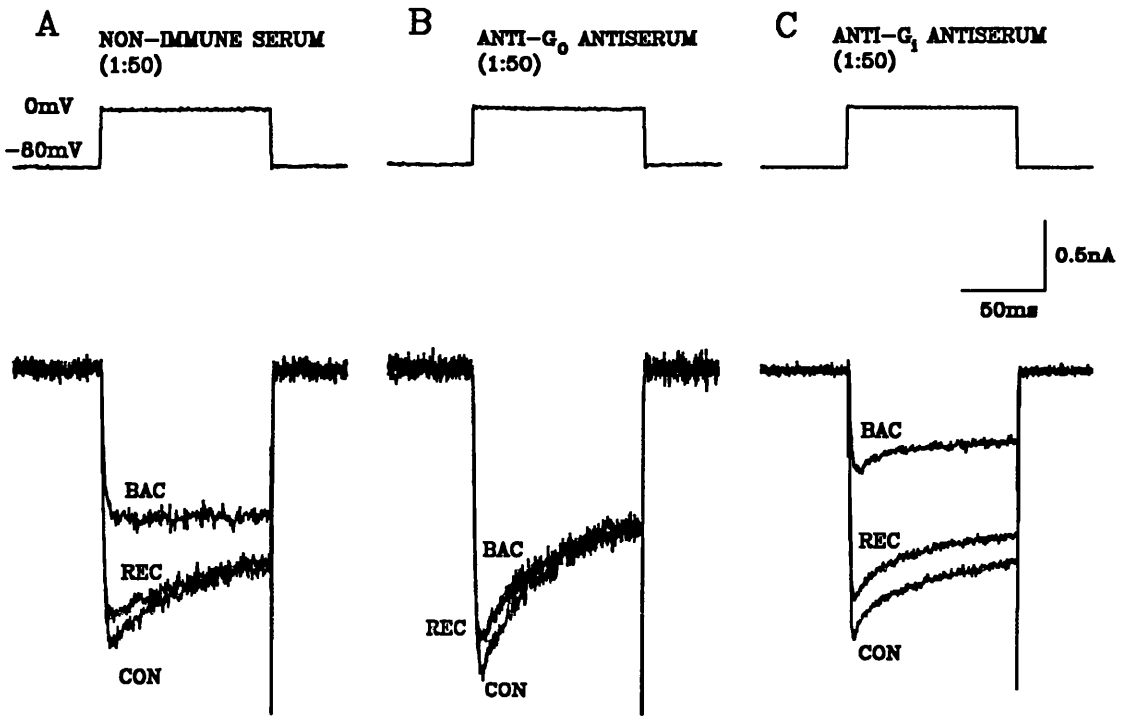

Figure 4.4 Baclofen inhibition of HVA calcium channel current in three groups of antiserum loaded cells.
A, shows the maximum inhibition by 50μM baclofen (BAC) and recovery (REC) in a cell replated in the presence of the non-immune rabbit serum (SER) at a dilution of 1:50.
B, shows a cell replated in the presence of the anti-$G\alpha_o$ antiserum (OC1) at a dilution of 1:50.
C, shows a cell replated in the presence of the anti-$G\alpha_i$ antiserum (SG1) at a dilution of 1:50.

4.2.3 The combined effect of replating DRGs with anti Gα antisera on baclofen inhibition of peak calcium channel current.

The maximum inhibition by baclofen (50μM) on the peak I_{Ba} in six groups of loaded cells are summarised in figure 4.5. The peak I_{Ba} was reversibly inhibited 28.4 ± 3.7% in control (CON) cells and this was similar (27.9 ± 3.9%) in cells that were replated in non-immune serum at a dilution of 1:50. When cells were replated with OC1 at a dilution of 1:100, baclofen inhibited I_{Ba} by 14.4 ± 3.6%, n=7. A higher concentration of OC1 (1:50) also reduced the inhibition by baclofen (10.1 ± 7.0% inhibition,n=4). Both concentrations of OC1 significantly reduced baclofen inhibition of peak I_{Ba}

($p<0.05$, compared with serum, Mann Whitney U-test). The Mann Whitney U-test was chosen because it makes no assumptions about the form of the distribution. The result of a Student's t-test on independent samples may be unsafe since we cannot be certain that the distribution of the observations is Gaussian or 'normal'.

The anti-$G\alpha_o$ antiserum raised against the N-terminal decapeptide of $G\alpha_o$ (ON1) at a dilution of 1:50, did not significantly prevent the inhibition by baclofen, which was 19.5 ± 4.4% (n=10). SG1 was unable at 1:50 (n=12) and 1:25 (n=8) to prevent baclofen inhibition of I_{Ba}; in the presence of SG1 (at both dilutions) baclofen produced 32.15 ± 3.51% inhibition (n=20).

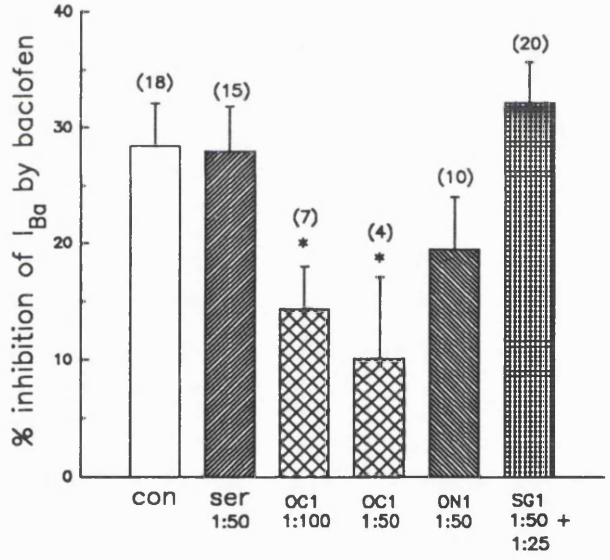

Figure 4.5 Summary of the effect of anti-Gα antisera on baclofen inhibition of peak HVA calcium channel current.
This bar chart shows the mean maximum inhibition of the peak HVA I_{Ba} by 50μM baclofen in six different groups of loaded cells. Significance ($p<0.05$) between groups (compared to non-immune serum) are represented by an asterisk. The number of cells are in parentheses.

4.2.4 The effect of the Anti-$G\alpha_o$ antiserum and the $G\alpha_o$ C-terminal decapeptide on baclofen inhibition of peak calcium channel current.

Antibody concentrations were diluted 1:25 in the replating medium during this study because the second anti-$G\alpha_o$ antiserum (OC2) came from a different rabbit and was ineffective at lower concentrations.

To evaluate if the effect of OC2 on baclofen inhibition was the result of specific binding to $G\alpha_o$, OC2 was preabsorbed with the peptide it was raised against. OC2 was pre-incubated with the $G\alpha_o$ (C-terminal) decapeptide conjugated to an extra cysteine. The extra cysteine was attached so that the 11-mer peptide could be conjugated to ovalbumin as opposed to the keyhole limpet hemocyanin for raising further anti-$G\alpha_o$ antiserum. The peptide (ANNLRGCGLYC) was screened in databases and its sequence was found not to correspond to any other proteins (N. Berrow, personal communication). The undecapeptide is so similar to the original decapeptide that it is referred to as the $G\alpha_o$ decapeptide throughout chapters 4 and 5.

In cells replated with non-immune rabbit serum (1:25), baclofen (50μM) inhibited the peak I_{Ba} by 32.97 ± 2.69%, n=20. This value was taken as the control. Cells replated with the OC2 significantly reduced baclofen inhibition of peak I_{Ba} to 22.49 ± 3.28%, n=22 ($p<0.05$, cf. non-immune serum, Mann Whitney U-test) as seen previously with OC1. When cells were replated with non-immune serum which had been pre-incubated with the $G\alpha_o$ decapeptide (80μg/ml) for one hour at 37°C, baclofen inhibition of I_{Ba} was also significantly reduced by 22.67 ± 3.64%, n=7 ($p<0.05$).

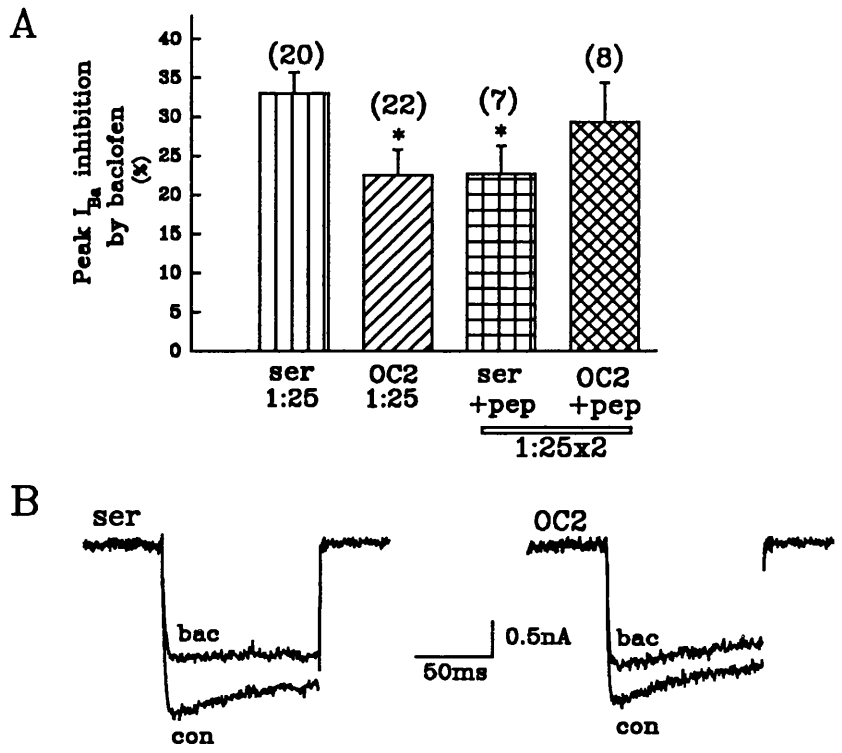

Figure 4.6 Summary of anti-$G\alpha_o$ antiserum and the $G\alpha_o$ decapeptide effect on baclofen inhibition of peak HVA calcium channel current.
A, this bar chart shows the mean maximum inhibition of the peak HVA I_{Ba} by baclofen (50μM) in four groups of loaded cells. Serum and OC2 pre-incubated with the $G\alpha_o$ decapeptide (80μg/ml) for one hour at 37°C are labelled with +pep. Significance ($p<0.05$) between groups (compared to non-immune serum) is shown by an asterisk. The number of cells in each group are shown in parentheses.
B, shows control current traces (con) and the maximum baclofen inhibition (bac) from the serum and OC2 groups. The two examples chosen have inhibition values similar to the mean values of their respective groups in the bar chart above.

The $G\alpha_o$ decapeptide is thought to be reducing baclofen inhibition of the peak HVA I_{Ba} by binding to the $GABA_B$ receptor in a way that mimics the C-terminus of $G\alpha_o$ and competes with native $G\alpha_o$ coupling. OC2 binds the native $G\alpha_o$ C-terminal to prevent coupling with the $GABA_B$ receptor. Pre-incubation of OC2 with the $G\alpha_o$ decapeptide for one hour at 37°C, reversed the action of OC2 and the $G\alpha_o$ decapeptide alone; and baclofen inhibition of I_{Ba} was 29.32 ± 5.04%, n=8.

Current traces showing baclofen inhibition of peak I_{Ba} in cells replated with serum and OC2 (1:25) are shown in figure 4.6B. These traces represent the mean inhibition by baclofen within their respective groups. The measurements of peak current inhibition were not made isochronally because the difference between isochronal and the peak current measurements of baclofen inhibition of the HVA I_{Ba} are very similar in acutely replated DRGs, see chapter 3.6. The degree of baclofen modulation of the rate of current activation is indicated by the time to peak values before during and after baclofen application. The results of the changes in the time to peak are summarised in table 4.1.

The increase in time to peak following baclofen application was only significant (Student's paired t-test, $p<0.05$) in the control, SG1, serum (1:25) and the OC2 groups which were the largest groups. The time to peak increased the least in the ON1 and the $G\alpha_o$ decapeptide groups. All the time to peak values recovered back to the control values in each group.

4.2.5 The effect of the Anti-$G\alpha_o$ antiserum and $G\alpha_o$ C-terminal decapeptide on the inhibition of the sustained calcium channel current by baclofen.

The modulation of peak I_{Ba} by baclofen and GTPγS infusion is more pronounced than for the sustained current component, especially in cells where the current activation kinetics were dramatically slowed. In addition a prepulse is significantly more effective at relieving baclofen or GTPγS inhibition of the peak current component than the sustained current component. Since baclofen inhibition of the sustained current component has the above differences, the effect of OC2 on baclofen inhibition of the sustained current component was investigated.

Table 4.1 showing the change in the time to peak with baclofen application in all the groups of loaded cells.

Group	Time to peak before bacofen (mean ± s.e.m)	Time to peak with baclofen	Time to peak with recovery	n
Control	8.8 ± 0.8	21.2 ± 5.6	8.0 ± 0.7	18
Serum (1:50)	7.9 ± 0.8	18.6 ± 5.6	7.8 ± 0.7	18
OC1 (1:100)	8.0 ± 0.6	21.7 ± 13.61	7.7 ± 1.2	7
OC1 (1:50)	7.2 ± 0.4	22.4 ± 13.78	6.4 ± 0.8	4
ON1 (1:50)	8.3 ± 0.6	9.4 ± 0.9	7.9 ± 0.5	10
SG1 (1:50+1:25)	7.3 ± 0.3	21.0 ± 5.8	7.5 ± 0.4	20
Second study				
Serum (1:25)	8.2 ± 0.4	34.1 ± 7.6	9.2 ± 0.8	20
OC2 (1:25)	7.0 ± 0.3	25.8 ± 7.2	7.6 ± 0.6	22
$G\alpha_o$ (80µg/ml) decapeptide	7.6 ± 0.6	8.8 ± 1.3	7.5 ± 0.5	7
OC2 + $G\alpha_o$ decapeptide	7.9 ± 0.5	40.3 ± 14.9	8.6 ± 0.9	8

The sustained I_{Ba} in cells replated with non-immune serum (1:25) was inhibited by baclofen by 24.32 ± 2.37%, n=20. When cells were replated in the presence of OC2 (1:25) baclofen inhibition of the sustained I_{Ba} was significantly reduced to 17.31 ± 2.19% (n=22),[$p<0.05$, cf. non-immune serum, Mann Whitney U-test]. Cells replated with non-immune serum (1:25) pre-incubated with the $G\alpha_o$ C-terminal decapeptide (80µg/ml) for one hour at 37°C, non-significantly reduced baclofen inhibition of the sustained I_{Ba} (20.42 ± 3.72%, n=7). Pre-incubation of OC2 with the $G\alpha_o$ decapeptide for one hour at 37°C reversed the significant protection provided by replating in the presence of OC2 alone, and the sustained I_{Ba} was inhibited by 23.08 ± 3.84%, n=8. These results are summarised in figure 4.7.

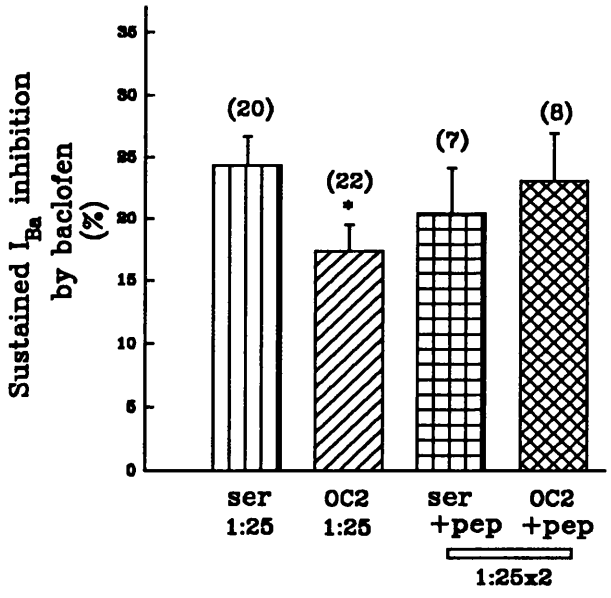

Figure 4.7 Summary of anti-$G\alpha_o$ antiserum and $G\alpha_o$ decapeptide on the ability of baclofen to inhibit the sustained calcium channel current. This bar chart shows the mean maximum inhibition of the sustained I_{Ba} by baclofen (50µM) in four groups of cells. Serum and OC2 pre-incubated with $G\alpha_o$ decapeptide (80µg/ml) for one hour at 37°C are labelled with +pep. Significance ($p<0.05$) between groups (compared to non-immune serum) is shown by an asterisk. The number of cells in each group are shown in parentheses.

A more accurate representation of the effect of replating with antisera, raised against $G\alpha_o$, is to show the distribution of baclofen inhibition of the peak I_{Ba}, see figure 4.8. The distribution of baclofen inhibition for cells replated in the presence of OC1 and OC2 is skewed to the left, this is confirmed by the Mann Whitney U-test which rejects the null hypothesis that the two groups come from the same population.
The range of baclofen action in anti-$G\alpha_o$ antiserum loaded cells is supported by the range of loading that can be seen in figure 4.9. The two pictures of figure 4.1, showing IgG loading with fluorescence microscopy and the localisation of the acutely replated DRGs with phase contrast microscopy have been superimposed. The range of loading can clearly be seen from no apparent to intense fluorescence.

4.2.6 The effect of replating DRGs in the presence of serum, anti-$G\alpha_o$ antiserum and the $G\alpha_o$ C-terminal decapeptide on the current density.

In order to investigate if the anti-Gα antisera were having any non-specific effect on the calcium channel current, the current density was calculated in each group of loaded cells. The current density was calculated by dividing the mean current (of three consecutive recordings before baclofen application) by the surface area of the cell and the values for each group are shown in table 4.2.
The mean current of all the DRGs replated in the presence of non-immune serum (1:25) is shown in figure 4.10. This group has a significantly greater current density than the previous serum group in the first antiserum loading experiments. The reasons for this increase were not investigated but the factors which have varied from the previous set of experiments are; (a) the intracellular recording saline was changed from CsAc to CsAsp and (b) a new aliquot of non-immune serum at a higher concentration was used in the replating medium.

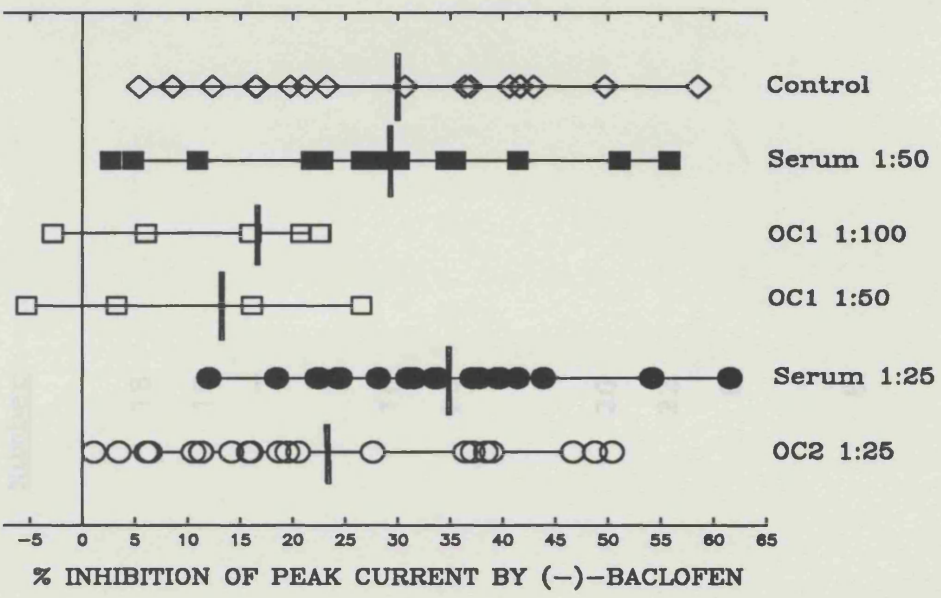

Figure 4.8 The distribution of baclofen inhibition of the peak calcium channel current in control, serum, OC1 and OC2 loaded cells.
This figure shows the distribution of baclofen inhibition within the control, serum (both studies), OC1 and OC2 groups. The mean inhibition for each group is shown by the vertical line.

Figure 4.9 Shows the range of IgG loading in acutely replated DRGs.
The fluorescence and phase images of figure 4.1 have been superimposed. The presence of IgG is shown in red and the phase contrast image of the acutely replated DRGs in grey. The scale bar is 100μm.

Table 4.2 shows the mean current density for all groups of DRGs replated in the presence of anti-G protein antisera and the $G\alpha_o$ decapeptide.

Group of antiserum	Current density ($pA/\mu m^2$)	Number
Control	1.54 ± 0.28	18
Serum (1:50)	0.97 ± 0.12	18
OC1 (1:100)	1.22 ± 0.29	7
OC2 (1:50)	1.39 ± 0.17	4
ON1 (1:50)	1.16 ± 0.18	10
SG1 (1:50 + 1:25)	1.10 ± 0.11	20
Second study		
Serum (1:25)	2.13 ± 0.16	20
OC2 (1:25)	1.74 ± 0.15	22
Serum + $G\alpha_o$ decapeptide (1:25 + 80µg/ml)	1.69 ± 0.37	8
OC2 + $G\alpha_o$ decapeptide (1:25 + 80µg/ml)	1.25 ± 0.24	8

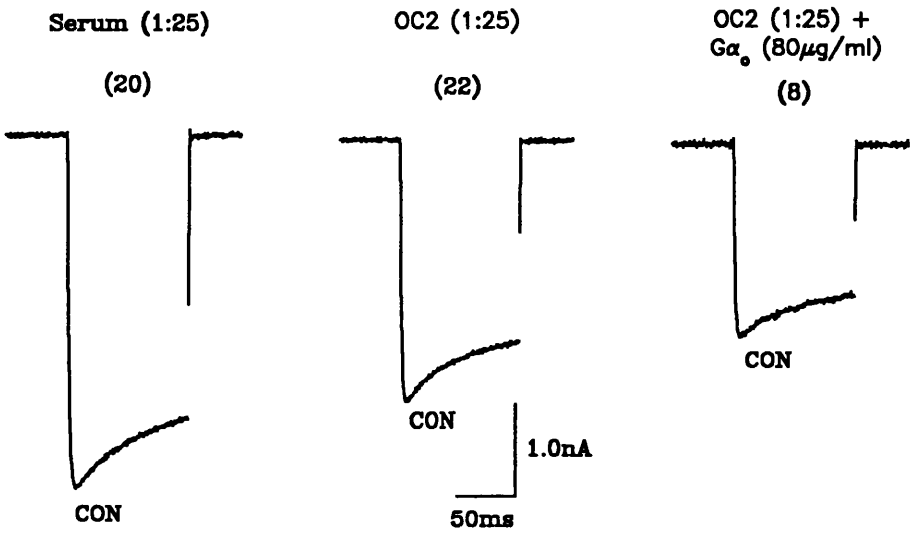

Figure 4.10 Shows mean current traces of all the DRGs in the groups replated in the presence of serum, OC2 and OC2 plus the $G\alpha_o$ decapeptide. This figure shows the mean of current trace before baclofen application from each acutely replated DRG recorded within the serum, OC2 and OC2 plus $G\alpha_o$ decapeptide groups. The number of cells recorded are given in parentheses. The mean current trace from cells replated with non-immune serum is shown on the right, OC2 the centre and cells replated with OC2 pre-incubated with the $G\alpha_o$ decapeptide on the left. The estimated current density values are given in table 4.2.

Baclofen inhibition of the peak I_{Ba} was significantly reduced in DRGs replated in the presence of OC2 or the $G\alpha_o$ decapeptide and their individual effects reversed with pre-incubation. This effect of pre-incubation of OC2 with the $G\alpha_o$ decapeptide on the current density however is completely opposite to the effect on baclofen inhibition. When cells were replated with OC2 pre-incubated with the $G\alpha_o$ decapeptide the effect of OC2 and the $G\alpha_o$ decapeptide alone was additive and the current density was significantly reduced ($p<0.01$, Mann Whitney U-test).

This result supports the specificity of the action of OC2 and the $G\alpha_o$ decapeptide on baclofen inhibition because the changes in current density do not match the effect on baclofen inhibition.

To further investigate if there was a relationship between the current density and baclofen inhibition a regression line was fitted to the data.
The linear correlation coefficient (r) between the current density and baclofen inhibition is shown in table 4.3.

Table 4.3 Shows the correlation between baclofen inhibition and the current density for DRGs replated with serum and OC2 ± the $G\alpha_o$ decapeptide groups.

Group	correlation (r)	probability	number
Serum	0.405	0.076	20
OC2	0.274	0.217	22
Serum + $G\alpha_o$ decapeptide	0.052	0.911	7
OC2 + $G\alpha_o$ decapeptide	0.849	0.008	8

There is only a significant ($p<0.01$) positive linear relationship in the DRGs replated with OC2 and the $G\alpha_o$ decapeptide. This is further supportive evidence that the effect of OC2 and the $G\alpha_o$ decapeptide on baclofen inhibition was specific. The DRGs replated in the presence of OC2 pre-incubated with the $G\alpha_o$ decapeptide have a significantly smaller current density and a highly significant positive relationship between current density and baclofen inhibition. Still baclofen inhibition of the peak and sustained current components was greater in the OC2 plus $G\alpha_o$ decapeptide group than in DRGs replated with OC2 or the $G\alpha_o$ decapeptide alone.

4.2.7 The effect of GTPγS infusion in cells replated in the presence of anti-Gα protein antibodies.

The effect of GTPγS infusion in control and OC1 loaded cells was compared. The effect on the current amplitude, the time to peak, the ability to fit a double exponential, the time constants of current activation and the relative contribution of the slow component were all analysed over time. Within all the parameters measured no significant difference was seen between the control and OC1 (1:100) loaded cells up to 300 seconds. After that time the number of cells that could be included in the study was reduced because baclofen or prepulses were applied or the current was too small to analyse.

The time point of 240 seconds was taken when GTPγS (200μM) infusion was fully effective. The sustained current amplitude at 240 seconds was 0.41 ± 0.05nA and 0.39 ± 0.06nA when GTPγS was in the patch pipette for control (n=18) and OC1 (1:100, n=22) loaded DRGs respectively. The sustained current amplitude in cells not infused with GTPγS at 240 seconds was 1.20 ± 0.15nA and 1.24 ± 0.25nA for the control and OC1 groups respectively, these results are shown in figure 4.12A.
The increase in the time to peak over time for the two groups is shown in figure 4.12B. The time to peak values at 240 seconds were 57.77 ± 8.69ms and 63.64 ± 8.77ms for the control and the OC1 groups respectively. The increase over time for the time to peak was also similar for both groups.

The ability to fit a double exponential to the activating current in cells of the control and OC1 groups infused with GTPγS was also similar. The mean time constants at 240 seconds were for τ_1, 2.19 ± 0.33ms and 1.58 ± 0.24ms and for τ_2, 37.62 ± 7.48ms and 34.43 ± 6.35ms for the control and the OC1 loaded groups respectively, these results are shown on figure 4.12C. At this time point, 10 of the current traces could be fitted by a double exponential in both the

control (n=18) and OC1 (n=22) groups. The relative proportion of the slow component (B/A+B) also increased in both groups to a similar extent over time. At 240 seconds the ratio of B/A+B was 0.22 ± 0.06 and 0.14 ± 0.04 in the control and the OC1 groups respectively. There was no significant difference between the current traces in both groups that could not be fitted with a double exponential. The change of the relative mean contribution of the slow component in control and OC1 cells infused with GTPγS over time are shown in figure 4.12D.

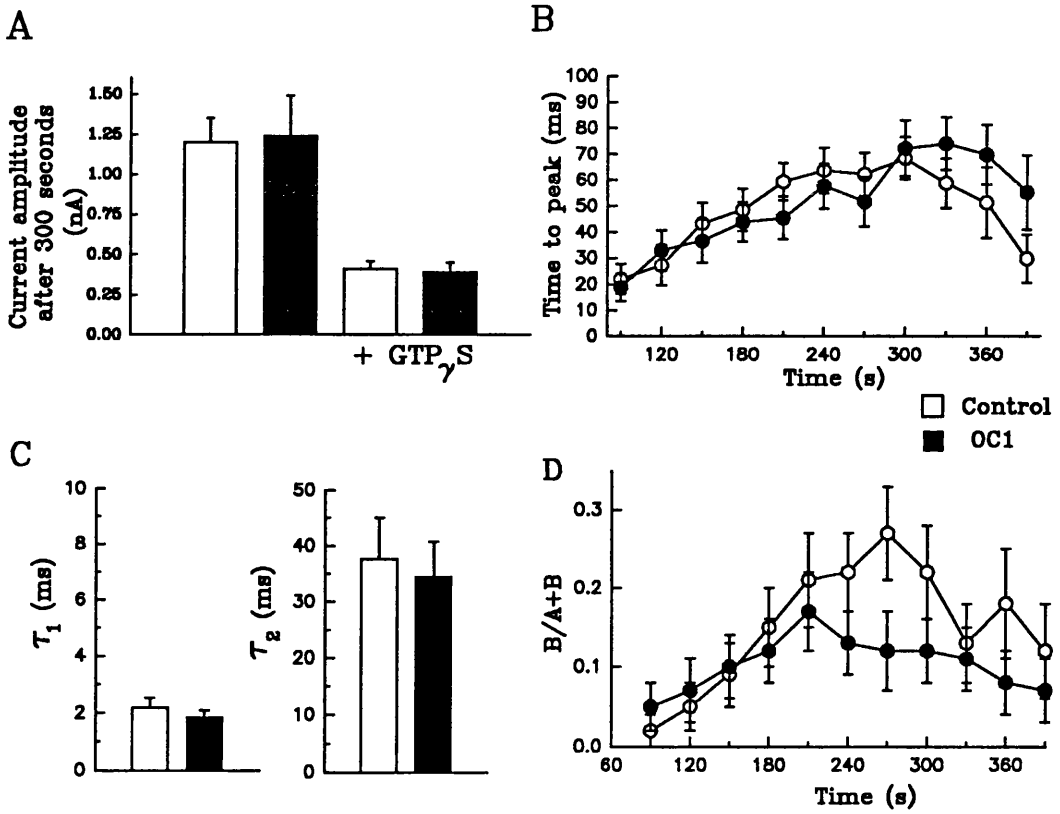

Figure 4.11 Shows the effect of GTPγS infusion in control and anti-$G\alpha_o$ loaded cells.

A, shows the sustained current amplitude with or without GTPγS in the patch pipette in control and OC1 loaded cells which are represented by the open and the filled bars respectively.

B, shows the change in the time to peak with GTPγS infusion in control (open circles) and OC1 (filled circles) loaded cells.

C, shows the mean values of the two time constants (τ_1 and τ_2) in cells where the activation of the current trace could be fitted with a double exponential at the time point of 240 seconds, n=10 for both groups. The control and OC1 loaded cells are represented by the open and the filled bars respectively.

D, shows the change in the relative contribution of the slow component (B/A+B) over time in control (n=18) and OC1 (n=22) loaded cells which are represented by the open and the filled circles respectively.

GTPγS modulation of the current in certain cells had activation kinetics complicated by an inactivating component during the voltage step or the current size was reduced to such an extent that no curve could be fitted. The results above were obtained using the extracellular saline with sodium chloride. The inability to fit a double exponential to the majority of currents was therefore thought to result in part from sodium influx through TTX-insensitive sodium channels. Using the extracellular saline with TEA replacing sodium, the effect of GTPγS infusion was again studied in cells replated with serum, OC2 and SG1 at dilutions of 1:25. In cells replated in the presence of non-immune serum the sustained current size at 240 seconds was 2.86 ± 0.32nA and 0.75 ± 0.21nA for the CsAsP intracellular saline alone and with GTPγS (200μM) in the patch pipette respectively. Cells replated with OC2 and SG1 had sustained currents reduced to 0.79 ± 0.28 nA (n=6) and 0.97 ± 0.42 nA (n=3) respectively these values are shown in figure 4.13.

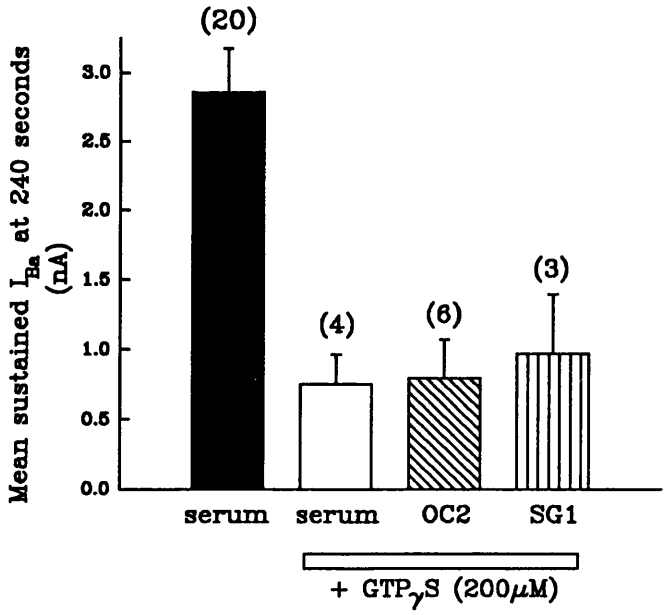

Figure 4.12 The effect of GTPγS infusion in cells replated in the presence of anti-Gα protein antibodies.
Shows the mean sustained current values after 240 seconds infusion with the CsAsp intracellular saline for DRGs replated with serum (1:25) and the inclusion of GTPγS (200μM) in the patch pipette for serum, OC2 and SG1 loaded cells (1:25). The number of recorded cells are given in parentheses.

The effect of GTPγS infusion in the serum, OC2 and SG1 loaded DRGs on the sustained current amplitude, time to peak and time constants of current activation are given in table 4.4. No significant difference was seen between the three groups of cells.

Table 4.4 Shows the effect of GTPγS on the sustained current amplitude, time to peak and time constants of current activation for serum, OC2 and SG1 loaded cells.

Group	n	Sustained current (nA)	Time to peak (ms)	τ_1 (ms)	τ_2 (ms)
Serum	4	0.75 ± 0.22	70.9 ± 8.9	1.2 ± 0.2	23.2 ± 5.6
OC2	6	0.79 ± 0.28	74.6 ± 5.5	1.2 ± 0.1	26.8 ± 6.4
SG1	3	0.97 ± 0.42	91.8 ± 1.6	1.3 ± 0.3	35.7 ± 2.8

4.3 DISCUSSION

4.3.1 Summary of results

1) Antibodies can be introduced into acutely replated DRGs during the replating procedure.
2) Replating DRGs in the presence of anti-$G\alpha_o$ antisera, OC1 (1:100 and 1:50) and OC2 (1:25), was able to significantly reduce baclofen inhibition of the HVA I_{Ba}.
3) Replating DRGs with the $G\alpha_o$ decapeptide (80µg/ml) alone was able to significantly reduce baclofen inhibition of the HVA calcium channel current.
4) The effect of OC2 and the $G\alpha_o$ decapeptide can be reversed if the two are pre-incubated together for one hour at 37°C.
5) The range of the reduced baclofen inhibition in DRGs replated with OC2 is complemented by the range of loading efficiency seen with fluorescence microscopy.
6) DRGs replated with OC2 pre-incubated with the $G\alpha_o$ decapeptide were additive in their effects and significantly reduced the current density. This effect is opposite to the result of pre-incubation on baclofen inhibition of the HVA I_{Ba}.
6) GTPγS modulation of the HVA I_{Ba} is not affected by replating DRGs with OC1, OC2 or SG1.

4.3.2 Introduction of antibodies into acutely replated DRGs.

4.3.2.1 The mechanism of antibody entry by acutely replating DRGs.

I have shown that antibodies can be introduced inside DRGs during the replating procedure and that there is a range of loading efficiency. The replating procedure is physically similar to scrape loading because the cell body is removed from the substratum. The antibodies enter the cells by diffusion through transient pores which are made as the attachment plaques and neurites are severed. The attachment plaque is the structure where the DRG cell body is attached

to the polyornithine/laminin coated coverslip. In the original evaluation of the scrape loading procedure it was estimated that transient pores were created wide enough for 500kD macromolecules to diffuse into Swiss 3T3 cells (McNeil *et al.*1984). The size of the transient pore made in acutely replated DRGs will depend on the size of the attachment plaque and the number of neurites of each cell replated.

4.3.2.2 An estimation of the average number of antibodies introduced per cell.

McNeil et al. (1984) looked at the extent of loading for a range of dextran sizes and concluded that on average 10^7 fluorescent dextran molecules (70kD) entered each cell during scrape loading with an extracellular concentration of 10mg/ml of fluorescent dextran. The extent of loading was heterogeneous and the fluorescent intensities ranged more than 100-fold across the population of loaded cells. They plotted the mean number of molecules loaded for three weights of dextran used and their loading curve would predict that less than 10^7 IgG molecules (150kD) would be loaded on average into each Swiss 3T3 cell.

(Ortiz *et al.*1987) estimated that 4×10^6 IgG molecules or 100fl of the extracellular medium with IgG (10mg/ml) were introduced into each L929 cell by the scrape loading procedure.

The final concentration of specific anti-Gα antiserum present in the replating medium was not known, however the weight of total serum protein was calculated to be 2.4mg/ml for the non-immune serum and OC2 at a dilution of 1:25. If 10% of the total antiserum protein is IgG and 1% of the total IgG concentration is specific for the $G\alpha_o$ decapeptide (G.Milligan, personal communication), then there is approximately 2.4µg/ml of specific IgG in the 1:25 dilution of OC2. If a similar proportion of extracellular IgG is loaded in acutely replated DRGs as in the L929 cells then the mean IgG loading will be approximately 10^3 IgG molecules introduced per cell.

Previously it has been calculated for cultured cerebellar granule neurones that 5 x 10^6 neurones have 5µg of membrane protein (E.Huston, personal communication). If a maximum of 0.7% of the total membrane protein is $G\alpha_o$ (Gierschik *et al.*1986), then the total protein weight of the $G\alpha_o$ subunits per cell is approximately 7 x 10^{-15}g. Since $G\alpha_o$ has a molecular weight of 39kD then 7 x 10^{-15}g is equivalent to 10^5 $G\alpha_o$ protein subunits per cell. The protein weight calculation for cultured cerebellar granule neurones includes extensive neurite outgrowth whilst acutely replated DRGs just consist of a cell body. The total protein concentration must therefore be less for acutely replated DRGs and therefore the number of $G\alpha_o$ per cell. The above calculation of the number of $G\alpha_o$ subunits per cell is probably an overestimate.
If the number of $G\alpha_o$ in acutely replated DRGs is approximately 10^4 and the amount of IgG loaded is proportional to the loading efficiency in Swiss 3T3 and L929 cells (ranging from 10^2 to 10^4), then the concentration of loaded IgG should theoretically be sufficient to record an effect in some cells.

4.3.3 The effect of replating DRGs in the presence of anti-Gα antisera.

4.3.3.1 The effect of baclofen inhibition of the HVA calcium channel current in DRGs replated in the presence of anti-Gα antisera.

The anti-$G\alpha_i$ antiserum was originally shown to be effective in GTPase assays at a dilution of 1:100 (McKenzie *et al.*1988). Assuming the same concentration dependence, anti-Gα antisera were then injected into NG108-15 cells in a volume calculated to be one hundredth the volume of the cell. The anti-$G\alpha_o$ antiserum (OC1) was shown to significantly reduce noradrenaline inhibition of the calcium channel current (McFadzean *et al.*1989).

In the present studies OC1 was diluted to 1:100 and 1:50 in the replating medium and both these dilutions were shown to significantly reduce baclofen inhibition of the HVA I_{Ba}, which is in agreement with McFadzean *et al.*(1989). When cells were replated with ON1 (1:50) baclofen inhibition of the HVA I_{Ba} was not significantly prevented. In agreement with this finding, it is the C-terminal of $G\alpha_o$ that is thought to be important in receptor and effector coupling whereas the N-terminal is thought to be coupling to the $G\beta\gamma$ subunits (Heideman and Bourne, 1990; Birnbaumer *et al.*1991). ON1 has however been shown to be effective at preventing baclofen stimulation of GTPase activity in neuronal membranes (Sweeney and Dolphin, 1992). This difference in the antiserum activity may be due the types of preparation used, the replating procedure introduces antisera into the cytoplasm of the DRGs whilst the GTPase assays were performed with rat brain membranes. ON1 recognised $G\alpha_o$ on immunoblots at a dilution of 1:4000 whilst OC1 was required at a dilution of 1:2500. SG1 at a dilution of 1:1000 recognised $G\alpha_i$ on immunoblots (Huston *et al.*1993).
Cells replated with SG1 at 1:50 and 1:25 did not reduce baclofen inhibition of the HVA I_{Ba}. These results indicate that in acutely replated DRGs, $G\alpha_o$ is responsible for transducing baclofen stimulation of the $GABA_B$ receptor to the N-type calcium channels.

4.3.3.2 The establishment of anti-$G\alpha_o$ antiserum specificity using pre-absorption with the $G\alpha_o$ (C-terminal) decapeptide.

The specificity of the anti-$G\alpha_o$ antiserum was established by pre-absorption of the antiserum with the peptide it was raised against. The immunocytochemical results established that 1.0µg/ml of $G\alpha_o$ decapeptide was sufficient to block $G\alpha_o$ immunoreactivity with OC2 (1:2000). Previously it has been shown that similar excessive peptide concentrations are required to pre-absorb out an antibody, Crouch (1991) used 1mg/ml to block affinity purified antibody binding to Balb/c3T3 cultured cells.

The second titre of anti-$G\alpha_o$ antiserum, OC2 was found ineffective in preventing baclofen inhibition at dilutions of 1:50 in the replating medium. When DRGs were replated with OC2 (1:25), baclofen inhibition of the HVA I_{Ba} was significantly prevented as before. When the non-immune serum was pre-incubated with the $G\alpha_o$ decapeptide (80µg/ml) for one hour at 37°C, baclofen inhibition of the HVA I_{Ba} was also significantly prevented. This concentration of $G\alpha_o$ decapeptide is equivalent to 1.0µg/ml used with OC2 (1:2000). The $G\alpha_o$ decapeptide is thought to be binding to $GABA_B$ receptor and interfering with native $G\alpha_o$ C-terminal coupling. The $G\alpha_o$ decapeptide sequence corresponds with the last 10 amino acids on the C-terminal of the $G\alpha_o$ subunit, the C-terminal is thought to be important in receptor coupling (Master *et al.*1988).

It has recently been shown that synthesised oligopeptides that correspond to part of the effector domain of the small GTP-binding protein Rab3a can stimulate complete exocytotic degranulation, like the whole Rab3a protein stimulated with GTPγS, in mouse mast cells (Oberhauser *et al.*1992). This result supports the proposed mechanism of the $G\alpha_o$ decapeptide mimicking the $G\alpha_o$ subunit and competing for the binding site on the $GABA_B$ receptor. The ability of the $G\alpha_o$ decapeptide to reduce baclofen inhibition of the peak HVA I_{Ba} independently, supports the thinking that the C-terminal of the $G\alpha_o$ subunit is involved in receptor coupling. This result is also interesting because the $G\alpha_o$ decapeptide sequence is virtually identical between the two known functional $G\alpha_o$ subunits, Go_1 and Go_2 (Hsu *et al.*1990). This result possibly indicates that the C-terminal decapeptide sequence on $G\alpha_o$ may be sufficient for receptor coupling and subsequent catalysis of GDP exchange for GTP on the $G\alpha_o$ subunit. However, if molecular diversity has functional relevance then the similarity of the C-terminal decapeptide sequences between $G\alpha_o1$ and the $G\alpha_o2$ subunits is puzzling.

It has recently been shown that specific Gß subunit subtypes are involved in specific signal transduction pathways. The muscarinic receptor inhibits calcium channel currents via the $G\beta_1$ subunit coupled to $G\alpha_o1$ whilst the somatostatin receptor inhibits calcium channel currents via the $G\beta_3$ subunit coupled to $G\alpha_o2$ (Kleuss *et al.*1992). The ability of a receptor to activate a specific $G\alpha_o$ subunit may possibly be regulated by the Gß subunit subtype in a particular heterotrimeric configuration thereby providing diversity in that signal transduction pathway. The functional role of the Gγ subunit is not yet known.

The significant prevention of baclofen inhibition induced when replating with OC2 and the $G\alpha_o$ decapeptide alone was reversed when the two were pre-incubated for one hour at 37°C. The $G\alpha_o$ decapeptide in the replating medium (80µg/ml) is in excess of OC2 (estimated as 2.4µg/ml), pre-incubation however appears to absorb a sufficient proportion of the $G\alpha_o$ subunits to partially reverse both the OC2 and the $G\alpha_o$ decapeptide independent effects on baclofen inhibition of the HVA I_{Ba}.

Both OC2 and the $G\alpha_o$ decapeptide partially reduced the current density. The independent effects of OC2 and the $G\alpha_o$ decapeptide were additive with pre-incubation and the current density was significantly reduced. How the antiserum and the decapeptide reduce the current density is not known but they seem to be acting by a mechanism that is different from their effect on signal transduction from the $GABA_B$ receptor to the calcium channel. Pre-incubation of OC2 and the $G\alpha_o$ decapeptide have opposite effects on baclofen inhibition of I_{Ba} than on the current density. A significant correlation between the current density and the percentage inhibition by baclofen on the peak current was only seen in DRGs replated in the presence of OC2 pre-incubated with the $G\alpha_o$ decapeptide. Since the current density is significantly reduced in the OC2 and $G\alpha_o$ decapeptide group and baclofen inhibition is not significantly different from the control, this is a further indication that the two effects on current density and

baclofen inhibition are independent.

4.3.4 The effect of GTPγS infusion in cells loaded with anti-Gα antiserum.

The ability to fit a double exponential to the current traces of acutely replated DRGs infused with GTPγS increased over time. This effect of GTPγS infusion was previously reported in cultured chick DRGs, once the rate of current activation had slowed sufficiently to fit a double exponential, the relative contribution of the slow component (B/A+B) increased to a final plateau value of 0.7 (Marchetti and Robello, 1989). It was rare in acutely replated DRGs for the relative proportion between the two current components to similarly change over time. The currents were slowed with GTPγS and this was clearly seen in the increase of time to peak current. However, the ability to fit a double exponential to all the current traces within a group was only seen with DRGs replated with SG1 (n=3). The inability to fit a double exponential may possibly be related to there being no DHP sensitive L-type calcium channels in acutely replated DRGs. There may also a higher proportion of the total HVA I_{Ba} in acutely replating DRGs being carried by calcium channels that have inactivation rates which complicate the activation kinetics over the test step.

The effect of GTPγS infusion on current amplitude and kinetics over time was compared between control and OC1 loaded DRGs. The ability of GTPγS to modulate the HVA I_{Ba} was not affected by replating DRGs in the presence of OC1 or OC2. The anti-$G\alpha_o$ antisera, OC1 and OC2 were raised against the C-terminal of the $G\alpha_o$ subunit and not the site that binds GDP and on activation GTP. Therefore it must be concluded that the C-terminal of the $G\alpha_o$ subunit is a sufficient distance from the GTPγS binding site for the antibody to be unable to occlude GTPγS activation.

This result contrasts with the pre-incubation of PTX, which ADP-ribosylates one amino acid in the same decapeptide sequence that OC1 and OC2 were raised against. PTX has been shown in some systems to affect GTPγS activation of the Gα subunit (Dolphin and Scott, 1987; Bergamaschi *et al.*1992). The ADP-ribosylation by PTX may possibly be creating a conformational change of the $G\alpha_o$ subunit.

4.3.5 Comparisons with other methods of anti-Gα antiserum and antibody entry into cells.

I started my investigation using the criteria of McFadzean et al (1989) where calcium channel currents were recorded after one hour from antiserum entry. The antiserum injection to a final dilution of 1:100 would provide nanomolar concentration of specific anti-$G\alpha_o$ antiserum inside NG108-15 cells. If NG108-15 cells have a similar number of $G\alpha_o$ subunits as cultured cerebellar granule neurones (10^5), then there was approximately three times as many specific antibodies injected inside the cell as $G\alpha_o$ subunits. Even with this excess of intracellular specific antibodies McFadzean *et al.*(1989) were unable to completely prevent noradrenaline inhibition of the calcium channel current with OC1. The anti-G_i antiserum injected had no significant effect. Noradrenaline inhibition of the calcium channel current in NG108-15 cells has however been shown to be prevented by pre-treatment with PTX (Kasai, 1992).
If the effect of OC1 injection is compared to the results of OC1 entry by scrape loading, with nanomolar concentrations in the replating medium, then either microinjection is not as efficient at introducing antiserum as calculated or the ability for OC1 to bind native $G\alpha_o$ subunits is limited in NG108-15 cells or facilitated in acutely replated DRGs.

Another approach using anti-Gα antibodies to study the involvement of specific G-protein subtypes in transduction pathways has been to include them in the patch pipette (Lledo *et al.*1992). In the whole cell configuration of the patch clamp technique the cell cytoplasm exchanges with the medium in the recording patch pipette (Pusch and Neher, 1988). In the investigation of Lledo et al they filled the tip of the patch pipette with affinity purified anti-G_o antibodies (180μg/ml). After 1-2 minutes from the onset of recording the calcium channel current was inhibited by the application of dopamine which in the rat anterior pituitary cells is working via the D_2 receptor. This inhibition was then taken as the control.
After 15 minutes infusion of the cell, dopamine inhibition of the calcium channel current was almost completely abolished and this was not due to receptor desensitisation. The authors stated that no consistent blockade was seen when the cells were infused for 10 minutes even though fluorescently labelled antibodies could be seen inside the cells after 6-7 minutes under ultraviolet light. The slowed onset of the antibody action probably reflects the rate of diffusion of the 150kD IgG molecule into the cell and binding to the $G\alpha_o$ subunit. The virtually complete block after 15 minutes shows that transduction was solely through G_o.

Finally, preliminary results have shown that anti-G_o antiserum diluted in the patch pipette (1:20) is capable of preventing μ-opioid receptor reduction of N-type calcium channel current in acutely dissociated DRGs (Wiley *et al.*1992). The antiserum was raised against the N-terminal of the $G\alpha_o$ subunit and a diffusion time of 20 minutes was required for the antiserum to be effective. All the results using anti-Gα antibodies to study PTX-sensitive modulation of calcium channels in neurones have indicated that $G\alpha_o$ is a common G protein subtype transducing the signal of receptor activation to calcium channels.

4.3.6 Conclusions

Only the anti-G_O antiserum reduced $GABA_B$ inhibition of the calcium channel current. The site of action of OC2 was most likely to be the C-terminal of $G\alpha_O$ because the action of OC2 was lost with pre-absorption with the $G\alpha_O$ decapeptide. In addition OC1 and OC2 were ineffective in reducing GTPγS modulation of the HVA I_{Ba}.

Since I have shown baclofen inhibits the ω-CTx-GVIA sensitive (N-type) calcium channels, it can be concluded that the $GABA_B$ receptor acts via G_O to inhibit N-type calcium channels in acutely replated DRGs.

CHAPTER FIVE

RESULTS III

5.1 The localisation of Gα subunit immunoreactivity in DRGs using anti-Gα peptide antisera and confocal microscopy.

5.1.1 INTRODUCTION

The aim of this section of my investigation was to use the anti-Gα antisera and confocal laser microscopy to localise Gα immunoreactivity in cultured DRGs. The electrophysiological findings described in chapter 1:6 and the prepulse results shown in chapter 3.2.8 predict that the Gα proteins involved in calcium channel modulation are closely localised with the calcium channels in the plasma membrane.

Using confocal laser microscopy it is possible to view a specimen in horizontal sections at specified vertical distances and acquire high resolution immunofluorescent images. This chapter only covers Gα immunoreactivity in cultured DRGs.

5.2 RESULTS

5.2.1 Anti-$G\alpha_O$ (C-terminal) antiserum staining in DRGs.

Using OC1 at a dilution of 1:2000 $G\alpha_O$ immunoreactivity was seen on DRG cell bodies and their neurites. Figure 5.1 shows eighteen consecutive cross sections taken at 1μm intervals through one unreplated DRG, which has been four days in culture. The top right section shows the attachment plaque of the DRG with neurites. As the scanning progresses up through the cell its morphological features become clear in relation to the cell's height above the coverslip. OC1 stains predominantly the cell membrane, neurites and attachment plaque.

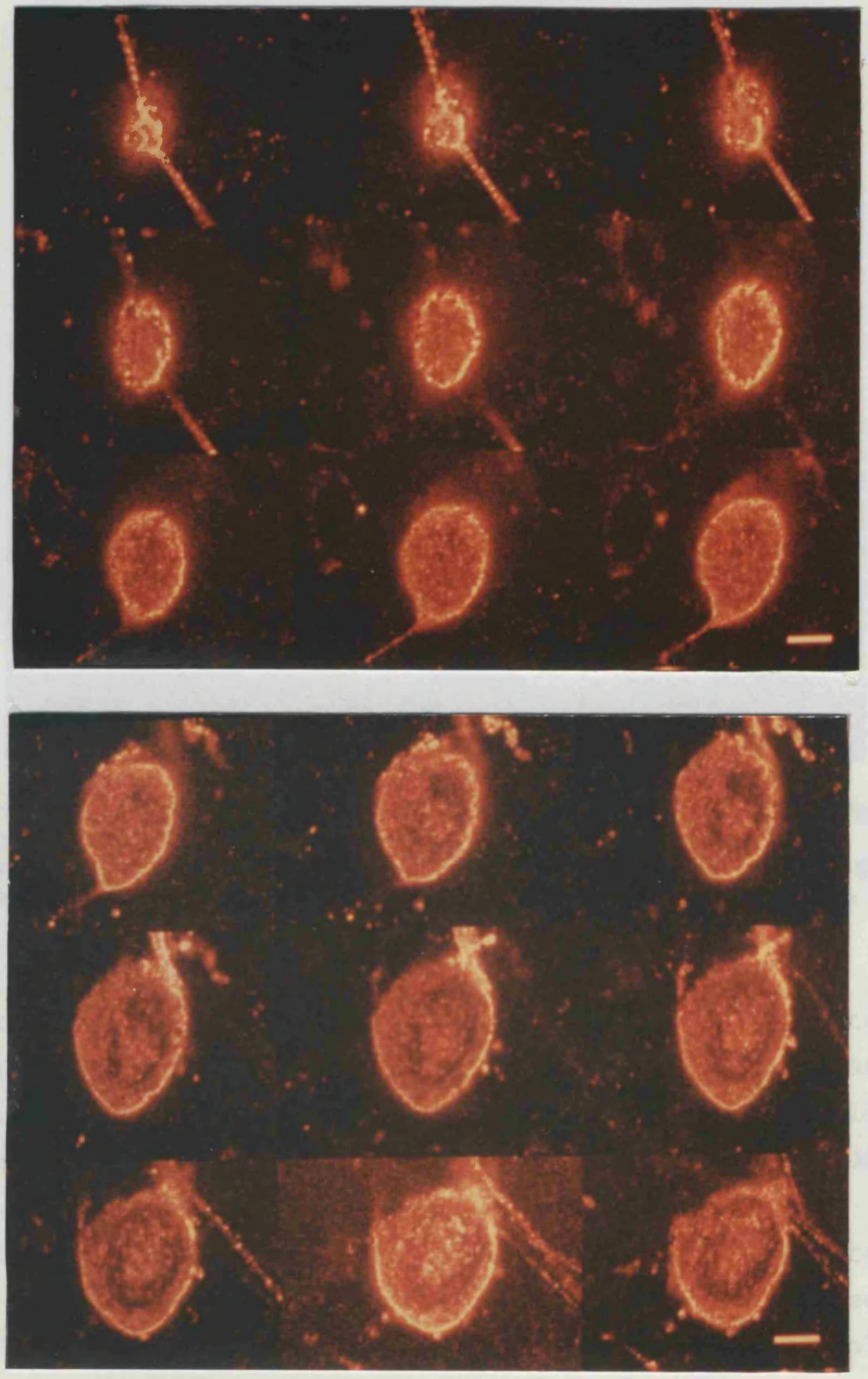

Figure 5.1 Shows anti-Gα_o (C-terminal) antiserum staining in cross sections through an unreplated DRG.
Shows eighteen consecutive cross sections of Gα_o (C-terminal) immuoreactivity taken at 1µm intervals through one unreplated DRG. OC1 (1:2000) stains predominantly the cell membrane, neurites and attachment plaque. The scale bars are 10µm.

All these images can be superimposed to create one picture showing α_o-immunoreactivity through the whole depth of the cell, see figure 5.2.

This picture is similar to conventional fluorescence microscopy except that the image is sharper because it has been built up from individual focused sections.

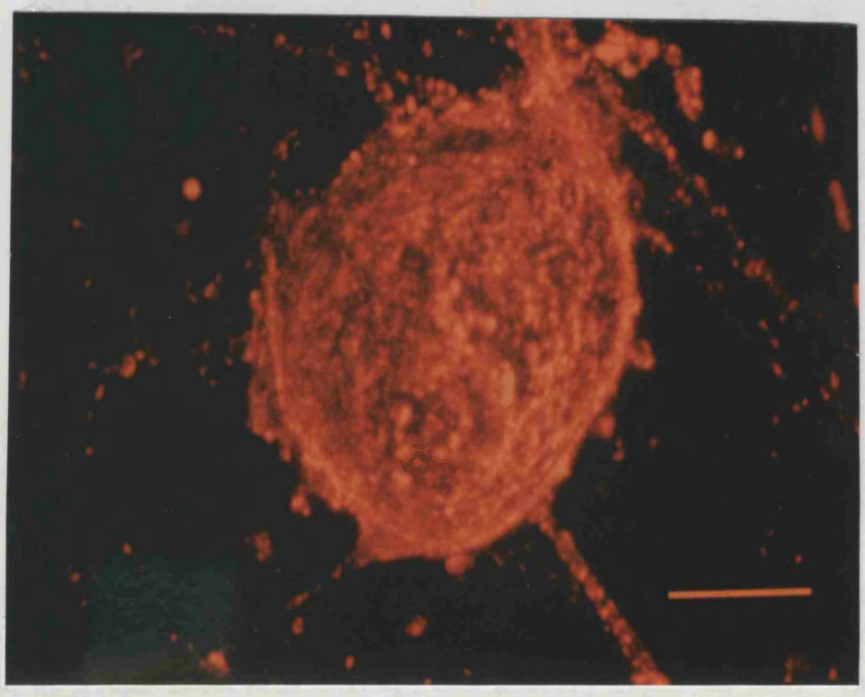

Figure 5.2 Shows a combined confocal section image of anti-$G\alpha_o$ (C-terminal) antiserum staining through an unreplated DRG
All the cross sections through the unreplated cell shown in figure 5.1 have been superimposed to give this combined image. The scale bar is 10μm.

In acutely replated DRGs OC1 was seen to produce intense $G\alpha_o$ immunoreactivity at the plasma membrane and attachment plaque, this is shown in figure 5.3. The distribution of $G\alpha_o$ immunoreactivity is very similar to unreplated DRGs. The attachment plaque in an acutely replated DRG is synthesised *de novo* once the cell suspension is plated out onto another coverslip following the replating procedure. The intense $G\alpha_o$ immunoreactivity of the attachment plaque possibly indicates a role for $G\alpha_o$ in attachment plaque function.

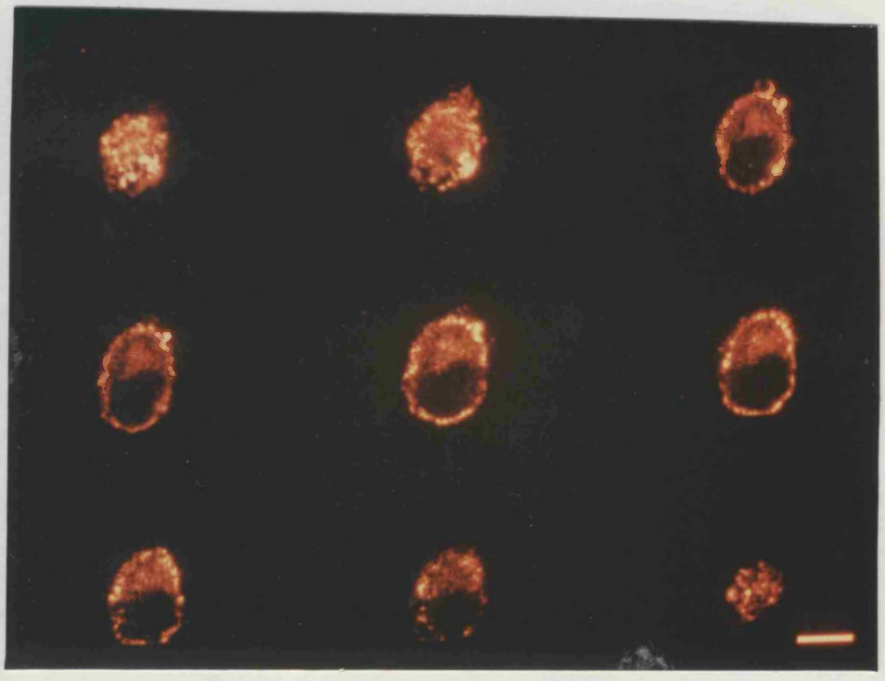

Figure 5.3 Shows confocal sections of anti-$G\alpha_o$ (C-terminal) antiserum staining in an acutely replated DRG.
The figure shows nine confocal section images of OC1 staining (1:2000) taken at 2.0μm intervals through one acutely replated DRG. The attachment plaque (top right hand image) and the plasma membrane show intense $G\alpha_o$ immunoreactivity. The scale bar is 10μm.

5.2.2 Anti-$G\alpha_o$ (N-terminal) antiserum staining in unreplated DRGs.

In contrast to OC1 (1:2000) the antiserum ON1 (1:2000) was unable to intensely stain DRGs. The brightest confocal section of N-terminal $G\alpha_o$ immunofluoresence and its corresponding phase contrast image are shown in figure 5.4. The non-neuronal cells had more immunoreactivity than the central DRG marked with the large arrow. Figure 5.5 shows the brightest confocal section of N-terminal $G\alpha_o$ immunofluoresence taken on a different day. The plasma membrane of the central DRG showed more immunoreactivity than the previous example (indicated by the small arrow). The most intense immunoreactivity was in the nucleus (indicated by the large arrow).

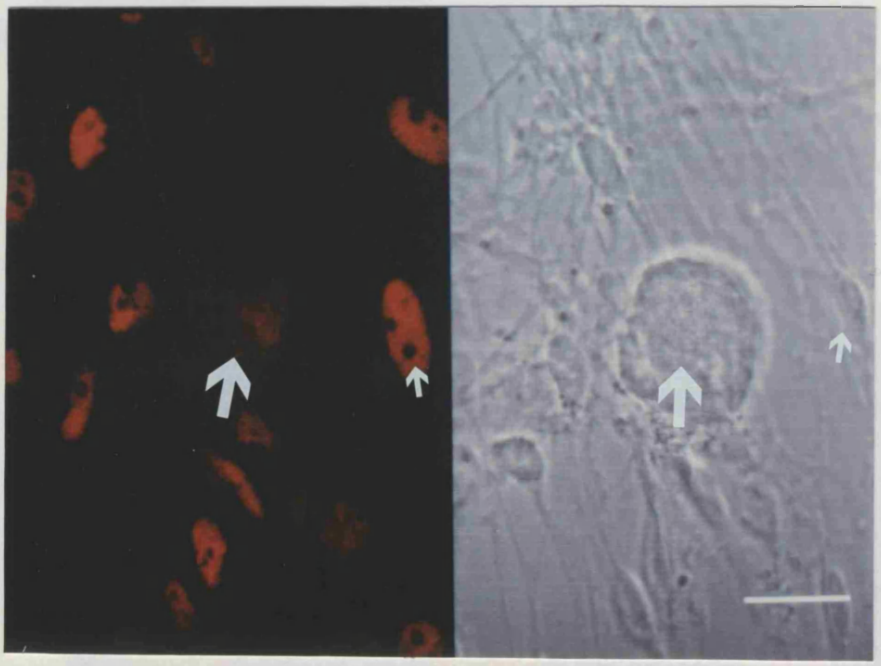

Figure 5.4 Shows anti-$G\alpha_o$ (N-terminal) antiserum staining of an unreplated cell with the corresponding phase contrast image.
This image is the brightest confocal section using ON1 (1:2000) showing $G\alpha_o$ (N-terminal) immunofluoresence on the left and the corresponding phase image on the right. The central DRG is indicated by a large arrow and one of the non-neuronal cells with the small arrow. The scale bar is 25μm.

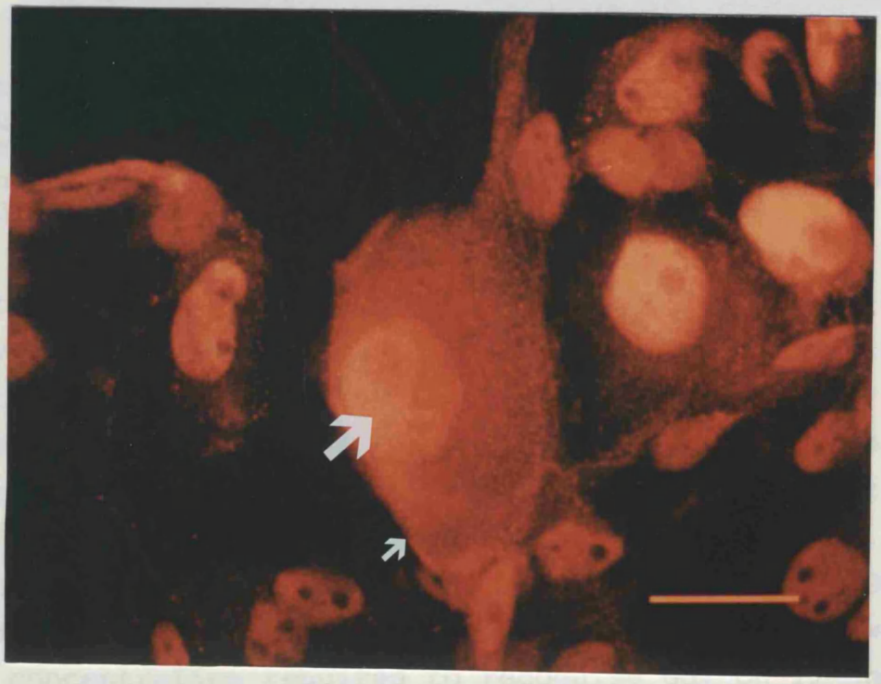

Figure 5.5 Shows the most intense anti-$G\alpha_o$ (N-terminal) antiserum immunoreactivity seen in an unreplated DRG.
The intense staining by ON1 of the nuclear region of the central DRG is indicated by the large white arrow and the immunoreactivity of the plasma membrane with the small arrow. The scale bar is 10μm.

5.2.3 Anti-$G\alpha_i$ (C-terminal) antiserum staining of unreplated DRGs.

SG1 was unable to stain the plasma membrane as intensely as OC1. The intensity of SG1 immunoreactivity in cultured DRGs was variable. Figure 5.6 shows nine confocal sections taken through one unreplated DRG incubated with SG1 (1:2000). The plasma membrane has intense immunoreactivity.

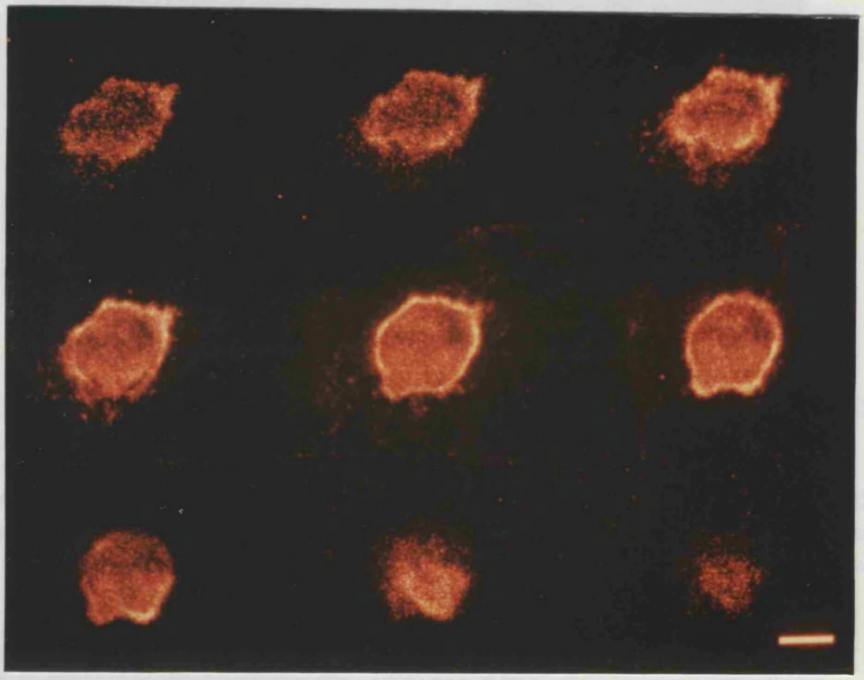

Figure 5.6 Shows confocal sections of anti-$G\alpha_i$ (C-terminal) antiserum staining in an unreplated DRG.
Shows nine confocal sections through one unreplated DRG. $G\alpha_i$ immunoreactivity is most intense at the plasma membrane. The scale bar is 10μm.

Another example of $G\alpha_i$ immunoreactivity with SG1 (1:2000) is shown in figure 5.7. In this confocal section showing a central DRG the distribution of $G\alpha_i$ immunoreactivity is not so specific. Only weak immunoreactivity can be seen in the plasma membrane and the neurite and most immunoreactivity can be seen in the cytoplasm and perinuclear region. In a later attempt to view intense $G\alpha_i$ immunoreactivity SG1 was used at a dilution of 1:500. This dilution of SG1 was twice the concentration required to recognise $G\alpha_i$ on immunoblots (Huston *et al.*1993). Figure 5.8 shows $G\alpha_i$ immunoreactivity with SG1 (1:500) in two plates of unreplated DRGs, only the cytoplasmic area shows weak immunoreactivity and none can be seen at the level of the plasma membrane (see arrows).

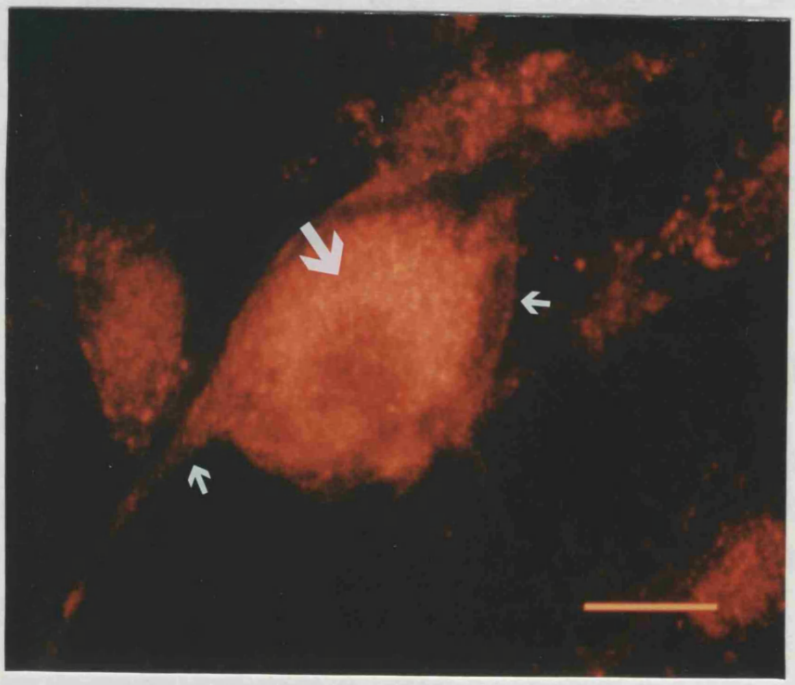

Figure 5.7 Shows a section of anti-$G\alpha_i$ (C-terminal) antiserum staining in an unreplated DRG.
This confocal fluorescent image shows the most intense $G\alpha_i$ immunoreactivity in the perinuclear and cytoplasmic regions of the DRG (large arrow). Weak $G\alpha_i$ immunoreactivity of the plasma membrane and the neurite are indicated by the small arrows. The scale bar is 10μm.

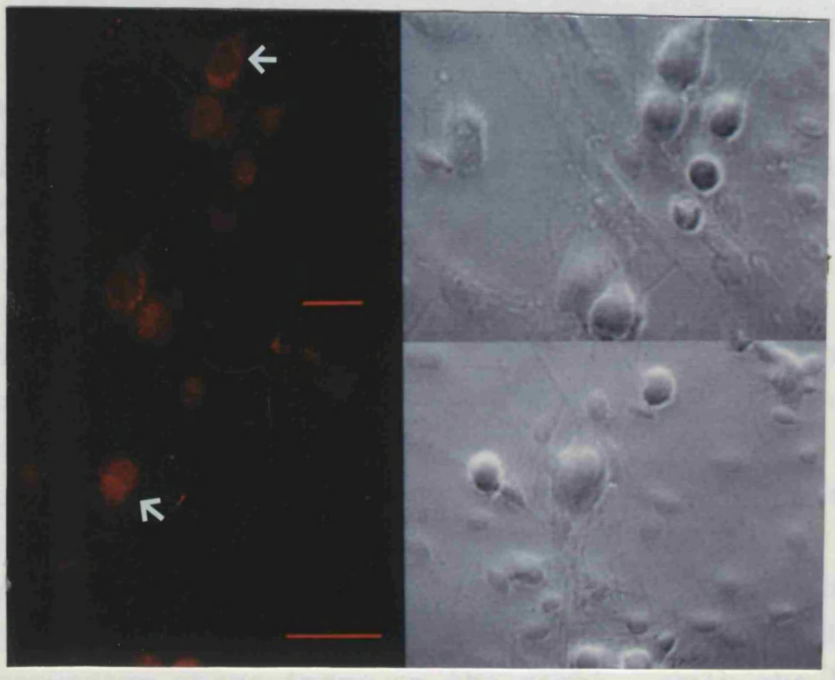

Figure 5.8 Shows $G\alpha_i$ immunoreactivity using anti-$G\alpha_i$ (C-terminal) antiserum in two plates of unreplated DRGs.
The two images on the left were stained with SG1 (1:500) and their corresponding phase images are on the right. $G\alpha_i$ immunoreactivity in these examples cannot be seen at the plasma membrane (arrows). The scale bars for the upper and lower images are 25 and 50μm respectively.

5.2.4 The localisation of anti-$G\alpha_s$ (C-terminal) antiserum in unreplated DRGs

CS1, an antiserum raised against the C-terminal decapeptide of the $G\alpha_s$ subunit was unable at a dilution of 1:2000 to stain the DRGs above the level of the non-immune serum control. Since no image was obtained with immunoreactivity greater than figure 5.9 no figure is shown.

5.2.5 Control immunofluorescence and anti-Neurofilament antibody staining of unreplated DRGs.

Figure 5.9 shows a confocal section through two closely associated unreplated DRGs incubated with non-immune serum (1:2000) and the corresponding phase image. No specific immunoreactivity can be seen.

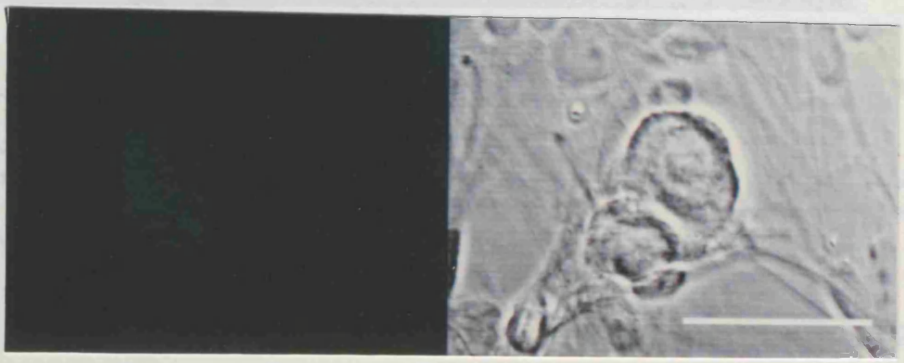

Figure 5.9 Shows a confocal section of unreplated DRGs stained with non-immune rabbit serum.
The figure shows two closely associated unreplated DRGs which have been incubated overnight with non-immune rabbit serum (1:2000). The fluorescent confocal image is on the left and the corresponding phase image is on the right. The scale bar is 50µm.

Neurofilament is a protein that is specifically expressed in neurones. In order to establish that the cells are neuronal, the cells were stained with a monoclonal anti-neurofilament antibody (1:2000), raised against the neurofilament of molecular weight 68 kD.
Figure 5.10 shows the brightest confocal section of anti-neurofilament 68 immunofluoresence on the left with the corresponding phase image on the right. Only the large diameter phase bright cells which are 25-30µm deep are seen to stain with their neurites. All non-neuronal cells lack immunoreactivity.

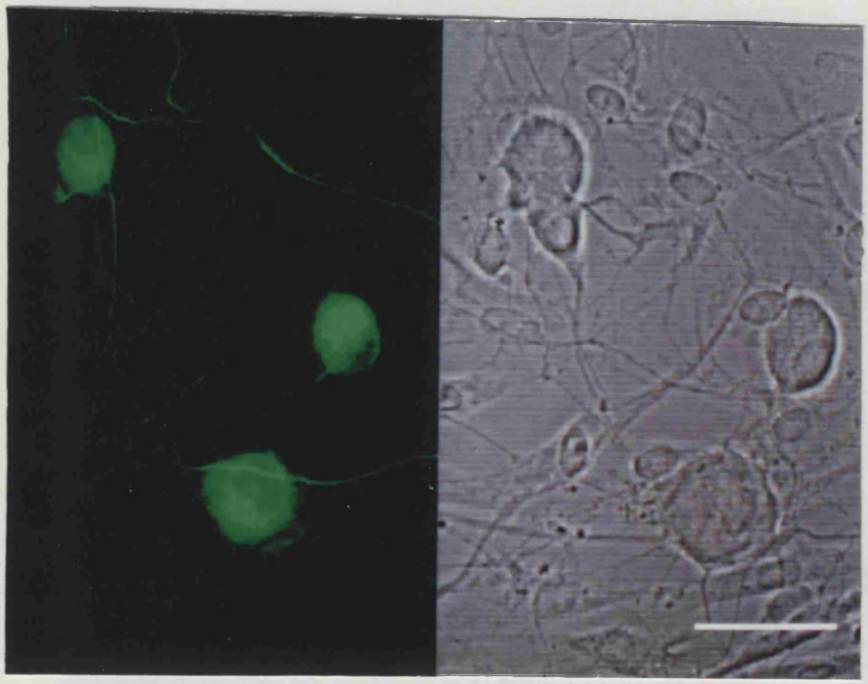

Figure 5.10 Shows anti-Neurofilament antibody staining of unreplated DRGs.
A confocal section of anti-neurofilament 68 monoclonal antibody (1:2000) immunoreactivity is shown on the left with the corresponding phase image on the right. Only the large diameter phase bright cells are seen to stain with their neurites. The scale bar is 50μm.

5.2.6 Anti-$G\alpha_o$ (C-terminal) antiserum staining in unreplated DRGs.

In agreement with the electrophysiological results, OC2 was also less effective than OC1 for immunocytochemistry. At a dilution of 1:2000 the OC2 stain of an unreplated DRG can be seen in figure 5.11. This figure shows consecutive confocal sections through one unreplated DRG. OC2 stained the DRGs less intensely and the distribution of $G\alpha_o$ immunoreactivity was also less specific. The antiserum still intensely stained the plasma membrane but the immunoreactivity of the attachment plaque was less pronounced whilst the immunoreactivity of the perinuclear region was greater.

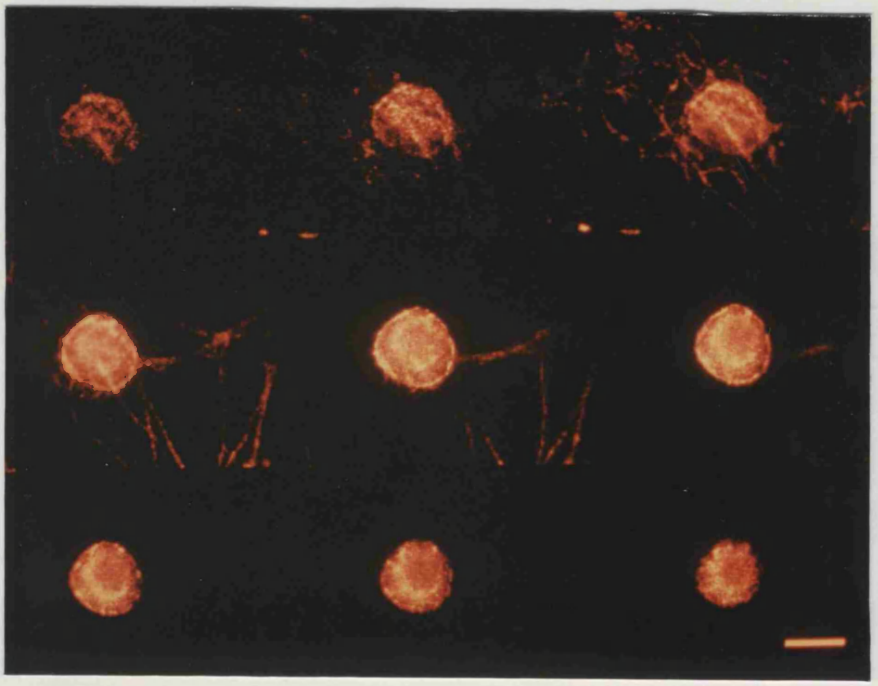

Figure 5.11 Shows confocal sections of anti-$G\alpha_o$ (C-terminal) antiserum staining in an unreplated DRG.
This picture consists of nine consecutive confocal sections taken at 1.6μm intervals through one unreplated DRG with OC2 (1:2000). OC2 intensely stained the plasma membrane, the immunoreactivity of the attachment plaque was less pronounced than with OC1 whilst the immunoreactivity of the perinuclear region was greater. The scale bar is 25μm.

OC2 was also seen to intensely stain areas of cell-cell contact in unreplated DRGs. The closely associated DRGs in figure 5.12 show most intense staining at the level of cell-cell contact.

5.2.7 The localisation and specificity of anti-$G\alpha_o$ (C-terminal) antiserum staining in unreplated DRGs.

Figure 5.13 is one confocal section showing $G\alpha_o$ immunoreactivity in an unreplated DRG using OC2 (1:2000). The intense $G\alpha_o$ immunoreactivity can be seen at the level of the plasma membrane and also in the perinuclear region. To show the localisation of the $G\alpha_o$ immunoreactivity in this unreplated DRG figure 5.13 has been superimposed on the corresponding phase image and this is shown in figure 5.14. The staining of the plasma membrane, neurite and perinuclear region clearly correspond with the phase image.

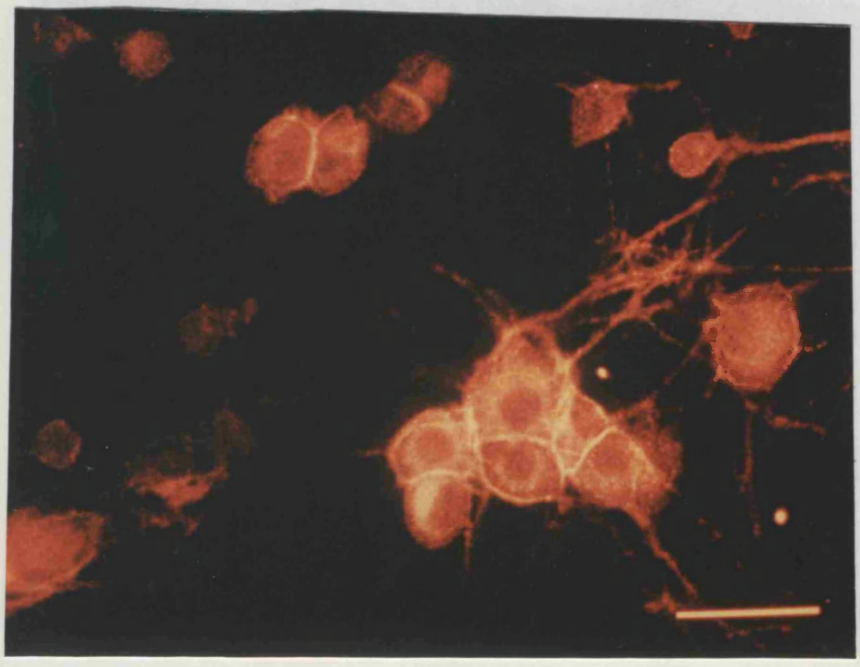

Figure 5.12 Shows anti-$G\alpha_o$ (C-terminal) antiserum staining of cell-cell contacts in unreplated DRGs
This figure shows a confocal section of unreplated DRGs in two closely associated groups of two and six cells. $G\alpha_o$ immunoreactivity is most intense at the points of cell-cell contact. The scale bar is 50µm.

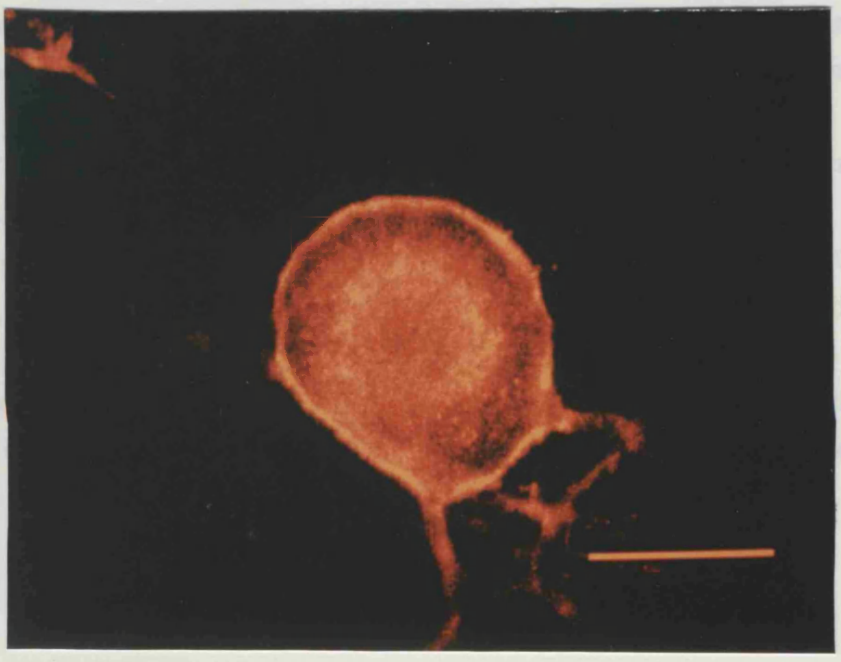

Figure 5.13 shows one confocal section of anti-$G\alpha_o$ (C-terminal) antiserum staining through an unreplated DRG.
Shows one confocal section taken through an unreplated DRG stained with OC2 (1:2000). $G\alpha_o$ immunoreactivity is seen intensely at the plasma membrane, the perinuclear region and the neurites which are only partly within the depth of the confocal sections. The scale bar is 25µm.

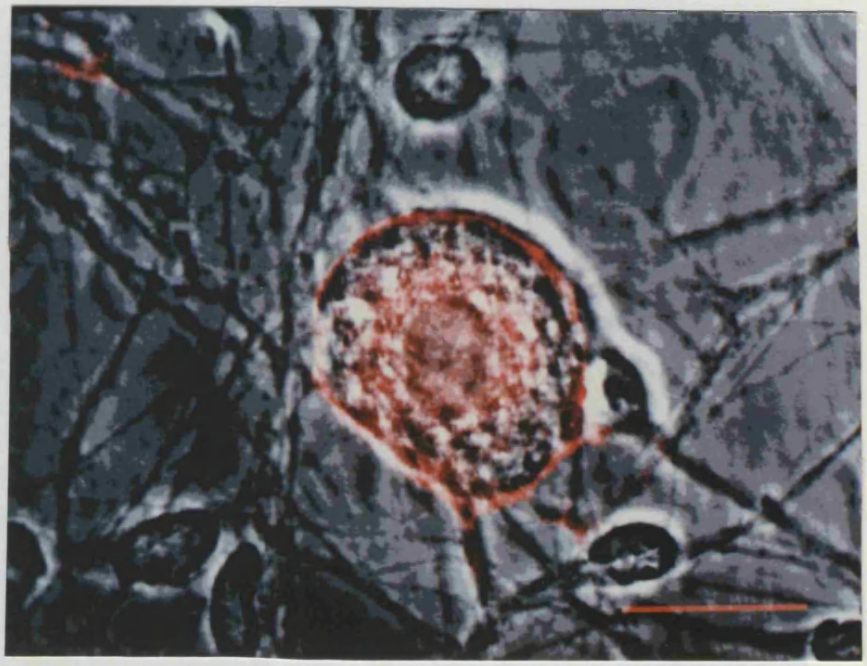

Figure 5.14 Shows anti-Gα_o (C-terminal) antiserum staining from one confocal section through an unreplated DRG superimposed on the corresponding phase contrast image.
This figure shows OC2 staining superimposed on the corresponding phase contrast image. Gα_o immunoreactivity corresponds with the plasma membrane, neurite and perinuclear region seen with the phase contrast image. The scale bar is 25μm.

In order to confirm the specificity of OC2 staining and complement the electrophysiological result, OC2 was pre-incubated with the Gα_o decapeptide (1.0μg/ml) for one hour at 37°C. OC2 alone was incubated at 37°C for one hour as a control, the staining can be seen in figure 5.13.
The brightest confocal section fluorescent image of OC2 plus the Gα_o decapeptide staining for one unreplated cell is shown in figure 5.15. Pre-absorption of OC2 with Gα_o decapeptide blocks α_o-immunoreactivity at the level of the plasma membrane but not in the perinuclear region (compare figures 5.13 and 5.15).

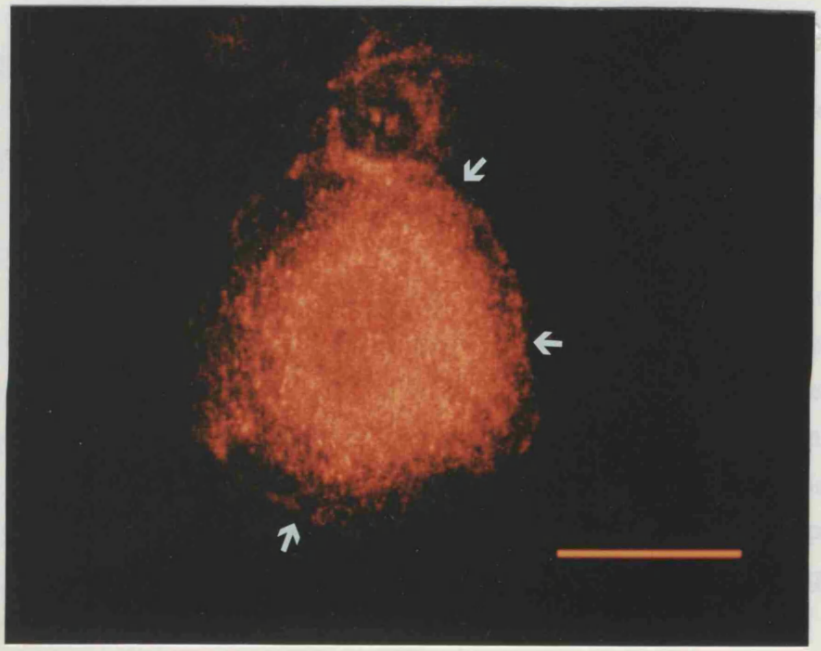

Figure 5.15 Shows $G\alpha_o$ immunoreactivity following pre-incubation of the anti-$G\alpha_o$ (C-terminal) antiserum with the $G\alpha_o$ decapeptide.
This figure shows the brightest confocal section of $G\alpha_o$ immunoreactivity taken through an unreplated DRG that was stained with OC2 (1:2000) following pre-incubation with the $G\alpha_o$ decapeptide (1.0µg/ml) for one hour at 37°C. $G\alpha_o$ immunoreactivity of the plasma membrane is blocked and this is indicated by the small arrows. The scale bar is 25µm.

5.3 DISCUSSION

5.3.1 Summary of results

1) OC1 intensely stains the plasma membrane, attachment plaque and the neurites of cultured DRGs.
2) The same profile of $G\alpha_o$ immunoreactivity is seen in acutely replated DRGs.
3) OC2 was less immunoreactive and the distribution of $G\alpha_o$ was different to OC1. The plasma membrane still stained intensely but the immunoreactivity of the attachment plaque was reduced and the perinuclear region greater.
4) OC2 immunoreactivity at the level of the plasma membrane was blocked by pre-absorption with the $G\alpha_o$ decapeptide whilst $G\alpha_o$ immunoreactivity in the perinuclear region was only slightly reduced.
5) SG1 was more variable than OC1 and OC2 staining; however, $G\alpha_i$ immunoreactivity was seen at the plasma membrane, neurites and perinuclear region.

5.3.2 Control immunocytochemical experiments.

5.3.2.1 Non-immune serum staining of cultured DRGs.

The level of autofluorescence and non-specific staining of the non-immune rabbit serum and the secondary antibody (goat anti rabbit conjugated to FITC) were evaluated. Using confocal laser scanning microscopy the gain of the photomultiplier tubes was adjusted so that the control background level was zeroed. The autofluoresence level was the same as incubation with the non-immune serum and the secondary antibody separately or together. This gain level was set so that the combined fluorescent image with the non-immune serum using the goat anti-rabbit FITC conjugate was zero and this is shown in the results.

5.3.2.2 Anti-neurofilament staining of cultured DRGs.

Cultured DRG immunofluorescence is easily identified from non-neuronal background cells by the height of the neurones above the coverslip which is easily calculated using confocal microscopy. Further confirmation is obtained by visualising the cells with phase contrast after the

fluorescent image has been recorded. DRGs are phase bright, characteristically round and range in diameter from 20-50μm. The fixed and permeabilized DRGs look very similar to the DRGs that were recorded electrophysiologically. However, in order to confirm this morphological identification, the neurones were incubated with a monoclonal antibody which was raised against neurofilament (M.W.68kD), a protein only found in neurones. The morphological identification of DRGs was confirmed. None of the background cells stained and are therefore non-neuronal.

5.3.3 The localisation of anti-$G\alpha_o$ (C-terminal) staining in cultured DRGs.

5.3.3.1 The distribution of C-terminal $G\alpha_o$ immunoreactivity in unreplated and replated DRGs using OC1.

$G\alpha_o$ is a membrane bound protein that accounts for up to one percent of the total membrane protein in specific regions of the brain (Gierschik *et al.*1986). The rapid and reversible relief of G-protein inhibition of the HVA I_{Ba} by a prepulse would predict a tightly coupled $G\alpha_o$ subunit and N-type calcium channel. This result predicts that most of the $G\alpha_o$ immunoreactivity to be found at the plasma membrane. The predominance of $G\alpha_o$ at the plasma membrane, localised alongside calcium channels, would also be expected from the result with $GTP_\gamma S$ infusion. $GTP_\gamma S$ is able to activate all the G-protein subtypes, yet when infused into acutely replated DRGs, it mimics the application of baclofen which I have shown is transduced by $G\alpha_o$. OC1 stained specifically the plasma membrane, neurites and the attachment plaque.

5.3.3.2 The distribution of C-terminal $G\alpha_o$ immunoreactivity in unreplated DRGs using OC2.

OC2 was less effective in my electrophysiological experiments and the dilution in the replating medium had to be doubled. $G\alpha_o$ immunoreactivity was also reduced and there were differences in the localisation of $G\alpha_o$ immunoreactivity. OC2 still intensely stained the plasma membrane whilst the attachment plaque stained less and the perinuclear region stained more intensely than before. OC2 was raised in another rabbit.

5.3.3.3 The investigation into the specificity of $G\alpha_o$ immunoreactivity using the $G\alpha_o$ decapeptide.

The intense $G\alpha_o$ immunofluorescence at the plasma membrane is blocked by pre-incubation of OC2 with the $G\alpha_o$ decapeptide. The $G\alpha_o$ decapeptide (1.0µg/ml) was in excess of OC2 (1:2000 = approximately 30ng/ml). In the electrophysiological experiments the OC2 concentration was sufficient to reverse the effect of the $G\alpha_o$ decapeptide alone on baclofen inhibition of the HVA I_{Ba}. In contrast to the $G\alpha_o$ immunoreactivity of the plasma membrane the perinuclear and cytoplasmic immunoreactivity was not blocked as effectively by pre-incubation with the $G\alpha_o$ decapeptide. Since the block of the plasma membrane $G\alpha_o$ immunoreactivity was so effective when OC2 was pre-incubated with the $G\alpha_o$ decapeptide then it is possible that OC2 is recognising another protein in addition to $G\alpha_o$ in the perinuclear and cytoplasmic regions.

5.3.3.4 The distribution of N-terminal $G\alpha_o$ immunoreactivity in unreplated DRGs.

ON1 did not intensely stain the DRG plasma membrane and most immunoreactivity was seen at the level of the nucleus. The ON1 immunoreactivity in the non-neuronal cells were also as intense as the DRGs. Even though this antiserum did not prevent baclofen inhibition of the HVA I_{Ba} in acutely replated DRGs, ON1 was effective in a preparation of neuronal membranes at blocking baclofen stimulation of GTPase activity (Sweeney and Dolphin, 1992). In immunoblots ON1 has been shown to recognise $G\alpha_o$ at a dilution of 1:4000 whilst OC1 only recognised $G\alpha_o$ at a dilution of (1:2500) (Huston *et al.*1993). The N-terminal of the Gα subunit is thought to couple Gßγ subunits in the cell membrane (Birnbaumer *et al.*1991). When the cultured DRGs were fixed with paraformaldehyde, this region may be fixed in a position unavailable for coupling with the antiserum or the N-terminal of $G\alpha_o$ was modified during the fixing procedure. The specificity of the stain on the non-neuronal cells was not evaluated further.

5.3.4 The localisation of anti-$G\alpha_i$ (C-terminal) antiserum staining in cultured DRGs.

The intensity of anti-G_i antiserum staining varied between DRGs. $G\alpha_i$ immunoreactivity was observed at the level of the plasma membrane, neurites and the perinuclear region. SG1 was shown to recognise $G\alpha_i$ in immunoblots at 1:1000 (Huston *et al.*1993). In some experiments no plasma membrane $G\alpha_i$ immunoreactivity was seen even with SG1 at a dilution of 1:500, the reason for this variability was not established. Since $G\alpha_i$ immunoreactivity was so variable , pre-absorption studies were not attempted. $G\alpha_i$ localisation in the plasma membrane would be expected because it is involved in inhibition of adenylyl cyclase activity. It has been shown in the cerebral cortex that the concentration of G_o is five times that of G_i (Gierschik *et al.*1986) therefore the concentration of $G\alpha_i$ subunits may possibly be much less than $G\alpha_o$ subunits in the plasma membrane of cultured DRGs.

5.3.5 Anti-$G\alpha_s$ antiserum staining in unreplated DRGs

The anti-$G\alpha_s$ antiserum has been shown to be effective at recognising $G\alpha_s$ on immunoblots at a dilution of 1:10000 (Huston *et al.*1993). However no immunoreactivity above the background was seen. The result from the immunoblot again does not agree with the immunocytochemistry result. The two procedures differ considerably in the way the Gα proteins are prepared.

5.3.6 Comparisons with other investigations using anti-Gα antisera.

Most of the studies of $G\alpha_o$ immunoreactivity have been performed using immunoblots of neuronal membrane fractions (Gierschik *et al.*1986; Inanobe *et al.*1990; Asano *et*

*al.*1992). Previously, the ultrastructural localisation of G_O had been shown in whole brain and cultured murine neurones, using affinity-purified polyclonal antibodies raised against the $G\alpha_O$ subunit (Gabrion *et al.*1989). The electron micrographs produced showed labelling on the cytoplasmic face of the plasma membrane lining the cell body and the neurites, especially in 'cell-cell' contacts, but also in the cytoplasmic matrix, between the endoplasmic reticulum and Golgi cisternae.

In cultured DRGs I too saw intense $G\alpha_O$-immunoreactivity at cell-cell contacts and the cytoplasmic matrix. $G\alpha_O$ immunoreactivity has also been seen in growth cones (data not shown). The functional significance of $G\alpha_O$ in these regions is not clear. However, $G\alpha_O$ represents a significant percentage (0.7%) of total membrane protein so it is probably involved in more roles than neurotransmitter modulation of calcium channel currents. There is evidence in PC12 cells that calcium influx through L- and N-type calcium channels is important for neurite outgrowth and this mechanism is sensitive to PTX (Doherty *et al.*1991).

The main finding of Gabrion et al. was that $G\alpha_O$ immunoreactivity was not observed on the inner face of the pre- or postsynaptic membranes in adult brain and cultured neurones. This last finding led them to conclude that there was a strong suggestion that $G\alpha_O$ protein is not involved in transducing chemical signals at the level of the synapse. If acutely replated DRGs are a reasonable model of their pre-synaptic terminal <u>in vivo</u> then my electrophysiological data disagrees with this suggestion.

5.3.7 Conclusion

Using immunocytochemical techniques I have shown that of the two PTX sensitive G-proteins subtypes found in neurones, the major PTX substrate $G\alpha_o$ shows the most immunoreactivity at the level of the DRG plasma membrane. Using concentrations of anti-G_i antiserum which have been shown to be effective in immunoblots I was unable to routinely visualise intense $G\alpha_i$ immunoreactivity at the plasma membrane. The predominant $G\alpha_o$ immunoreactivity in the plasma membrane complements the electrophysiological results that $G\alpha_o$ is the PTX sensitive G-protein responsible for calcium channel modulation by $GABA_B$ receptors.

CHAPTER SIX

DISCUSSION

6.1 CONCLUSIONS

I have shown that the G-protein responsible for transduction of $GABA_B$ receptor inhibition of calcium channel currents in acutely replated DRGs, is $G\alpha_o$. The calcium channel subtype which is modulated through the $G\alpha_o$ pathway is the ω-CTX-GVIA sensitive, N-type calcium channel. The rapid and reversible relief of G protein inhibition by a pre-pulse, would predict that this G-protein and calcium channel were tightly coupled at the plasma membrane. This prediction is supported by the result that $G\alpha_o$ immunoreactivity is intensely localised at the plama membrane in cultured DRGs. Both the reduction of baclofen inhibition of the calcium channel current and the intense immunofluorescence produced with the anti-$G\alpha_o$ antisera were reversed by pre-incubation with the $G\alpha_o$ decapeptide.

6.2 Future investigations

Four $G\alpha_o$-type proteins have been purified from the bovine brain (Inanobe *et al.*1990) and two forms of $G\alpha_o$ have been shown to exist by immunocytochemical (Asano *et al.*1992) and electrophysiological experiments (Kleuss *et al.*1991). The anti-$G\alpha_o$ antisera (OC1 and OC2) were raised against the end C-terminal decapeptide (residues 344-345) that correspond to the $G\alpha_o1$ sequence (ANNLRGCGLY), the $G\alpha_o2$ C-terminal decapeptide sequence differs from $G\alpha_o1$ by one amino acid residue in this region. The Asparagine (N) is replaced by a Lysine residue. OC1 and OC2 antisera are probably able to identify both forms of $G\alpha_o$ because there is insufficient variability for specific antiserum generation in the C-terminal decapeptide region.

It may be possible to differentiate between the two $G\alpha_o$ subtypes by loading DRGs with antisera that have already been generated which distinguish between $G\alpha_oA$ and $G\alpha_oB$ on immunoblots (Asano *et al.*1992). Asano et al. raised specific antisera with amino acid sequences from G_oA and G_oB ($G\alpha_o1$ and $G\alpha_o2$) that had no homology (between residues 294-311). These sequences are still within the last 40% of Gα subunit that is thought to be responsible for coupling to the receptor (Heideman and Bourne, 1990; Masters *et al.*1988).

Since the $G\alpha_o$ decapeptide was effective at preventing baclofen inhibition of the HVA I_{Ba}, then another approach that could be used to distinguish between the Gα subtypes involved in a transduction pathway would be to replate cells with specific peptide fragments of Gα subunit subtypes. This approach was used originally to evaluate the role of Gα subunits in signal transduction. Following pre-incubation with PTX, neurotransmitter inhibition was restored by infusing cells with purified Gα subunits from the pipette. Reconstitution studies have indicated that calcium channel currents are not inhibited exclusively by $G\alpha_o$ because $G\alpha_i$ can also restore neurotransmitter inhibition of calcium channel currents (Hescheler *et al.*1987; Toselli *et al.*1989; Linder *et al.*1990). Intracellular application of anti-Gα antiserum however, have implicated that $G\alpha_o$ and not $G\alpha_i$ transduce neurotransmitter inhibition of the calcium channel current (McFadzean *et al.*1989; Lledo *et al.*1992).

Recently microinjection of $G\alpha_o1$, $G\alpha_o2$ and $G\alpha_i3$ peptides, activated with $GTP_\gamma S$ or Gpp(NH))p, have shown that $G\alpha_o2$ selectively reduces the HVA calcium current in Helisoma B5 neurones. $G\alpha_o1$ and $G\alpha_i3$ are ineffective at 10 times the concentration of $G\alpha_o2$ (Man-Son-Hing *et al.*1992). The specificity of this result using pre-activated Gα subunits compared to the reconstitution studies may result from the

different concentrations used in the two preparations. The investigation of Hescheler et al.(1987) included purified G_i and G_o in the patch pipette at concentrations of 3.8 and 0.4nM respectively to restore DADLE inhibition of the calcium channel current in neuroblastoma x glioma cells. The intracellular dialysis of $G\alpha_o$ at the same concentration (10nM) as the holo-protein (G_o) was also shown to be as effective at restoring acetylcholine inhibition of the calcium channel currents in hippocampal neurones (Toselli *et al.*1989). Linder et al.(1989) used 100nM of recombinant Gα subunits in the patch pipette, the subtypes $G\alpha_i1$, $G\alpha_i2$, $G\alpha_i3$ and $G\alpha_o$ were all able to reconstitute bradykinin inhibition, while $G\alpha_i2$ was inactive at restoring neuropeptide Y inhibition of the calcium channel current in DRGs. Man-Son-Hing et al.(1992) however, estimate that the microinjection solution (1nM) is diluted 1:100 when injected into cells. The threshold concentration for pre-activated $G\alpha_o2$ inhibition of the calcium channel current was therefore estimated to be about 10pM.

The use of peptides or peptide fragments is especially suited for the acutely replated DRG model because these relatively small molecules would be efficiently loaded during the replating procedure. My results of baclofen inhibition of the HVA I_{Ba} in DRGs replated in the presence of the anti-Gα antisera and the $G\alpha_o$ decapeptide were taken 60-90 minutes following the replating procedure. This time was sufficient for cell adhesion and to record an effect.

Replated DRGs were able to put out extensive neurites after 90 minutes and could be successfully maintained, at their lower density, in culture. The introduction of macromolecules by the replating procedure can therefore be studied over longer time periods. This approach has been used to introduce active enzymes, missing because of a genetic defect, in the L929 cell line (Ortiz *et al.*1987) as well as the evaluation of ras oncogene proteins in the intracellular signal transduction pathway of neurotrophic factors (Borasio *et al.*1989). The replating procedure could also be used for the introduction of DNA oligonucleotides.

6.3 Molecular biological approaches to investigate G-protein modulation of calcium channels.

During my investigation using anti-G-protein antibodies two molecular biological approaches have also been used by others to evaluate G protein tranduction pathways. The first technique is to block the synthesis of a specific protein at the level of the DNA by the introduction of antisense DNA. This technique manipulates the continual cycle of protein degradation and synthesis which occurs in all cells. Once the antisense DNA has bound to a specific sequence of DNA the transcription of that DNA sequence, translation and subsequent protein synthesis is blocked (Hélène and Toulmé, 1990). The total level of the protein falls as the rate of degradation and turnover exceeds production until finally that protein is not expressed in the cell. Antisense DNA specific for the DNA sequences of $G\alpha_o1$ and $G\alpha_o2$ have been injected into GH3 cells. Modulation of calcium channel currents by muscarinic receptor activation is only blocked with antisense DNA for $G\alpha_{o1}$ whilst antisense DNA for $G\alpha_{o2}$ blocks calcium channel modulation by somatostatin receptor activation (Kleuss *et al.*1991). This study was extended using antisense DNA specific to DNA sequences that encode the Gß subunits, to investigate the involvement of Gß subunits in this transduction process. It was shown that of the four Gß subunits tested, Gß1 and Gß3 were selectively involved in signal transduction from muscarinic M4 and somatostatin receptors respectively, to inhibit voltage-operated calcium channels (Kleuss *et al.*1992). This result highlights the importance of the Gß subunit for specific receptor coupling and also expands the possible number of combinations of heterotrimeric G proteins which may be specifically associated to a receptor subtype.

The second molecular biological approach used to study G protein transduction pathways has been to generate using site directed mutagenesis a $G\alpha_{O}A$ subunit that is PTX resistant (Taussig *et al.*1992). The DNA template of NG108-15 cells was hybridized with the mutated oligonucleotide sequence and a modified DNA template was created which encoded a $G\alpha_{O}A$ subunit with a cysteine to serine change (4 residues from the carboxyl terminus). This is the site of ADP-ribosylation by PTX. Modified DNA was then transfected into an NG108-15 cell line. After treatment with PTX, the mutant $G_{\alpha O}A$ rescued the Leu-enkephalin and noradrenaline pathways but not the somatostatin inhibition of calcium channel currents in NG108-15 cells.

Both of these techniques take advantage of the wealth of molecular biological information available for G proteins. In combination with the recent advances in calcium channel cloning and expression it is now possible to accurately investigate G-protein transduction and modulation of calcium channels.

REFERENCES

Adams, M.E., V. P. Bindokas, A. C. Dolphin, and R. H. Scott. 1989. The inhibtion of Ca^{2+} channel currents in cultured rat dorsal root ganglion (DRG) neurones by w-agatoxin 1A (a funnel web spider toxin). *J. Physiol.* 418:34P.(Abstr.)

Adams, M.E., R. A. Myers, J. Imperial, and B. M. Olivera. 1992. Toxityping calcium channels in the mammalian brain with radiolabelled ω-Agatoxins and ω-conotoxins. *Society for Neuroscience* 10.6:(Abstr.)

Akaike, N. 1991. T-type calcium channel in mammalian CNS neurones. *Comp. Biochem. Physiol. [C]* 98C:31-40.

Aosaki, T. and H. Kasai. 1989. Characterization of two kinds of high-voltage-activated Ca- channel currents in chick sensory neurons. *Pflügers Arch* 414:150-156.

Arshavsky, V.Yu. and M. D. Bownds. 1992. Regulation of deactivation of photoreceptor G protein by its target enzyme and cGMP. *Nature* 357:416-417.

Artalejo, C.R., S. Rossie, R. L. Perlman, and A. P. Fox. 1992. Voltage-dependent phosphorylation may recruit Ca^{2+} current facilitation in chromaffin cells. *Nature* 358:63-66.

Asano, T., R. Morishita, and K. Kato. 1992. Two forms of G_o Type G Proteins: Identification and Distribution in Various Rat Tissues and Cloned Cells. *J. Neurochem.* 58:2176-2181

Asano, T., M. Ui, and N. Ogasawara. 1985. Prevention of the agonist binding to y-aminobutyric acid B receptors by guanine nucleotides and islet-activating protein, pertussis toxin, in bovine cerebral cortex. *J. Biol. Chem.* 260, No.23:12653-12658.

Augustine, G.J., E. M. Adler, and M. P. Charlton. 1991. The calcium signal for transmitter secretion from presynaptic nerve terminals. *Ann. N. Y. Acad. Sci.* 635:365-381.

Axelrod, J., R. M. Burch, and C. L. Jelsema. 1988. Receptor-mediated activation of phospholipase A2 via GTP-binding proteins: arachidonic acid and its metabolites as second messengers. *TiNS* 11:117-123.

Bailey, C.H. and M. Chen. 1983. Morphological Basis of Long-Term Habituation and Sensitization in Aplysia. *Science* 220:91-93.

Barlow, H.B. 1987. General principles: the senses considered as physical instruments. In The senses. H. B. & Mollon Barlow,J.D., editor. Cambridge University Press, Cambridge, London, NY, New Rochelle, Melbourne, Sydney.

Bean, B.P. 1989. Neurotransmitter inhibition of neuronal calcium currents by changes in channel voltage-dependence. *Nature* 340:153-155.

Beech, D.J., L. Bernheim, and B. Hille. 1992. Pertussis Toxin and Voltage Dependence Distinguish Multiple Pathways Modulating Calcium Channels of Rat Sympathetic Neurons. *Neuron* 8:97-106.

Bergamaschi, S., S. Govoni, F. Battaini, M. Trabucchi, S. Del Monaco, and M. Parenti. 1992. G Protein Modulation of ω-Conotoxin Binding Sites in Neuroblastoma X Gliamo NG 108-15 Hybrid Cells. *J. Neurochem.* 59:536-543.

Berridge, M.J. and R. F. Irvine. 1989. Inositol phosphates and cell signalling. *Nature* 341:197-205.

Berstein, G., J. L. Blank, D-Y. Jhon, J. H. Exton, S. G. Rhee, and E. M. Ross. 1992. Phospholipase C-ß1 Is a GTPase-Activating Protein for $G_{q/11}$, Its Physiological Regulator. *Cell* 70:411-418.

Birnbaumer, L., E. Perez-Reyes, P. Bertrand, T. Gudermann, X. Y. Wei, H. Kim, A. Castellano, and J. Codina. 1991. Molecular diversity and function of G proteins and calcium channels. *Biol. Reprod.* 44:207-224.

Blaustein, M.P. 1988. Calcium transport and buffering in neurons. *TiNS* 11:438-443.

Bley, K.R. and R. W. Tsien. 1990. Inhibition of Ca^{2+} and K^{+} channels in sympathetic neurons by neuropeptides and other ganglionic transmitters. *Neuron* 4:379-391.

Borasio, G.D., J. John, A. Wittinghofer, Y. -A. Barde, M. Sendtner, and R. Heumann. 1989. ras p21 protein promotes survival and fiber outgrowth of cultured embryonic neurons. *Neuron* 2:1087-1096.

Bourne, H.R., D. A. Sanders, and F. McCormick. 1991. The GTPase superfamily: conserved structure and molecular mechanism. *Nature* 349:117-127.

Brehm, P. and R. Eckert. 1978. Calcium entry leads to inactivation of calcium channel in Paramecium. *Science* 202:1203-1206.

Brown, A.M. 1991. A cellular logic for G protein-coupled ion channel pathways. *FASEB J.* 5:2175-2179.

Brown, D.A. 1990. G-Proteins and Potassium Currents in Neurons. *Ann. Rev. Physiol.* 52:215-242.

Campbell, K.P., A. T. Leung, and A. H. Sharp. 1988. The biochemistry and molecular biology of the dihydropyridine-sensitive calcium channel. *TiNS* 11:425-430.

Camps, M., A. Carozzi, P. Schnabel, A. Scheer, P. J. Parker, and P. Gierschik. 1992. Isozyme-selective stimulation of phospholipase C-ß2 by G protein ßγ-subunits. *Nature* 360:684-686.

Carbone, E. and H. D. Lux. 1984. A low voltage-activated, fully inactivating Ca channel in vertebrate sensory neurones. *Nature* 310:501-502.

Cervero, F. 1986. Dorsal Horn Neurons and their Sensory Inputs. In Spinal Afferent Processing. T. L. Yaksh, editor. Plenum Press, New York and London. 197-213.

Cox, D.H.; Dunlap,K. 1992. Pharmacological Discrimination of N-Type from L-Type Calcium Current and its Selective Modulation by Transmitters. *J. Neurosci.* 12:906-914.

Crouch, M.F. 1991. Growth factor-induced cell division is paralleled by translocation of $G_{i\alpha}$ to the nucleus. *FASEB J.* 5:200-206.

Curtis, B.M. and W. A. Catterall. 1984. Purification of the Calcium Antagonist Receptor of the Voltage-Sensitive Calcium Channel from Skeletal Muscle Transverse Tubules. *Biochemistry* 23:2113-2118.

De Waard, M., M. Seagar, A. Feltz, and F. Couraud. 1992. Inositol Phosphate Regulation of Voltage-Dependent Calcium Channels in Cerebellar Granule Neurons. *Neuron* 9:497-503.

Delcour, A.H. and R. W. Tsien. 1993. Neurotransmitter Inhibition of Unitary N-type Calcium Channel Activity by Altered Equilibria Between Gating Modes. *Science* (In Press)

DeRiemer, S., J. Strong, K. Albert, P. Greengard, and L. Kaczmarek. 1987. Enhancement of calcium current in Aplysia neurones by protein kinase C. *Nature* 313:313-316.

Docherty, R.J. and I. McFadzean. 1989. Noradrenaline-induced inhibition of voltage-sensitive calcium currents in NG108-15 hybrid cells. *Eur. J. Neurosci.* 1, No.2:132-140.

Dodge, F.A.,Jr. and R. Rahamimoff. 1967. Co-operative action of calcium ions in transmitter release at the neuromuscular junction. *J. Physiol.* 193:419-432.

Doherty, P., S. V. Ashton, S. E. Moore, and F. S. Walsh. 1991. Morphoregulatory activities of NCAM and N-Cadherin can be accounted for by G Protein-dependent activation of L- and N-Type neuronal Ca^{2+} channels. *Cell* 67:21-33.

Dolphin, A.C. 1987. Nucleotide binding proteins signal transduction and disease. *TiNS* 10:53-57.

Dolphin, A.C. 1990. G-Proteins and the Regulation of Ion Channels. In G-Proteins as Mediators of Cellular Signalling Processes. M. D. Houslay and G. Milligan, editors. John Wiley

& Sons Ltd, 125-150.

Dolphin, A.C. 1991.
Ca^{2+} channel currents in rat sensory neurones: Interaction between guanine nucleotides, cyclic AMP and Ca^{2+} channel ligands. *J. Physiol.* 432:23-43.

Dolphin, A.C. 1992. The effect of phosphatase inhibitors and agents increasing cyclic-AMP-dependent phosphorylation on calcium channel currents in cultured rat dorsal root ganglion neurones: interaction with the effect of G protein activation. *Pflügers Arch* 421:138-145.

Dolphin, A.C., E. Huston, H. A. Pearson, A. Menon-Johansson, M. I. Sweeney, M. E. Adams, and R. H. Scott. 1991. G protein modulation of calcium entry and transmitter release. In Calcium entry and action at the presynaptic terminal. E. F. Stanley, M. C. Nowycky, and D. J. Triggle, editors. Annals of NY Acad of Sciences, New York. 139-152.

Dolphin, A.C., S. M. McGuirk, and R. H. Scott. 1989. An investigation into the mechanisms of inhibition of calcium channel currents in cultured sensory neurones of the rat by guanine nucleotide analogues and (-)-baclofen. *Br. J. Pharmacol.* 97:263-273.

Dolphin, A.C. and S. A. Prestwich. 1985. Pertussis toxin reverses adenosine inhibition of neuronal glutamate release. *Nature* 316:148-150.

Dolphin, A.C. and R. H. Scott. 1987. Calcium channel currents and their inhibition by (-)-baclofen in rat sensory neurones: modulation by guanine nucleotides. *J. Physiol.* 386:1-17.

Dolphin, A.C. and R. H. Scott. 1989. Interaction between calcium channel ligands and guanine nucleotides in cultured rat sensory and sympathetic neurones. *J. Physiol.* 413:271-288.

Doroschenko, P.A., P. G. Kostyuk, and A. I. Martynyuk. 1982. Intracellular metabolism of adenosine 3'-5'-cyclic monophosphate and calcium inward current in perfused neurones of *Helix pomatia*. *Neuroscience* 7:2125-2134.

Dubel, S.J., T. V. B. Starr, J. Hell, M. K. Ahlijanian, J. J. Enyeart, W. A. Catterall, and T. P. Snutch. 1992. Molecular cloning of the α-1 subunit of an ω-conotoxin-sensitive calcium channel. *Proc. Natl. Acad. Sci. U. S. A.* 89:5058-5062.

Dumuis, A., M. Sebben, L. Haynes, J. -P. Pin, and J. Bockaert. 1988. NMDA receptors activate the arachidonic acid cascade system in striatal neurons. *Nature* 336:68-70.

Dunlap, K. and G. D. Fischbach. 1978. Neurotransmitters decrease the calcium component of sensory neurone action potentials. *Nature* 276:837-839.

Elmslie, K.S., W. Zhou, and S. W. Jones. 1990. LHRH and GTPγS modify calcium current activation in bullfrog sympathetic neurons. *Neuron* 5:75-80.

Ewald, D.A., P. C. Sternweis, and R. J. Miller. 1988. Guanine nucleotide-binding protein Go-induced coupling of neuropeptide Y receptors to Ca^{2+} channels in sensory neurons. *Proc. Natl. Acad. Sci. USA* 85:3633-3637.

Fatt, P. and B. L. Ginsborg. 1958. The ionic requirements for the production of action potentials in crustacean muscle fibres. *J. Physiol.* 142:516-543.

Findlay, J. and E. Eliopoulos. 1990. Three-dimensional modelling of G protein-linked receptors. *TiPS* 11:492-499.

Formenti, A. and V. Sansone. 1991. Inhibitory action of acetylcholine, baclofen and GTP-gamma- *S* on calcium channels in adult rat sensory neurons. *Neurosci. Lett.* 131:267-272.

Forscher, P., G. S. Oxford, and D. Schulz. 1986. Noradrenaline modulates calcium channels in avian dorsal root ganglion cells through tight receptor-channel coupling. *J. Physiol.* 379:131-144.

Fox, A.P., M. C. Nowycky, and R. W. Tsien. 1987. Single-channel recordings of three types of calcium channels in chick sensory neurons. *J. Physiol.* 394:173-200.

Fox, A.P., M. C. Nowycky, and R. W. Tsien. 1987. Kinetics and pharmacological properties distinguishing three types of calcium currents in chick sensory neurones. *J. Physiol.* 394:149-172.

Fulton, B.P. 1987. Postnatal changes in conduction velocity and soma action potential parameters of rat dorsal root ganglion neurones. *Neurosci. Lett.* 73:125-130.

Gabrion, J., P. Brabet, B. Nguyen Than Dao, V. Homburger, A. Dumuis, M. Sebben, B. Rouot, and J. Bockaert. 1989. Ultrastructural localisation of the GTP-binding protein G_o in neurones. *Cellular Signalling* 1:107-123.

Gierschik, P., G. Milligan, M. Pines, P. Goldsmith, J. Codina, W. Klee, and A. Spiegel. 1986. Use of specific antibodies to quantitate the guanine nucleotide-binding protein G_o in brain. *Proc. Natl. Acad. Sci. U. S. A.* 83:2258-2262.

Gilman, A.G. 1987. Guanine nucleotide binding proteins: transducers or receptor-generated signals. *Ann. Rev. Biochem.* 56:615-619.

Grassi, F. and H. D. Lux. 1989. Voltage-dependent GABA-induced modulation of calcium currents in chick sensory neurons. *Neuroscience Letters* 105:113-119.

Gray, W.R. and B. M. Olivera. 1988. Peptide Toxins from

Venomous Conus Snails. *Ann. Rev. Biochem.* 57:665-700.

Green, K.A. and G. A. Cottrell. 1988. Action of baclofen on components of the Ca-current in rat and mouse DRG neurones in culture. *Br. J. Pharmacol.* 94:235-245.

Hagiwara, S. and S. Nakajimi. 1966. Effects of intracellular Calcium ion concentration upon the excitability of the muscle fiber membrane of barnacle. *J. Gen. Physiol.* 49:807-818.

Hamill, O.P., A. Marty, E. Neher, B. Sakmann, and F. J. Sigworth. 1981. Improved patch-clamp techniques for high resolution current recording from cells and cell-free membrane patches. *Pflügers Arch* 391:85-100.

Hamilton, S.L., J. Codina, M. J. Hawkes, A. Yatani, T. Sawada, F. M. Strickland, S. C. Froehner, A. M. Spiegel, L. Toro, E. Stefani, L. Birnbaumer, and A. M. Brown. 1991. Evidence for direct interaction of $G_s\alpha$ with the Ca^{2+} channel of skeletal muscle. *J. Biol. Chem.* 266:19528-19535.

Hammond, D.L. 1988. Control Systems for Nociceptive Afferent Processing The Descending Inhibitory pathways. In Spinal Afferent Processing. T. L. Yaksh, editor. Plenum Press, New York and London. 363-390.

Harper, A.A. and S. N. Lawson. 1985. Conduction velocity is related to morphological cell type in rat dorsal root ganglion neurones. *J. Physiol.* 359:31-46.

Hartzell, H.C., P. -F. Méry, R. Fischmeister, and G. Szabo. 1991. Sympathetic regulation of cardiac calcium current is due exclusively to cAMP dependent phosphorylation. *Nature* 351:573-576.

Haydon, P.G., H. J. Man-Son-Hing, R. T. Doyle, and M. Zoran. 1991. FMRFamide Modulation of Secretory Machinery Underlying Presynaptic Inhibition of Synaptic Transmission Requires a Pertussis Toxin-Sensitive G-protein. *J. Neurosci.* 11:3851-3860.

Heideman, W. and H. R. Bourne. 1990. Structure and Function of G-Protein α Chains. In G Proteins. Academic Press,Inc., 17-40.

Herrero, I., M. T. Miras-Portugal, and J. Sánchez-Prieto. 1992. Positive feedback of glutamate exocytosis by metabotropic presynaptic receptor stimulation. *Nature* 360:163-166.

Hescheler, J., W. Rosenthal, W. Trautwein, and G. Schultz. 1987. The GTP-binding protein, Go, regulates neuronal calcium channels. *Nature* 325:445-447.

Hescheler, J., W. Rosenthal, M. Wulfern, M. Tang, M. Yajima, W. Trautwein, and G. Schultz. 1988. Involvement of the guanine nucleotide-binding protein, N_o, in the inhibitory regulation of neuronal calcium channels. *Adv. Second Messenger Phosphoprotein Res.* 21:165-174.

Hess, P. 1990. Calcium Channels in Vertebrate Cells. *Ann. Rev. Neurosci.* 13:337-356.

Hélène, C. and J. J. Toulmé. 1990. Specific regulation of gene expression by antisense, sense and antigene nucleic acids. *BBA* 1049:99-125.

Hille, B. 1984. Ionic Channels of Excitable Membranes. Sinauer Associates Inc., Sunderland, Massachusetts.

Hille, B. 1992. G Protein-Coupled Mechanisms and Nervous Signalling. *Neuron* 9:187-195.

Hillyard, D.R., V. D. Monje, I. M. Mintz, B. P. Bean, L. Nadasdi, J. Ramachandran, G. Miljanich, A. Azimi-Zoonooz, J. M. McIntosh, L. J. Cruz, J. S. Imperial, and B. M. Olivera. 1992. A New Conus peptide ligand for Mammalian Presynaptic Ca^{2+} channels. *Neuron* 9:69-77.

Hirokawa, N., K. Sobue, K. Kanda, A. Harada, and H. Yorifugi. 1989. The cytoskeletal architecture of the presynaptic terminal and molecular structure of synapsin 1. *J. Cell. Biol.* 108:111-126.

Hockberger, P.E., M. Toselli, D. Swandulla, and H. D. Lux. 1989. A diacylglycerol analogue reduces neuronal calcium currents independently of protein kinase C activation. *Nature* 338:340-342.

Holz, G.G., R. M. Kream, A. Spiegel, and K. Dunlap. 1989. G proteins couple α-adrenergic and $GABA_b$ receptors to inhibition of peptide secretion from peripheral sensory neurons. *Neuroscience* 9:657-666.

Holz, G.G., S. G. Rane, and K. Dunlap. 1986. GTP-binding proteins mediate transmitter inhibition of voltage-dependent calcium channels. *Nature* 319:670-672.

Horne, W.A., P. T. Ellinor, I. Inman, M. Zhou, R. W. Tsien, and T. L. Schwartz. 1992. Multiple calcium channel clones isolated from a marine ray. *Society for Neuroscience* 479.2:(Abstr.)

Horne, W.A., P. T. Ellinor, I. Inman, M. Zhou, R. W. Tsien, and T. L. Schwarz. 1993. Molecular diversity of Ca^{2+} channel α_1 subunits from the marine ray *Discopyge ommata. Proc. Natl. Acad. Sci. U. S. A.* (In Press)

Hsu, W.H., U. Rudolph, J. Sanford, P. Bertrand, J. Olate, C. Nelson, L. G. Moss, A. E. Boyd, J. Codina, and L. Birnbaumer. 1990. Molecular cloning of a novel splice variant of the α subunit of the mammalian G_o protein. *J. Bio. Chem.* 265:11220-11226.

Huston, E., G. Cullen, M. I. Sweeney, H. Pearson, M. S. Fazeli, and A. C. Dolphin. 1993. Pertussis toxin treatment increases glutamate release and dihydropyridine binding sites in cultured rat cerebellar granule neurons. *Neuroscience* In press:

Hymel, L., J. Striessning, H. Glossmann, and H. Schindler. 1988. Purified skeletal muscle 1,4-dihydropyridine receptor forms phosphorylation-dependent oligomeric calcium channels in planar bilayers. *Proc. Natl. Acad. Sci. USA* 85:4290-4294.

Iggo, A. 1987. Cutaneous sensory mechanisms. In The senses. H. B. & Mollon Barlow,J.D., editor. Cambridge University Press, Cambridge, London, NY, New Rochelle, Melbourne, Sydney.

Imredy, J.P. and D. T. Yue. 1992. Submicroscopic Ca^{2+} Diffusion Mediates Inhibitory Coupling between Individual Ca^{2+} Channels. *Neuron* 9:197-207.

Inanobe, A., H. Shibasaki, K. Takahashi, I. Kobayashi, U. Tomita, M. Ui, and T. Katada. 1990. Characterization of four G_o-type proteins purified from bovine brain membranes. *FEBS* 263:369-372.

Kalsner, S. 1990. Heteroreceptors, Autoreceptors, and Other Terminal Sites. In Presynaptic Receptors and the Question of Autoregulation of Neurotransmitter Release. S. ; Westfall Kalsner,T.C., editor. Annals of The New York Academy of Sciences, 2 East 63rd Street, New York. 1-6.

Kasai, H. 1992. Voltage- and Time-Dependent inhibition of Neuronal calcium channels by a GTP-binding protein in a mammalian cell line. *J. Physiol.* 448:189-209.

Kasai, H. and T. Aosaki. 1989. Modulation of Ca-channel current by an adenosine analog mediated by a GTP-binding protein in chick sensory neurons. *Pflügers Arch* 414:145-148.

Katz, A., W. Dianqing, and M. I. Simon. 1992. Subunits ßγ of heterotrimeric G protein activate ß2 isoform of phospholipase C. *Nature* 360:686-689.

Katz, B. 1967. Nerve, Muscle and Synapse. McGraw-Hill book company, N.Y.; St.Louis; S.F.; Toronto; London; Sydney..

Katz, B. 1969. The release of Neural Transmitter substances. Liverpool University Press, Liverpool.

Kaziro, Y., H. Itoh, T. Kozasa, M. Nakafuku, and T. Satoh. 1991. Structure and function of signal-transducing GTP-binding proteins. *Annu. Rev. Biochem.* 60:349-400.

Kerr, L.M. and D. Yoshikami. 1984. A venom peptide with a novel presynaptic blocking action. *Nature* 308:282-284.

Kim, D., D. L. Lewis, L. Graziadei, E. J. Neer, D. Bar-Sagi, and D. E. Clapham. 1987. G-protein ßy-subunits activate the cardiac muscarinic K^+-channel via phospholipase A_2. *Nature* 337:557-559.

Kleuss, C., J. Hescheler, C. Ewel, W. Rosenthal, G. Schultz, and B. Wittig. 1991. Assignment of G-protein subtypes to specific receptors inducing inhibition of calcium currents. *Nature* 353:43-48.

Kleuss, C., H. Scherübl, J. Hescheler, G. Schultz, and B. Wittig. 1992. Different ß-subunits determine G-protein interaction with transmembrane receptors. *Nature* 358:424-426.

Kostyuk, P., N. Akaike, Yu. Osipchuk, A. Savchenko, and Ya. Shuba. 1989. Gating and Permeation of Different Types of Ca Channels. *Ann. N. Y. Acad. Sci.* 560:63-79.

Kostyuk, P.G., Ya Shuba,M., and A. N. Savchenko. 1988. Three types of calcium channels in the membrane of mouse sensory neurons. *Pflugers Arch* 411:661-669.

Kostyuk, P.G., N. S. Veselovsky, and A. Y. Tsyndrenko. 1981. Ionic currents in the somatic membrane of rat dorsal root ganglion neurons-I.sodium currents. *Neuroscience* 12:2423-2430.

Kramer, R.H., L. K. Kaczmarek, and E. S. Levitan. 1991. Neuropeptide inhibition of voltage-gated calcium channels mediated by mobilization of intracellular calcium. *Neuron* 6:557-563.

Kurachi, Y., H. Ito, T. Sugimoto, T. Shimizu, I. Miki, and M. Ui. 1989. Arachadonic acid metabolites as intracellular modulators of the G protein-gated cardiac K^+ channel. *Nature* 337:555-557.

Lacerda, A.E., H. S. Kim, P. Ruth, E. Perez-Reyes, V. Flockerzi, F. Hofmann, L. Birnbaumer, and A. M. Brown. 1991. Normalization of current kinetics by interaction between the α_1 and ß subunits of the skeletal muscle dihydropyridine-sensitive Ca^{2+} channel. *Nature* 352:527-530.

Leonard, J.P., J. Nargeot, T. P. Snutch, N. Davidson, and H. A. Lester. 1987. Ca channels induced in Xenopus oocytes by injection of rat brain mRNA. *J. Neurosci.* 7:3:875-881.

Lester, R.A.J. and C. E. Jahr. 1990. Quisqualate receptor-mediated depression of calcium currents in hippocampal neurons. *Neuron* 4:741-749.

Linden, J. and T. M. Delahunty. 1989. Receptors that inhibit PI breakdown. *TiPS* 10:117-120.

Linder, M.E., D. A. Ewald, R. J. Miller, and A. G. Gilman. 1990. Purification and characterization of $G_{o\alpha}$ and three types of $G_{i\alpha}$ after expression in *Escherichia coli*. *J. Biol. Chem.* 265:8243-8251.

Lipscombe, D., S. Kongsamut, and R. W. Tsien. 1989. α-Adrenergic inhibition of sympathetic neurotransmitter release mediated by modulation of N-type calcium-channel gating. *Nature* 340:639-642.

Lledo, P.M., V. Homburger, J. Bockaert, and J. -D. Vincent. 1992. Differential G protein-mediated coupling of D_2 dopamine receptors to K^+ and Ca^{2+} currents in rat anterior pituitary cells. *Neuron* 8:455-463.

Llinás, R., I. Z. Steinberg, and K. Walton. 1981. Relationship between presynaptic calcium current and postsynaptic potential in squid giant synapse. *Biophysical Journal* 33:323-352.

Llinás, R., M. Sugimori, D. E. Hillman, and B. Cherksey. 1992. Distribution and functional significance of the P-type voltage-dependent Ca^{2+} channels in the mammalian central nervous system. *TiNS* 15:351-355.

Llinás, R., M. Sugimori, J. -W. Lin, and B. Cherksey. 1989. Blocking and isolation of a calcium channel from neurons in mammals and cephalopods utilizing a toxin fraction (FTX) from funnel-web spider poison. *Proc. Natl. Acad. Sci. USA* 86:1689-1693.

Logothetis, D.E., Y. Kurachi, J. Galper, E. J. Neer, and D. E. Clapham. 1987. The ßγ subunits of GTP-binding proteins activate the muscarinic K^+ channel in heart. *Nature* 325:321-326.

Lopez, H.S. and A. M. Brown. 1991. Correlation between G protein activation and reblocking kinetics of Ca^{2+} channel currents in rat sensory neurons. *Neuron* 7:1061-1068.

Lundy, P.M., R. Frew, T. W. Fuller, and M. G. Hamilton. 1991. Pharmacological evidence for an w-conotoxin, dihydropyridine insensitive neuronal Ca^{2+} channel. *Eur. J. Pharmacol.* 206:61-68.

Mackler, S.A., B. P. Brooks, and J. H. Eberwine. 1992. Stimulus-Induced Coordinate Changes in mRNA Abundance in Single Postsynaptic Hippocampal CA1 Neurons. *Neuron* 9:539-548.

Man-Son-Hing, H.J., J. Codina, J. Abromowitz, and P. G. Haydon. 1992. Microinjection of the α-subunit of the G protein G_o2, but not G_o1, reduces a voltage-sensitive calcium current. *Cellular Signalling* 4:429-441.

Marchetti, C. and M. Robello. 1989. Guanosine-5'-0-(3-thiotriphosphate) modifies kinetics of voltage- dependent calcium current in chick sensory neurons. *Biophys. J.* 56:1267-1272.

N. G. Lopez, J. Ramachandran, and H. R. Bourne. 1988. Carboxyl terminal Domain of $G_{s\alpha}$ specifies coupling of receptors to stimulation of adenylyl cyclase. *Science* 241:448-451.

Matthews, G. 1991. Ion channels that are directly activated by cyclic nucleotides. *TiPS* 12:245-247.

McCobb, D.P. and K. G. Beam. 1991. Action Potential Waveform Voltage-Clamp Commands Reveal Striking Differences in Calcium Entry via Low and High Voltage-Activated Calcium Channels. *Neuron* 7:119-127.

McEnery, M.W., A. M. Snowman, A. H. Sharp, M. E. Adams, and S. H. Snyder. 1991. Purified ω-conotoxin GVIA receptor of rat brain resembles a dihydropyridine-sensitive L-type calcium channel. *Proc. Natl. Acad. Sci. USA* 88:11095-11099.

McFadzean, I. and R. J. Docherty. 1989. Noradrenaline- and Enkephalin-Induced Inhibition of Voltage-Densitive Calcium Currents in NG108-15 Hybrid Cells. *Eur. J. Neurosci.* 1:141-147.

McFadzean, I., I. Mullaney, D. A. Brown and G. Milligan. 1989. Antibodies to the GTP binding protein, G_o, antagonize noradrenaline-induced calcium current inhibition in NG108-15 hybrid cells. *Neuron* 3:177-182.

McKenzie, F.R., E. C. Kelly, C. G. Unson, A. M. Spielel, and G. Milligan. 1988. Antibodies which recognize the C-terminus of the inhibitory guanine-nucleotide-binding protein (G_i) demonstrate that opioid peptides and foetal-calf serum stimulate the high affinity GTPase activity of two separate pertussis-toxin substrates. *Biochem. J.* 249:653-659.

McLaughlin, S.K., P. J. McKinnon, and R. F. Margolskee. 1992. Gustducin is a taste-cell-specific G protein closely related to the transducins. *Nature* 357:563-569.

McNeil, P.L., R. F. Murphy, F. Lanni, and D. Lansing Taylor. 1984. A method for incorporating macromolecules into adherent cells. *J. Cell. Biol.* 98:1556-1564.

Melzack, R. and P. D. Wall. 1965. Pain Mechanisms: A New Theory. *Science* 150:971-979.

Mikami, A., K. Imoto, T. Tanabe, T. Niidome, Y. Mori, H. Takeshima, S. Narumiya, and S. Numa. 1989. Primary structure and functional expression of the cardiac dihydropyridine-sensitive calcium channel. *Nature* 340:230-233.

Miller, R.J. 1990. Receptor-mediated regulation of calcium channels and neurotransmitter release. *FASEB J.* 4:3291-3299.

Mintz, I.M., M. E. Adams, and B. P. Bean. 1992a. P-Type calcium channels in rat central and peripheral neurons. *Neuron* 9:85-95.

Mintz, I.M., M. E. Adams, and B. P. Bean. 1992b. Use of Spider toxins to discriminate between neuronal calcium channels. *Society for Neuroscience* 10.5:(Abstr.)

Mintz, I.M., V. J. Venema, M. E. Adams, and B. P. Bean. 1991. Inhibition of N- and L-type Ca^{2+} channels by the spider venom toxin ω-Aga-IIIA. *Proc. Natl. Acad. Sci. USA* 88:6628-6631.

Mintz, I.M., V. J. Venema, K. M. Swiderek, T. D. Lee, B. P. Bean, and M. E. Adams. 1992. P-type calcium channels blocked by the spider toxin ω-Aga-IVA. *Nature* 355:827-829.

Mori, Y., T. Friedrich, M. -S. Kim, A. Mikami, J. Nakai, P. Ruth, E. Bosse, F. Hofmann, V. Flockerzi, T. Furuichi, K. Mikoshiba, K. Imoto, T. Tanabe, and S. Numa. 1991. Primary structure and functional expression from complementary DNA of a brain calcium channel. *Nature* 350:398-402.

Mulkey, R.M. and R. S. Zucker. 1991. Action potentials must admit calcium to evoke transmitter release. *Nature* 350:153-155.

Nahorski, S.R. 1988. Inositol polyphosphates and neuronal calcium homeostasis. *TiNS* 11:444-448.

Neer, E.J., J. M. Lok, and L. G. Wolf. 1984. Purification and Properties of the inhibitory Guanine Nucleotide Regulatory Unit of Brain Adenylate Cyclase. *J. Biol. Chem.* 259:14222-14229.

Nicoll, R.A. and B. E. Alger. 1979. Presynaptic Inhibition: Transmitter and ionic mechanisms. *Int. Rev. Neurobiol.* 21:217-258.

Niesen, C.E., O. T. Jones, and P. L. Carlen. 1992. Novel Snake toxin blocks selectively the L-type calcium current in rat dentate granule neurons. *Society for Neuroscience* 10.3:(Abstr.)

Niidome, T., K. Man-Suk, T. Friedrich, and Y. Mori. 1992. Molecular cloning and characterization of a novel calcium channel from rabbit brain. *FEBS* 308:7-13.

Nowycky, M.C., A. P. Fox, and R. W. Tsien. 1985. Three types of neuronal calcium channel with different calcium agonist sensitivity. *Nature* 316:440-446.

Oberhauser, A.F., J. R. Monck, W. E. Balch, and J. M. Fernandez. 1992. Exocytotic fusion is activated by Rab3a peptides. *Nature* 360:270-273.

Offermanns, S., M. Gollasch, J. Hescheler, K. Spicher, A. Schmidt, G. Schultz, and W. Rosenthal. 1991. Inhibition of voltage-dependent Ca^{2+} currents and activation of pertussis toxin-sensitive G-proteins via muscarinic receptors in GH_3 cells. *Mol. Endocrinol.* 5:995-1002.

Olivera, B.M., W. R. Gray, R. Zeikus, J. M. McIntosh, J. Varga, J. Rivier, V. de. Santos, and L. J. Cruz. 1985. Peptide Neurotoxins from Fish-hunting Cone Snails. *Science* 230:1338-1343.

Olivera, B.M., J. S. Imperial, L. J. Cruz, V. P. Bindokas, V. J. Venema, and M. E. Adams. 1991. Calcium channel-targeted polypeptide toxins. *Ann. N. Y. Acad. Sci.* 635:114-122.

Olsen, R.W. and A. J. Tobin. 1990. Molecular biology of $GABA_A$ receptors. *FASEB J.* 4:1469-1480.

Ortiz, D., M. M. Baldwin, and J. J. Lucas. 1987. Transient correction of genetic defects in cultured animal cells by introduction of functional proteins. *Mol. Cell. Biol.* 7:3012-3017.

Paupardin-Tritsch, D., H. M. Gerschenfeld, A. Nairn, and P. Greengard. 1986. cGMP-dependent protein kinase enhances Ca^{2+} current and potentiates the serotonin-induced Ca^{2+} current increases in snail neurones. *Nature* 323:812-814.

Pearson, H.A. and A. C. Dolphin. 1992. Internal Mg/ATP levels alter Ca^{2+} channel current characteristics and responses to (-)baclofen in cultured rat cerebellar granule neurones. *J. Physiol.* (Abstract) In press.

Penington, N.J., J. S. Kelly, and A. P. Fox. 1991. A study of the mechanism of Ca^{2+} current inhibition produced by serotonin in rat dorsal raphe neurons. *J. Neurosci.* 11:3594-3609.

Perez-Reyes, E., H. S. Kim, A. E. Lacerda, W. Horne, X. Wei, D. Rampe, K. P. Campbell, A. M. Brown, and L. Birnbaumer. 1989. Induction of calcium currents by the expression of the α_1- subunit of the dihydropyridine receptor from skeletal muscle. *Nature* 340:233-236.

Perez-Reyes, E., X. Wei, A. Castellano, and L. Birnbaumer. 1990. Molecular Diversity of L-type Calcium Channels. *J. Biol. Chem.* 265:20430-20436.

Perney, T.M., L. D. Hirning, S. E. Leeman, and R. J. Miller. 1986. Multiple calcium channels mediate neurotransmitter release from peripheral neurons. *Proc. Natl. Acad. Sci. USA* 83:6656-6659.

Piomelli, D., A. Volterra, N. Dale, S. Siegelbaum, E. R. Kandel, J. H. Schwartz, and F. Belardetti. 1987. Lipoxygenase metabolites of arachadonic acid as second messengers for presynaptic inhibition of Aplysia sensory cells. *Nature* 328:38-43.

Plummer, M.R., D. E. Logothetis, and P. Hess. 1989. Elementary properties and pharmacological sensitivities of calcium channels in mammalian peripheral neurons. *Neuron* 2:1453-1463.

Plummer, M.R., A. Rittenhouse, M. Kanevsky, and P. Hess. 1991. Neurotransmitter modulation of calcium channels in rat sympathetic neurons. *J. Neurosci.* 11:2339-2348.

Pugh, E.N. and T. D. Lamb. 1990. Cyclic GMP and calcium: the internal messengers of excitation and adaptation in vertebrate photoreceptors. *Vision Research* 30:1923-1948.

Pumplin, D.W., T. S. Reese, and R. Llinás. 1981. Are the presynaptic membrane particles the calcium channels? *Proc. Natl. Acad. Sci. U. S. A.* 78:7210-7213.

Purves, D. 1989. Body and the brain- a trophic theory of neural connections. Harvard University Press,

Pusch, M. and E. Neher. 1988. Rates of diffusional exchange between small cells and a measuring patch pipette. *Pflugers Arch* 411:204-211.

Rane, S.G. and K. Dunlap. 1986. Kinase C activator 1,2-oleoylacetylglycerol attenuates voltage-dependent calcium current in sensory neurones/. *Proc. Natl. Acad. Sci. U. S. A.* 83:184-188.

Rang, H.P. and M. M. Dale. 1987. Pharmacology. Churchill Livingstone, Edinburgh London Melbourne and New York.

Regan, L.J., D. W. Y. Sah, and B. P. Bean. 1991. Ca^{2+} channels in rat central and peripheral neurons: High-threshold current resistant to dihydropyridine blockers and w-conotoxin. *Neuron* 6:269-280.

Regan, L.J., D. W. Y. Sah, and B. P. Bean. 1991. Ca^{2+} channels in rat central and peripheral neurons: High-Threshold current resistant to Dihydropyridine blockers and ω-conotoxin. *Neuron* 6:269-280.

Reuter, H. 1983. Calcium channel modulation by neurotransmitters, enzymes and drugs. *Nature* 301:569-574.

Sakamoto, J. and K. P. Campbell. 1991. A monoclonal antibody to the ß subunit of the skeletal muscle dihydropyridine receptor immunoprecipitates the brain ω- conotoxin GVIA receptor. *J. Biol. Chem.* 266:18914-18919.

Sather, W.A., T. Tanabe, Y. Mori, M. E. Adams, G. Miljanich, S. Numa, and R. W. Tsien. 1992. Contrasts between cloned BI and Cardiac L-type calcium channels expressed in Xenopus oocytes. *Society for Neuroscience* 10.11:(Abstr.)

Schmidt, A., J. Hescheler, S. Offermanns, K. Spicher, K. D. Hinsch, F. J. Klinz, J. Codina, L. Birnbaumer, H. Gausepohl, R. Frank, and et al. 1991. Involvement of pertussis toxin-sensitive G-proteins in the hormonal inhibition of dihydropyridine-sensitive Ca^{2+} currents in an insulin-secreting cell line (RINm5F). *J. Biol. Chem.* 266:18025-18033.

Schofield, G.G. 1991. Norepinephrine inhibits a Ca^{2+} current in rat sympathetic neurons via a G-protein. *Eur. J. Pharmacol. Mol. Pharmacol.* 207:195-207.
Scholz, K.P. and R. J. Miller. 1992. Inhibition of Quantal Transmitter Release in the Absence of Calcium Influx by a G Protein-Linked Adenosine Receptor at Hippocampal Synapses. *Neuron* 8:1139-1150.

Scott, R.H. and A. C. Dolphin. 1986. Regulation of calcium currents by GTP analogue: potentiation of (-)-baclofen-mediated inhibition. *Neuroscience Letters* 69:59-64.

Scott, R.H. and A. C. Dolphin. 1987. Activation of a G protein promotes agonist responses to calcium channel ligands. *Nature* 330:760-762.

Scott, R.H. and A. C. Dolphin. 1990. Voltage dependent modulation of cultured rat sensory neurone calcium channel currents by G protein activation: differential effects on kinetics and amplitude. *J. Physiol.* 424:40P.(Abstr.)

Scott, R.H., H. A. Pearson, and A. C. Dolphin. 1991. Aspects of vertebrate neuronal voltage-activated calcium currents and their regulation. In . Prog.Neurobiol., 485-520.

Scroggs, R.S. and A. P. Fox. 1991. Distribution of dihydropyridine and ω-conotoxin-sensitive calcium currents in acutely isolated rat and frog sensory neuron somata: Diameter-dependent L channel expression in frog. *J. Neurosci.* 11:1334-1346.

Scroggs, R.S. and A. P. Fox. 1992. Calcium current variation between acutely isolated adult rat dorsal root ganglion neurons of different size. *J. Physiol.* 445:639-658.

Sher, E. and F. Clementi. 1991. ω-conotoxin-sensitive voltage-operated calcium channels in vertebrate cells. *Neuroscience* 42:301-307.

Silver, R.A., A. G. Lamb, and S. R. Bolsover. 1990. Calcium hotspots caused by L-channel clustering promote morphological changes in neruonal growth cones. *Nature* 343:751-754.

Snutch, T.P., J. P. Leonard, M. M. Gilbert, H. A. Lester, and N. Davidson. 1990. Rat brain expresses a heterogeneous family of calcium channels. *Proc. Natl. Acad. Sci. U. S. A.* 87:3391-3395.

Snutch, T.P. and P. B. Reiner. 1992. Ca^{2+} channels: diversity of form and function. *Curr. Op. Neurobiol.* 2:247-253.

Snutch, T.P., W. J. Tomlinson, J. P. Leonard, and M. M. Gilbert. 1991. Distinct Calcium Channels Are Generated by Alternative Splicing and Are Differentially Expressed in the Mammalian CNS. *Neuron* 7:45-57.

Song, S.-Y., K. Saito, K. Noguchi, and S. Konishi. 1989.

Different GTP-binding proteins mediate regulation of calcium channels by acetylcholine and noradrenaline in rat sympathetic neurons. *Brain Research* 494:383-386.
Soong, T.-W. and T. P Snutch. 1992. cDNA cloning of a calcium channel highly expressed in the hippocampus. *Society for Neuroscience* 479.6:(Abstr.)

Stanley, E.F. and G. Goping. 1991. Characterization of a calcium current in a vertebrate cholinergic presynaptic nerve terminal. *J. Neurosci.* 11(4):985-993.

Starr, T.V.B., W. Prystay, and T. P. Snutch. 1991. Primary structure of a calcium channel that is highly expressed in the rat cerebellum. *Proc. Natl. Acad. Sci. USA* 88:5621-5625.

Sternweis, P.C. and J. D. Robishaw. 1984. Isolation of Two Proteins with High Affinity for Guanine Nucleotides from Membranes of Bovine Brain. *J. Biol. Chem.* 259:13806-13813.

Strange, P.G. 1988. The structure and mechanism of neurotransmitter receptors. *Biochem. J.* 249:309-318.

Strittmatter, S.M., D. Valenzuela, T. E. Kennedy, E. J. Neer, and M. C. Fishman. 1990. G_o is a major growth cone protein subject ot regulation by GAP- 43. *Nature* 344:836-841.

Strong, S.A., A. P. Fox, R. W. Tsien, and L. K. Kaczmarek. 1987. Stimulation of protein kinase C recruits covert calcium channels in Aplysia bag cell neurons. *Nature* 325:714-717.

Surprenant, A., K. -Z. Shen, R. A. North, and H. Tatsumi. 1990. Inhibition of calcium currents by noradrenaline, somatostatin and opioids in guinea-pig submucosal neurones. *J. Physiol.* 431:585-608.

Südhof, T.C. and R. Jahn. 1991. Proteins of Synaptic Vesicles Involved in Exocytosis and Membrane Recycling. *Neuron* 6:665-677.

Sweeney, M.I. and A. C. Dolphin. 1992. 1,4-Dihydropyridines modulate GTP hydrolysis by G_o in neuronal membranes. *FEBS Lett.* 310:66-70.

Takemura, M., H. Kiyama, H. Fukui, M. Tohyama, and H. Wada. 1989. Distribution of the ω-Conotoxin receptor in rat brain. An autoradiographic mapping. *Neuroscience* 32:405-416.

Tanabe, T., H. Takeshima, A. Mikami, V. Flockerzi, H. Takahashi, K. Kangawa, M. Kojima, H. Matsuo, T. Hirose, and S. Numa. 1987. Primary structure of the receptor for calcium channel blockers from skeletal muscle. *Nature* 328:313-318.

Tang, C.M., F. Presser, and M. Morad. 1988. Amiloride selectively blocks the low threshold (T) calcium channel. *Science* 240:213-215.

Tatebayashi, H. and N. Ogata. 1992. Kinetic analysis of the

GABAB-mediated inhibition of the High-Threshold Ca^{2+} current in cultured rat sensory neurones. *J. Physiol.* 447:391-407.

Taussig, R., S. Sanchez, M. Rifo, A. G. Gilman, and F. Belardetti. 1992. Inhibition of the w-Conotoxin-sensitive Calcium Current by Distinct G Proteins. *Neuron* 8:799-809.

Toselli, M., J. Lang, T. Costa, and H. D. Lux. 1989. Direct modulation of voltage-dependent calcium channels by muscarinic activation of a pertussis toxin-sensitive G-protein in hippocampal neurons. *Pflügers Arch* 415:255-261.

Triggle, D.J., M. Hawthorn, M. Gopalakrishnan, A. Minarini, S. Avery, A. Rutledge, R. Bangalore, and W. Zheng. 1991. Synthetic organic ligands active at voltage-gated calcium channels. *Ann. NY Acad. Sci.* 635:123-138.

Tsien, R.W. and R. Y. Tsien. 1990. Calcium channels, Stores, and Oscillations. *Annu. Rev. Cell Biol.* 6:715-760.

Turner, T.J., M. E. Adams, and K. Dunlap. 1992. Calcium Channels Coupled to Glutamate Release Identified by ω-Aga-IVA. *Science* 258:310-313.

VanDongen, A.M.J., J. Codina, J. Olate, R. Mattera, R. Joho, L. Birnbaumer, and A. M. Brown. 1988. Newly identified brain potassium channels gated by the Guanine Nucleotide binding protein Go. *Science* 242:1433-1436.

Varadi, G., P. Lory, D. Schultz, M. Varadi, and A. Schwartz. 1991. Acceleration of activation and inactivation by the ß subunit of the skeletal muscle calcium channel. *Nature* 352:159-162.

Wang, H-.Y., D. C. Watkins, and C. C. Malbon. 1992. Antisense oligodeoxynucleotides to G_s protein α-subunit sequence accelerate differentiation of fibroblasts to adipocytes. *Nature* 358:334-337.

Wanke, E., A. Ferroni, A. Malgaroli, A. Ambrosini, T. Pozzan, and J. Meldolesi. 1987. Activation of Muscarinic receptor selectively inhibits a rapidly inactivated Ca^{2+} current in rat sympathetic neurons. *Proc. Natl. Acad. Sci. U. S. A.* 84:4313-4317.

Westenbroek, R.E., M. K. Ahlijanian, and W. A. Catterall. 1990. Clustering of L-type Ca^{2+} channels at the base of major dendrites in hippocampal pyramidal neurons. *Nature* 347:281-284.

Wiley, J.W., R. A. Gross, and R. L. Macdonald. 1992. The peptide CGRP increases a high-threshold Ca^{2+} current in rat nodose neurones via a pertussis toxin-sensitive pathway. *J. Physiol.* 455:367-381.

Wiley, J.W., R. A. Gross, H. Moises, and R. L. Macdonald. 1992. Dynorphin A-mediated reduction of calcium currents in

rat dorsal root ganglion neurons is antagonized by anti-$G_o\alpha$ antiserum. *Society for Neuroscience* 535.3:(Abstr.)

Williams, M.E., P. F. Brust, D. H. Feldman, S. Patthi, S. Simerson, A. Maroufi, A. F. McCue, G. Veliçelebi, S. B. Ellis, and M. M. Harpold. 1992. Structure and Functional Expression of an ω-Conotoxin-Sensitive Human N-type Calcium Channel. *Science* 257:389-395.

Williams, M.E., D. H. Feldman, A. F. McCue, R. Brenner, G. Velicelebi, S. B. Ellis, and M. M. Harpold. 1992. Structure and Functional Expression of α_1, α_2 and ß Subunits of a Novel Human Neuronal Calcium Channel Subtype. *Neuron* 8:71-84.

Yatani, A., R. Mattera, J. Codina, R. Graf, K. Okabe, E. Padrell, R. Iyengar, A. M. Brown, and L. Birnbaumer. 1988. The G protein-gated atrial K^+ channel is stimulated by three distinct $G_{i\alpha}$-subunits. *Nature* 336:680-682.

Zucker, R.S. and P. G. Haydon. 1988. Membrane potential has no direct role in evoking neurotransmitter release. *Nature* 335, :360-362.